Titre: Title:	Study of the behaviour of acetals in the proton exchange fuel cell's cathode
Auteur: Author:	Geoffrey Longtin
Date:	2006
Type:	Mémoire ou thèse / Dissertation or Thesis
Référence: Citation:	Longtin, G. (2006). Study of the behaviour of acetals in the proton exchange fuel cell's cathode [Mémoire de maîtrise, École Polytechnique de Montréal]. PolyPublie. https://publications.polymtl.ca/7845/

URL de PolyPublie: PolyPublie URL:	https://publications.polymtl.ca/7845/
Directeurs de recherche: Advisors:	
Programme: Program:	Non spécifié

UNIVERSITÉ DE MONTRÉAL

STUDY OF THE BEHAVIOUR OF ACETALS IN THE PROTON EXCHANGE FUEL CELL'S CATHODE

GEOFFREY LONGTIN

DÉPARTEMENT DE GÉNIE CHIMIQUE

ÉCOLE POLYTECHNIQUE DE MONTRÉAL

MÉMOIRE PRÉSENTÉ EN VUE DE L'OBTENTION

DU DIPLÔME DE MAÎTRISE ÈS SCIENCES APPLIQUÉS

(GÉNIE MÉTALLURGIQUE)

DÉCEMBRE 2006

Your file Votre référence
ISBN: 978-0-494-25554-4
Our file Notre référence
ISBN: 978-0-494-25554-4

UNIVERSITÉ DE MONTRÉAL

ÉCOLE POLYTECHNIQUE DE MONTRÉAL

Ce mémoire intitulé:

STUDY OF THE BEHAVIOUR OF ACETALS IN THE PROTON EXCHANGE FUEL CELL'S CATHODE

présenté par: LONGTIN Geoffrey

en vue de l'obtention du diplôme de: Maîtrise ès sciences appliqués

a été dûment accepté par le jury d'examen constitué de:

M.CHARTRAND Patrice, Ph.D., président

M. SAVADOGO Oumarou, Doct. d'état, membre et directeur de recherche

M. ROCHEFORT Dominic, Ph.D., membre

REMERCIEMENTS

Dans les lignes qui suivent, je voudrais prendre le temps de remercier tous ceux qui ont pu m'apporter de l'aide tout au long de mes études. Premièrement, je tiens à remercier toute ma famille qui, au cours de mon cheminement scolaire, m'a montré l'importance d'une bonne éducation. J'aurai toujours l'inspiration de mon grand-père maternel qui m'a servit de modèle dans la vie afin de devenir le meilleur de soi-même et persister dans ces études. Également, je tiens à remercier Oumarou Savadogo qui a su m'épauler durant mes études universitaires et qui a aussi accepté de diriger mon projet de maîtrise. Mes remerciements vont aussi au professeur Zempachi Ogumi, qui a si gentiment accepté que je poursuive ma maîtrise dans son laboratoire à l'Université de Kyoto au Japon. L'expérience était des plus enrichissante tant au niveau académique que personnel. Je tiens donc à remercier les gens suivant (par ordre alphabétique), qui m'ont apporté une aide grandement appréciée : Takeshi Abe, Annie Bourdon, Yanick Cyr, Taro Kinumoto, Josée Laviolette, Carole Massicotte, Koji Matsuoka, Shigenori Mitsushima, Kohei Miyazaki, Teko Napporn, Éric Nguo, Zempachi Ogumi, Sebastien Potvin, Oumarou Savadogo, Hironori Shirakata, à ma famille, à mes amis, ainsi que les membres du jury, et je tiens aussi à remercier tout ceux dont je n'ai pas eu la chance de nommer ci haut.

RÉSUMÉ

Les réserves de pétrole se faisant de plus en plus rares et le problème de pollution s'y reliant qui s'aggrave, il devient urgent de trouver une alternative pour nos besoins énergétiques. Une avenue prometteuse nous renvoie à l'utilisation des piles à combustible. Plusieurs efforts on déjà été faits afin d'améliorer les piles à combustible qui carburent au méthanol. Or, ce dernier est trop toxique pour l'être humain. De récentes études ont opté d'utiliser les acétals comme combustible. Ce présent rapport suit la route tracé par Narayanan, Savadogo, et plus précisément, le mémoire de Yanick Cyr. Notre attention se portera principalement sur la détermination du comportement des acétals dans la cathode de la pile à combustible à membrane échangeuse de protons. De nos jours, il est communément reconnu que le passage du combustible se fait en diffusant au travers la membrane selon un processus de *crossover*. Jusqu'à ce jour, nous ne pouvons qu'espérer de minimiser le *crossover* puisqu'il est impossible d'éradiquer ce phénomène. Les options qui s'offrent à nous consistent à réduire la perméabilité de la membrane électrolytique, ou de trouver de catalyseurs qui seront moins affectés par la présence de combustible dans la cathode. C'est cette seconde option que nous irons explorer subséquemment.

L'ensemble des tests a été réalisé à l'aide d'une cellule électrochimique afin de simuler les conditions d'opérations d'une pile à combustible consommant des acétals. Différents catalyseurs ont été utilisés afin de voir leur comportement suite au *crossover*. Le catalyseurs utilisés sont: Pt, Pt/C, PtRu/C, PtIr/C et PtSn/C. En plus de nos trois

acétals (méthylal, éthylal et 1,3-dioxolane), nous avons utilisé le méthanol comme référence. La voltammétrie cyclique a été utilisé pour déterminer les propriétés électrochimiques et la cinétique des combustibles. De plus, l'usage du chromatographe liquide à haute performance et du spectromètre de masse nous ont permis de faire une analyse des produits d'oxydation sur une période de quelques heures.

Il a été observé que l'oxydation des combustibles (0,5M) sur la plaque lisse de platine nuit grandement au processus de réduction d'oxygène. En effet, en ajoutant du méthylal en présence d'oxygène, le potentiel de début de réduction de l'oxygène chute de 1,00V/RHE à 0,41V. Il en va dans le même sens lors qu'on utilise comme combustible l'éthylal, le 1,3-dioxolane et le méthanol puisque le potentiel de début de réduction de l'oxygène 0,47V, 0,44V et 0,70V respectivement.

En poursuivant l'étude sur des catalyseurs de platine dispersé sur un support de poudre de carbone (Pt/C), il a été mesuré que le potentiel de début de réduction de l'oxygène est de 0,91V. Or, en présence du méthanol, le potentiel tombe à 0,69V. Pour l'éthylal on obtient 0,56V, le 1,3-dioxolane 0,51V et le méthylal 0,41V. En utilisant le catalyseur PtRu/C, le méthanol est le combustible qui démontre le potentiel de début de réduction de l'oxygène le plus élevé avec 0,54V. Les acétals suivent avec le 1,3-dioxolane, l'éthylal et le méthylal qui ont respectivement 0,47V, 0,42V et 0,41V. Dans l'ensemble, on constate que pour le platine lisse, les pics d'oxydation des combustibles sont plus larges et ont les valeurs les plus élevées pour les potentiels plus

faibles comparativement à ceux observés sur le Pt/C. Avec le PtIr/C comme catalyseur, on observe que le méthanol est le combustible qui s'oxyde le moins efficacement en présence d'oxygène. Or, c'est le méthylal qui offre le potentiel de réduction de l'oxygène le plus élevé avec 0,70V, suivi du méthanol à 0,56V, du 1,3-dioxolane à 0,53V et de l'éthylal 0,47V. En somme, on constate que la réaction de réduction de l'oxygène est affectée tant par la nature du catalyseur que par le type de combustible qui se retrouve dans le comportement de la cathode. Par conséquent, sur le Pt/C, la présence du méthanol est la moins néfaste pour la réaction de réduction de l'oxygène, tandis que sur le PtRu/C et PtIr/C ce sont le méthanol et le méthylal qui inhibent moins la réaction de réduction de l'oxygène (RRO).

Par la suite, on a étudié l'effet de la différence (ΔR) entre le rayon atomique du platine et celui de l'élément d'alliage sur le pic d'oxydation du combustible. On a pu donc établir que c'est avec le PtIr/C, avec un ΔR avoisinant 3Å, qu'on obtient les courant de pics d'oxydation les plus faibles. En établissant une courbe similaire qui relie la variation du potentiel de début de réduction de l'oxygène à celle de (ΔR), il semble que le catalyseur ayant un ΔR proche de 3Å offre les potentiels les plus élevés. Cependant, cette conclusion n'inclut pas le 1,3-dioxolane car les résultats montrent que pour ce combustible, les potentiels de début de réduction les plus élevés sont obtenus lorsque ΔR se rapproche de 0.

L'analyse chromatographique et de spectromètre de masse a permis de chiffrer et d'identifier les éléments qui constituent les produits des réactions électrochimiques. En utilisant le méthanol sur le Pt/C, il semble que seul le méthanol est détectable à la sortie des détecteurs. Mais en utilisant le méthanol avec le PtRu/C, PtIr/C ou le PtSn/C, on détecte en plus une présence de formaldéhyde. Le méthylal et l'éthylal présentent aussi des quantités de formaldéhyde en utilisant n'importe quel catalyseur. En présence de 1,3-dioxolane, on peut aussi détecter du formaldéhyde en utilisant les quatre catalyseurs. Mais avec les catalyseurs à alliage binaire, on détecte en plus la présence d'acide formique. En guise de conclusion, on constate que pour le méthylal, le Pt/C réduit le moins le méthylal. Pour ce qui est de l'éthylal et du 1,3-dioxolane, il semble que le PtIr/C est le catalyseur le moins susceptible de réduire ces combustibles. Quand au méthanol, il semble ne pas avoir une grande différence en utilisant l'un des trois catalyseurs à alliages métalliques binaire.

À la fin de ce document, une liste des recommandations est énumérée afin de faciliter la poursuite et l'amélioration de l'étude sur les piles à combustibles à acétals.

ABSTRACT

With the predicted limitations of the fossil reserves around the world and the growing pollution related to their consumption, it is in the human being's interest that we find some alternative less polluting energy resources or vectors for our needs. A promising road leads us to the usage of fuel cells. Efforts have been made to improve the already promising DMFC (direct methanol fuel cell). Methanol being too toxic to humans, studies, including those developed recently in our group, have contributed in the increase in the performances of Direct Acetal Fuel Cells (DAFC) .This work follows previous works of Narayanan, Savadogo, and more closely, Yanick Cyr's Master Thesis. For the first time, the present research focuses on determining the effect of acetal's cross-over on the DAFC cathode behavior. It is widely demonstrated that the liquid fuels like alcohols or acetals cross over to the cathode by permeation through the electrolyte membrane. Until now the fuel cross-over problem was expected, in general, to be minimized through an appropriate choice of the polymer electrolyte membrane. In this work we will show that one other elegant approach consists in looking for acetals tolerant cathode for the Oxygen Reduction Reaction (ORR).

All tests were conducted in an electrochemical cell in order to simulate the working conditions of an acetal fuel cell. Several different catalysts (Pt, Pt/C, PtRu/C, PtSn/C, and PtIr/C) where used to see their behavior in the instance of fuel crossover. The fuels used in this study were methylal, ethylal, 1,3-dioxolane, and for comparison, methanol. The latter will serve as a referral since acetals are not well documented. Cyclic

voltammograms and potentiostatic tests helped to determine the electrochemical properties and reaction kinetics of the fuels. Furthermore, the use of the HPLC (high performance liquid chromatograph) and the mass spectrometer, a semi-quantitative analysis of the products was made over a period of 10 000 seconds.

It was observed that the oxidation of the fuels (0,5M) on pure platinum electrode hindered greatly the process of the oxygen reduction. When adding methylal in presence of oxygen, the oxygen reduction reaction (ORR) onset potential would drop from 1,00V/RHE to 0,41V. Using éthylal, 1,3-dioxolane and methanol, we come to the same conclusions since we obtain ORR potentials of 0,47V, 0,44V and 0,77V respectively for each fuel.

When platinum electro-catalyst dispersed onto carbon (Pt/C) was used, we obtained an ORR onset potential of 0,91V without any fuel. However, in the presence of methanol, the onset potential dropped to 0,69V. In the presence of ethylal the onset potential is was 0,56V. This onset potential was 0,51 and 0,41 when 1,3-dioxolane and methylal respectively used. When electro-catalyst based on platinum-ruthenium dispersed onto carbon (PtRu/C) as a catalyst, we find that methanol yield the highest ORR onset potential among all fuels with 0,54V. The acetals exhibited the ORR onset potentials of 0,47V, 0,42V and 0,41V for 1,3-dioxolane, ethylal and methylal respectively. In the case of PtIr/C based electro-catalyst, it is observed that methylal yields the highest ORR onset potential with 0,70V, followed by methanol 0,56V, 1,3-dioxolane 0,53V and ethylal 0,47V. Overall, it is noticed that the ORR is affected by the nature of the fuel as

well as that of the catalyst. Consequently, on Pt/C, the presence of methanol is the least harmful to the ORR, as for PtRu/C and PtIr/C, it is the respective presence of methanol and methylal that are the least harmful.

The variation of the acetal oxidation peak with the difference of the atomic radius of the alloying element and that of platinum (ΔR) was shown. A volcano plot of the oxidation peak current with (ΔR) was obtained. It was established that with PtIr/C, with a ΔR close to 3Å, we obtained the lowest oxidation peaks currents. While establishing a parallel between the onset potentials of the ORR and the nature of the catalyst, it seems that catalysts with ΔR near 3Å yielded the highest onset potentials. However this conclusion cannot be applied to 1,3-dioxolane since it was observed that the highest potentials were obtained with a ΔR value close to 0; indicated a more complex behavior related to the variation of the onset potential with ΔR.

The chromatographic and mass spectrometric methods were used to identify the elements which constituted the products of the electrochemical reactions. When methanol was used as fuel on Pt/C electro-catalyst, it seemed that only methanol was detectable as reaction product. However, when methanol used on PtRu/C, PtIr/C or PtSn/C, the presence of formaldehyde was detected as reaction product. When Methylal, ethylal and 1,3-dioxolane were used as fuel in the cell, quantities of formaldehyde were detected as reaction products on all catalysts tested. On the other hand, when

1,3-dioxolane was the fuel on a binary all the alloyed electro-catalyst, formic acid was detected.

In conclusion, we observe that among all catalysts used, the Pt/C based electro-catalyst is the cathode which exhibited the smallest onset potential. In a similar way, it was shown that the lowest onset potentials were obtained when PtIr/C catalyst was used as electro-catalyst for ethylal and 1,3-dioxolane fuels. The onset potential of methanol contacting the electro-catalyst cathode is higher on Pt/C than all the other binary electro-catalyst, indicating that the ORR might be less affected by the presence of this fuel in the case of Pt/C.

At the end of the document we listed the recommendations which will help to improve the development of direct acetal fuel cells.

CONDENSÉ EN FRANÇAIS

En ce début de 21^{ième} siècle, nous nous confrontons au problème du réchauffement de la Terre. Depuis des années déjà, on entend dire que nos émissions de gaz à effet de serre augmentent sans cesse, mettant ainsi en péril le fragile équilibre de l'atmosphère terrestre. Les émissions provenant des voitures restent à ce jour l'un des principaux facteurs du réchauffement de notre planète. Les immenses marchés économiques en expansion comme, l'Inde et la Chine vont contribuer à faire accélérer le processus de réchauffement déjà entamé. On se doit de trouver une alternative qui saura réduire ou prévenir ce phénomène. Des normes de réglementation tels les protocoles de Kyoto sauront sûrement nous diriger dans la bonne direction. Depuis plus de cent ans, les automobiles sont essentiellement propulsées à l'aide du moteur à combustion. Les piles à combustible semblent présentement offrir une partie de la solution, en remplaçant les présents moteurs pollueurs et moins efficaces. Heureusement, la voie optant pour les piles à combustible semble prendre de l'ampleur en voyant que des milliards de dollars sont investis dans la recherche par des gouvernements et des corporations à travers le globe. Au centre de ce domaine de recherche, les piles à combustible carburant à l'hydrogène semblent prometteuses puisqu'elles ne produisent que de l'eau. Or, en portant un regard sur l'ensemble de cette technologie, on s'aperçoit que l'usage de l'hydrogène pose quelques obstacles. Les principaux inconvénients de l'utilisation de l'hydrogène sont directement reliés à son entreposage ainsi qu'à l'infrastructure de distribution. Une approche qui permettrait de résoudre le problème consisterait à utiliser le méthanol. Ce dernier, qui est liquide, offre l'avantage de ne pas avoir à altérer

le système de distribution actuel de l'industrie pétrolière. Mais comme le méthanol est considéré toxique pour l'être humain, de nouveaux combustibles ont été investigué. Par exemple, des chercheurs de la NASA ont proposé pour la première fois d'utiliser les acétals comme combustibles. Des recherches liées à ce sujet ont été développées en détail au Laboratoire de nouveaux matériaux pour l'électrochimie et l'énergie de l'École Polytechnique de Montréal. Les résultats préliminaires obtenus semblent indiquer une plus grande puissance électrique des piles à combustible aux acétals comparativement à celle des piles à combustible au méthanol. L'objectif de ce présent travail consiste à poursuivre l'étude de la viabilité et de l'amélioration de la pile à combustible à consommation directe d'acétals. Notre attention se portera plus précisément sur l'effet des acétals sur la performance des cathodes pour la réaction de réduction de l'oxygène.

Les études ont été faites en utilisant une cellule électrochimique dans un montage à trois électrodes. La cellule électrochimique est constituée d'une électrode de travail (le site des réactions), d'une contre électrode (collecte du courant), d'un électrolyte de support et d'une électrode de référence (servant à jauger le potentiel). Dans la cellule, nous introduisons un électrolyte de référence constitué d'acide sulfurique 0.5M afin d'assurer la mobilité des ions. Aussi, afin de bien simuler les conditions cathodiques de la pile à combustible, nous saturerons la solution d'oxygène. De plus, la configuration de la cellule, nous permet de permuter les électrodes de travail afin d'en changer la nature.

Nous avons aussi utilisé la voltammetrie cyclique pour caractériser les réactions d'oxydation et de réduction dans la cellule électrochimique. Le voltammétrie peut être utilisée de diverses manières. L'une d'entre elle consiste à balayer le potentiel entre deux bornes et d'en mesurer le courant. C'est de cette façon qu'il est possible de déterminer les potentiels d'oxydation ou de réduction des espèces en solution. De plus, on peut découvrir le courant associé à chacun de ces pics. L'évolution de l'adsorption/désorption d'hydrogène et de la réduction de l'oxygène est aussi possible grâce à ce dispositif. Nous avons aussi utilisé le mode potentiostatique qui consiste à appliquer un potentiel et à mesurer le courant en fonction du temps. De tels essais permettent de déterminer la composition chimique des produits de réaction en fonction du temps.

Le chromatographe liquide à haute performance a été utilisé pour déterminer la nature et la quantité des produits en solution après 10 000 secondes. Cette méthode d'analyse est bien indiquée pour ce type d'étude parce que son principe est basé sur la détection des temps de rétention des produits à travers une colonne. Ainsi, les produits analysés sont identifiés et classifiés à leur sortie d'un détecteur en fonction de leur temps de rétention dans la colonne. Le spectromètre de masse peut parvenir aux mêmes conclusions que le chromatographe. Or, son fonctionnement en est totalement différent. On se doit d'injecter un échantillon dans une chambre sous vide. Grâce à un bombardement d'électrons, les produits sont fractionnés en ions. Ces mêmes ions traversent un champ magnétique suivant une trajectoire d'un demi-cercle. Ce processus permet de classer

les produits relativement à leur poids et à leur électronégativité. Ainsi, chaque produit présente une signature distincte et leur quantification devient possible grâce à l'utilisation de référence. Afin de maximiser la puissance d'analyse, nous avons couplé le chromatographe à un spectromètre de masse. De cette manière, il sera possible de dissocier les produits afin de les quantifier plus précisément grâce au spectromètre de masse. Dans le présent montage, un tel arrange était toutefois impossible à réaliser.

Au cours de nos études, nous utilisons le méthylal, l'éthylal, le 1,3-dioxolane et le méthanol comme combustibles sous différentes conditions expérimentales. Les résultats obtenus avec le méthanol ont été utilisés comme référence parce que les résultats obtenus sur les acétals sont très peu documentés. La première étape a consisté à étudier la réaction de réduction de l'oxygène et le voltamogramme obtenu est pris comme référence. La réalisation de la courbe voltamétrique de la réaction de réduction de l'oxygène des électrodes de platine lisse à une vitesse de balayage de 5mV/sec a permis de déterminer le potentiel de début de la réaction de réduction de l'oxygène (*onset potential of the oxidation reduction reaction - ORR*) à 1,00V.

Lorsque le platine lisse est utilisé comme électro-catalyseur en contact de 0,5M de méthylal comme combustible en présence d'oxygène on voit que l'oxydation de ce dernier est favorisée au détriment de la réduction de l'oxygène. On peut aussi conclure que le potentiel de début de réduction de l'oxygène chute à 0,41V. Aussi, on constate que le courant de réduction de l'oxygène est environ le dixième de celui obtenu sans

méthylal. En comparant les courbes de polarisation de cette interface en présence de l'oxygène ou de l'azote, on voit que la réaction liée à la décomposition du méthylal est plus intense lorsque l'oxygène n'est pas présent. L'effet de l'oxygène sur la réaction d'oxydo-réduction de l'éthylal est similaire à celle du méthylal. Le potentiel de début de réduction de la réaction de réduction de l'oxygène est de 0,47V. En ce qui concerne le 1,3-dioxolane et le méthanol, le début de réduction de l'oxygène est respectivement à 0,44V et 0,70V en leur présence. Pour une même concentration donnée, il semble que c'est le 1,3-dioxolane qui s'oxyde le plus en présence d'oxygène; ensuite vient l'éthylal, le méthanol et le méthylal. Ces résultats montrent que le méthanol semble être le combustible qui est moins nuisible à la réaction de réduction de l'oxygène.

Dans le cas où l'électro-catalyseur est à base d'une électrode de platine dispersé dans une poudre de carbone (Pt /C), on peut observer un effet de double couche beaucoup plus prononcé que sur le voltamogramme de référence d'une électrode de platine lisse. En présence d'une atmosphère saturée d'oxygène, on remarque que le début de la réduction de l'oxygène est 0,91V, ce qui est 0,09V plus faible que celui obtenu sur le platine pur. Si le 1,3-dioxolane est utilisé comme combustible, cette valeur tombe à 0,51V, dans le cas du méthylal elle tombe à 0,41V; alors que pour l'éthylal est de 0,56V et 0,69V pour le méthanol. La comparaison des voltammogrammes obtenus avec les différents acétals en présence de l'oxygène sur les catalyseurs de PtRu/C et de Pt/C montre que les pics d'oxydation sont plus faibles et larges pour PtRu/C, et que leurs potentiels sont à des valeurs plus faibles. De plus, on constate que le méthanol offre le

potentiel de début de réduction le plus élevé avec 0,54V. Avec l'électrode de Pt-Ru, l'utilisation du 1,3-dioxolane, de l'éthylal ou du méthylal qui ont respectivement des potentiels de début de réduction de l'oxygène de 0,47V, 0,42V et 0,41V. Le dernier des trois catalyseurs étudiés est le PtIr/C. Avec ce catalyseur, on remarque que le méthanol s'oxyde le moins en présence de l'oxygène, or c'est le méthylal qui offre le potentiel de réduction de l'oxygène le plus élevé avec 0,70V, suivi du méthanol (0,56V), du 1,3-dioxolane (0,53V) et de l'éthylal (0,47V). En résumé, la réaction de réduction de l'oxygène est influencée par la nature du catalyseur et le type de combustible utilisé. Sur le platine lisse, le potentiel du début de la réaction de réduction le l'oxygène est optimum en présence du méthanol. Sur les catalyseurs Pt/C, PtRu/C et PtIr/C le potentiel de réaction de la réduction de l'oxygène est optimum en présence de 1,3-dioxolane, du méthanol, et du méthylal respectivement pour chacun des trois catalyseurs.

La hauteur des pics d'oxydation du combustible est aussi liée à la valeur du potentiel de début de réduction de l'oxygène. D'autre part, la variation de la densité de courant des pics d'oxydation de chaque combustible avec la différence entre le rayon atomique de l'élément d'alliage et celui du platine (ΔR) donne des courbes en forme de volcan. On observe que les sommets les plus faibles sont obtenus avec un ΔR avoisinant 3Å. De plus, c'est le catalyseur PtIr/C qui donne les plus faibles courants d'oxydation en présence d'oxygène. L'effet volcano est aussi observable lorsqu'on trace les potentiels de début de la réaction de réduction de l'oxygène en fonction de ΔR, en présence de

chaque combustible. On remarque qu'avec le méthylal et l'éthylal, les potentiels les plus élevés sont obtenus avec le catalyseur PtIr/C, c'est-à-dire avec un ΔR de 3 à 4Å. Le méthanol semble avoir un effet « volcanique » plus faible étant donné que pour les catalyseurs de PtIr/C et PtRu/C on obtient des potentiels similaires. Le 1,3-dioxolane semble échapper à la règle car on obtient plutôt une droite linéaire par conséquent, plus la différence de rayon atomique est grande, plus on observe des potentiels faibles.

Dans la dernière partie de cette étude, nous avons déterminé les produits de réaction pour chacun des catalyseurs en fonction des combustibles utilisés en présence d'oxygène. Ces produits ont été d'abord été déterminés avec Pt/C. Pour les acétals on retrouve comme produit de réaction intermédiaire du formaldéhyde. C'est avec le méthylal qu'on a détecté le plus de formaldéhyde. Si on utilise le méthanol comme combustible, on ne retrouve aucun autre produit de réactions autre que le méthanol. En utilisant le PtRu/C comme catalyseur, on retrouve le formaldéhyde pour chacun des combustibles utilisés, incluant le méthanol. En plus, pour le 1,3-dioxolane, on peut noter la présence d'acide formique. L'utilisation du méthylal comme combustible semble conduire à plus de produits intermédiaires, suivit du 1,3-dioxolane, de l'éthylal et du méthanol. Avec le catalyseur PtIr/C, on trouve du formaldéhyde lorsque chacun des quatre combustibles est utilisé. En plus avec le 1,3-dioxolane, on dénote la présence d'acide formique. C'est avec le 1,3-dioxolane qu'on obtient le plus de produits intermédiaires. L'utilisation du catalyseur à base de PtSn/C conduit aux produits de réactions semblables à ceux obtenus avec les autres alliages binaires. C'est-à-dire qu'on retrouve

du formaldéhyde pour tous les combustibles, et en plus de l'acide formique est produit lorsque le 1,3-dioxolane est utilisé comme combustible. En tenant compte de la combinaison des matériaux d'électrodes et de combustible, le 1,3-dioxolane et l'éthylal produisent le plus de produits de réactions intermédiaires.

Ce travail se termine avec l'étude de l'effet du combustible sur le type de catalyseurs. Dans le cas du méthylal, on observe que la plus grande production de formaldéhyde est obtenue en présence de PtRu/C. Lorsque le méthylal est toujours utilisé comme combustible, c'est avec le Pt/C qu'on mesure la plus grande quantité de méthylal produit après 10 000 secondes de fonctionnement de la cellule. On peut aussi dire que c'est en présence de PtIr/C qu'il semble que la réaction de réduction de l'oxygène en présence de méthylal se produit le plus rapidement. En se basant sur les valeurs des potentiels de début de réduction de l'oxygène et du pic d'oxydation du combustible, on observe que dans le cas de l'éthylal comme combustible l'activité de la réaction de réduction de l'oxygène diminue lorsqu'on passe de PtIr/C, PtSn/C, PtRu/C à Pt/C, respectivement L'utilisation du 1,3-dioxolane comme combustible semble produire de l'acide formique en plus du formaldéhyde en présence de catalyseur à alliage binaire. C'est avec le PtIr/C qu'on obtient une activité de réaction de réduction de l'oxygène est la plus faible possible, suivit du PtRu/C, du PtSn/C et du Pt/C, respectivement. L'utilisation du méthanol combustible semble produire des résultats similaires en utilisant les catalyseurs binaires. Avec de tels catalyseurs, la réaction de réduction est moins prédominante qu'avec un catalyseur de Pt/C.

Suite aux résultats obtenus dans ce travail, les recommandations suivantes peuvent être suggérées afin d'accélérer le développement de ce type de piles :

i) Il faudrait corroborer l'ensemble des résultats ci-dessus à la nature et la quantité des espèces intermédiaires. Ceci peut se faire en reliant le spectromètre de masse, le chromatographe à phase liquide à une cellule électrochimique afin de mieux quantifier et de détecter les produits de réaction contenus dans l'électrolyte. Le spectromètre de masse peut aussi être couplé directement à la cellule électrochimique afin de mieux détecter les espèces produites. L'emphase devrait aussi être portée sur l'automatisation de l'échantillonnage qui servirait à injecter le liquide directement dans le chromatographe, permettant ainsi d'accélérer le processus.

ii) Il faudra utiliser le FTIR (*Fourier Transform InfraRed*) pour déterminer les intermédiaires réactionnels. Les résultats obtenus avec ces différentes analyses donneraient des indications sur les espèces adsorbées à la surface du catalyseur

iii) Afin de permettre l'optimisation de la composition des catalyseurs, il faudra faire des expériences en fonction de la fonction de la température d'opération, la concentration du combustible et du pH de l'électrolyte et la composition du catalyseur;

iv) Des études devraient aussi être effectuées en fonction du type de catalyseur avec de nouvelles combinaisons de matériaux;

v) Finalement, les tests devraient être faits dans une vraie pile à combustible afin d'évaluer les effets de ces améliorations sur la cathode.

TABLE OF CONTENTS

LIST OF FIGURES

LIST OF TABLES

LIST OF NOTATIONS AND SYMBOLS

CCD: Charge-Couple Device

DOFC: Direct Oxidation Fuel-Cell

DMFC: Direct Methanol Fuel Cell

DMM: Dimethoxymethane (methylal)

FTIR: Fourier Transform Infrared

GC: Gas Chromatography

GCNF: Graphitic Carbon Nanofiber

HPLC: High Performance Liquid Chromatograph

MEA: Membrane Electrolyte Assembly

MeOH: Methanol

MOR: Methanol Oxidation Reaction

MS: Mass spectrometry

ORR: Oxygen Reduction Reaction

P1: Positive scan fuel oxidation peak

P2: Negative scan fuel oxidation peak

PBI: polybenzimidazole

RHE: Reversible Hydrogen Electrode

SCE: Saturated Calomel Electrode

SEIRAS: Surface-Enhanced Infrared Absorption Spectroscopy

TEM: Transmission Electron Microscopy

TMM: Trimethoxymethane

TON: Turnover Number

WE: Working Electrode

XRD: X-Ray Diffraction

XPS: X-ray photo electron spectroscopy

$_{ad}$: Adsorbed specie

INTRODUCTION

Global warming is still increasing with the growing utilization of the fossil fuels for transportation in particular. Scientists worldwide are currently debating the long term effects of this problem. If nothing is done to slow down the emissions of green house gases in the Earth's atmosphere, the world's fragile ecosystem could be less hospitable for future generations. From the present standpoint, with the ever growing demand for fossils fuels, the future doesn't look so bright. China's new open market politics will have a large scale impact because of its population growing need of energy and transport systems. If appropriate regulations are not found, the increase of the fossil energy will further degrade the world ecosystem. But with international regulations like the Kyoto Protocol, we can hope that they can steer us to achieve our goals of reducing the green house gases. The transportation systems used worldwide until now are based on the internal combustion motors. A cleaner approach is now being proposed: the powering of automobiles by fuel cells. Currently this optimistic route seems to gain popularity because billions of dollars are being invested in this field of research by major car companies and by governments around the world.

At the core of this research field, fuel cells powered by hydrogen seem very promising because their byproducts consist only of pure water. But if we look on a larger scale of this precise technology, we can observe that hydrogen fuel utilization has serious limitations. The principal disadvantages of using hydrogen are related to the fabrication, the storage of gaseous hydrogen and the lack of the distribution infrastructure. One of

the approaches to solve those problems is to replace hydrogen by methanol as a fuel. Methanol, which is a liquid fuel, offers the big advantage of not altering the current system of gasoline distribution. Unfortunately the methanol electrooxdiation process involves more complex reaction steps thus resulting in lesser power output. Novel sources of energy have since then been looked into. In the present case, it is worth mentioning the innovative research of NASA's Jet Propulsion laboratory[1] which proposed the utilization of acetals as a fuel for PEM fuel cell applications. In our laboratory of New Materials of l'École Polytechnique de Montréal, Savadogo and Yang[2, 3] pursued this promising approach. The preliminary results of their studies showed greater power generation compared to the direct methanol fuel cell (DMFC).

The main goal of this work is to further study the possibility of using acetals as liquid fuels for PEM fuel cell applications. The work initiated in our laboratory was based on the optimization of the acetal fuel cell power output. This work was continued in the master thesis of Yanick Cyr[4], which was on the effect of various catalyst combinations on the optimization of the fuel cell performances for various acetals. The main objective of this work is to study the oxygen reduction reaction (ORR) and the effect of acetal crossover on the performance for various electrocatalysts.

In the first part, we will show a concise literature review in which we will cover several important subjects which may help in understanding the core of the project. This part includes an abstract on principals of fuel cells, the techniques used to investigate fuel cell

performances and an overview of catalyst issues for the electro-oxidation of PEM cells using light organic fuels. The second part will be devoted to the experimental procedures. It includes the experimental setup, electrode fabrication, cyclic voltammetry, high performance liquid chromatography, mass spectrometry, and experimental procedures for MEA preparation. The third part focuses on the results and discussion. The discussion will cover the analysis of the experimental results of various cyclic voltammograms taken under different conditions to the effect of the cathode catalyst and the fuel compositions. Results from the mass spectrometer analysis and the HPLC will be used to include conclusions on the composition of the reaction products of the electrolyte under simulated working conditions. A thorough conclusion will summarize all the different observations that were made during the study of the behavior of the acetals in the fuel cell's cathodic compartment. Finally, the work will end with several recommendations that could serve as a guide to help further the research relative to the present work.

CHAPTER 1

LITERATURE REVIEW

This present study is the continuation of the ongoing project of acetals fuel cells at l'École Polytechnique de Montréal. My predecessor Yanick Cyr's memoir : "*Mise au point d'une pile à combustible à consommation direct d'acétals liquides*"[4] focused on of the viability of acetal fuel cells. In this present project, we will study the reactions and the interactions of cathodes catalysts with methanol and acetals in the fuel cell. The subject of methanol will be covered in this work because it will serve as a reference for the new and not yet well documented field of acetal fuels.

1.1 History

In a general consensus, Sir William Grove is thought to be the father of the fuel cell dating back to 1839.[5] Around the same time Volta's pile was invented, Schoenbein was the first to publish results about the 'fuel cell effect'. During lectures in France and Switzerland in the summer of 1838[6, 7], he demonstrated that a voltage and current could be obtained from a hydrogen/oxygen chain. But no longer than one month later, Grove wrote a paper with similar conclusions.[8] In spite of this tardiness, Sir William Grove is recognized as the inventor of the fuel cell because he was the first person who presented it as an electricity generator. It wasn't until 1845 that he published an article about the complete fuel cell electricity generator[9], marking the starting point of fuel cell technology. Later on, other researchers, such a Walter Nernst who is famous for his

equilibrium potential in ionic solution, furthered the study of this promising field. But the progress of their combined research was slow because their main focus was on determining equilibrium thermodynamics, not investigating the kinetics of the reaction, and their search was also hindered because no better catalyst than platinum could be found. It wasn't until Francis Thomas Bacon's pioneer work with NASA's Apollo space mission in 1968 that we could see for the first time a tangible application for the fuel cells. Despite those promising results, since this fuel cell worked with potassium hydroxide solution, ultra-pure hydrogen was needed to make the fuel cell work properly. Therefore, the transfer of fuel cells never made it to the commercial market up to this date because of the difficulty and the costs related to pure hydrogen production. Gladly, in the 1990's, the Canadian company Ballard Power revived the hope of seeing a fuel cell marketed with their improved DMFCs. Since then, major companies around the world have been investing time and money to research this now promising technology in the hope of seeing soon a first breakthrough of fuel cells in the global market. The future applications of fuel cells will span across three major branches: the car market, portable electronics and power generators for private of public needs.

1.2 Techniques for studying fuel cells

The study of fuel cell can be very complex. For example, it took scientists around three decades to fully understand the methanol oxidation reaction on platinum. So it is important to stress that research can only move forward faster if people work in closer relation and use similar techniques.

1.2.1 Techniques for studying reactions

The study of fuel cells requires using several different techniques. Modern instrumental tools for analytical chemistry are being listed in Wasmus et al. article.[10] Among theses several techniques, programmed current or programmed voltage electrochemical methods can be cited as the first foremost useful methods for analyzing fuel cells. Theses powerful techniques can help us understand the electrical aspect of the working fuel cell. The listing of their every possible usage will not be discussed here because they are too numerous. Our attention will be brought upon those who can help us learn about the reactions that occur in the cell. Only then, with both of theses classes of instruments, can a proper comprehension of fuel cells can be achieved.

We will start off by discussing gas chromatography (GC). In steady state studies, reactions products can be clearly and precisely identified with GC.[1] But given the fact that GC requires several minutes to analyze the products of the electrochemical reaction, it cannot therefore be used successfully in real-time monitoring conditions. To overcome this problem, infra-red (IR) techniques have been used. On-line Fourier Transformed Infra-Red (FTIR) spectroscopy is commonly used for studying the products in a real-time environment. Research groups have been using on-line FTIR for determining the products of the methanol oxidation reaction under different conditions.[11] This technique can also be used according to two different modes in order to detect either absorbed species or species that are in the electrolyte. FTIR has been used to study several aspect of the fuel cell, such as the cathode exhaust products.[12] But also, it was

a key element for determining the oxidation steps of the methanol oxidation reaction (MOR).[13] In 1996, Fan, Q. et al. reported, with the *in situ* FTIR, the presence of absorbed CO on a Pt-Ru anode.[14] These same conclusions have been confirmed later on by other groups.[15] In reference to acetals, other papers have cited the usage of FTIR for studying methylal and it's conformers,[16, 17] and the ring opening reaction of 1-3,doxolane[18]. But, as reported by Fan's research group, FTIR has some limitations for detecting certain species when the signal is lost in the background noise[19]. To overcome this problem, Miki, A et al. have pushed the limits of this technique reaching signals 30 to 75 times higher than FTIR with the surface-enhanced infrared absorption spectroscopy (SEIRAS).[20]

The mass spectrometer (MS) also greatly contributes to the study of the products of the fuel cell. Complementing the findings done by FTIR, the mass spectrometer helped researchers to achieve their goal of determining the MOR.[21] The work of Jusys and Behm have led to establish an on-line mass spectrometry technique by solving the mass transport problem of the old system.[15] Later on, others have reused this novel technique to further the study of methanol oxidation in a direct methanol fuel cell.[22]

1.2.2 Techniques for studying the catalyst

In essence, the electrochemical reactions happening in the fuel cell all depend on the nature and morphology of the catalyst. To better understand the effect of these

parameters on the reactions, we need to be able to analyze the catalyst at the atomic scale. Methods using X-ray radiation have proven to be very useful for characterizing the catalyst, the support, and the electrodes. X-ray diffraction (XRD) and X-ray photo electron spectroscopy (XPS) have the advantages of giving information concerning the crystallinity, the particle size, the composition, among others. For example, XRD and XPS have been used to study the alloying of Pt-Ru, the preferred structure, the particles sizes, and they even detected a $RuO_2 \cdot xH_2O$ species with the help of XPS and it's specific binding energy.[23, 24] The characterization of the catalyst can be done via transmission electron microscopy (TEM). TEM, on top of giving information on the size of the particle and its crystallinity, it can also be very useful for determining the surface area and the particle shape.[23]

Table 1.1: Summary of techniques used for general electrochemical catalysis research and for the characterization of fuel cell components

Technique	Subject of investigation	Advantages	Disadvantages
In-situ FTIR	Products and adsorbed species formed at smooth electrodes	Detection of volatile and non-volatile products	Restriction to smooth electrodes with sufficient reflectivity and to liquid electrolytes
		Identification of adsorbed species	Sometimes significant *IR*-drop in experimental setup due to thin layer techniques
		Separation of adsorbed and non-adsorbed species using IR-light of different polarization	Potential sweep techniques are difficult
			Difficult adjustment of electrochemical cell and optical system
			Electrodes need frequent polishing
Differential Electrochemical Mass Spectrometry (DEMS)	Volatile products formed at sputtered, lacquer-type and, in some cases, technical electrodes	Detection of volatile products using galvanostatic, potentiostatic and potential sweep methods	Restriction to liquid electrolytes
		Separation of overlapping electrode processes and reaction pathways	No detection of non-volatile products
			Sweep rates of less than 50 mV s^{-1}
			Simultaneous formation of a larger number of products may lead to overlapping of mass signals
			No ready-to-use setup is available on the market for analytical instrumentation

Table 1.1 (*continued*)

X-ray radiation methods (e.g. XRD, XPS and EXAFS)	Characterization of technical electrodes	Qualitative and, under certain conditions, quantitative analysis of catalyst or support surface composition	Quantitative analysis needs careful calibration
		Different elements can be studied separately from each other	Sensitivity to contamination
		In some cases, the oxidation/bonding state of elements can be determined	Sometimes difficult interpretation (especially EXAFS, see Refs [177,178])
Transmission Electron Microscopy (TEM)	Characterization of technical electrodes	Determination of particle size and shape	Substrate must be electronically conductive
			Sensitive to electrostatic charge
FTIR	Characterization of technical electrodes	Nature of surface groups can be determined	Weak sensitivity due to strong IR-absorption of carbon materials
			Not suited to all types of carbon
Electrochemical Impedance Spectroscopy	Characterization of technical electrodes	Electrode structure and kinetic parameters can be determined	Equilibrium conditions are required
		Fully automated setups including complete software package are readily available	Sensitive to artefacts
			Frequently used concept of equivalent circuits may not always work for data analysis
Multi-Purpose Electrochemical Mass Spectrometry (MPEMS)	Volatile products formed at sputtered, lacquer-type and technical electrodes including fuel cells	DEMS mode with sweep rates of up to 1000 mV s^{-1}	Simultaneous formation of a larger number of products may lead to overlapping of mass signals
		Detection of volatile fuel cell reaction products	No ready-to-use setup is available on the market for analytical instrumentation
		Setup can be adapted to other non-electrochemical applications with minimum reconstruction	

Technique	Subject of investigation	Advantages	Disadvantages
On-line FTIR	Volatile products formed in fuel cells	Detection of volatile fuel cell reaction products	No ready-to-use setup is available on the market for analytical instrumentation
		Complementary to MPEMS due to the possibility of product identification in cases where MPEMS shows problems with fragment overlapping	
FTIR Diffuse Reflection Spectroscopy	Volatile products and adsorbates formed in fuel cells	Volatile products and adsorbed intermediates can be studied under fuel cell conditions	
NMR-spectroscopy	Polymer electrolytes	Reactions within the polymer matrix can be studied	Sample preparation is critical for reproducible results
		Identity and behavior of sorbed species can be investigated	Complex and expensive instrumentation in the case of solid-state-techniques
		Sorbed species and polymer matrix can be studied separately	
		In case of solid-state-techniques, even non-mobile phases can be investigated	
Thermogravimetric Analysis (TGA) and related techniques (TGA/MS and TGA/FTIR)	Polymer electrolytes	Thermal stability of polymer electrolytes can be assessed	Care has be exercised for applying the results of TGA measurements to long term stability
		In case of TGA/MS and TGA/FTIR, even a thermal degradation mechanism can be established	
		Relatively simple techniques suitable for routine investigations	
		Instrumentation readily available	

Here above, in Table 1.1 taken from Wasmus, S. et al. article "*Methanol oxidation and direct methanol fuel cell : a selective review*",[10] we can view a summary of different techniques used for the characterization of the fuel cell. This table was made to guide people in selecting the proper techniques required for their own research. By consulting the advantages and disadvantages list, they can then choose according to their own needs.

1.3 Catalysts overview

The choice of the nature and crystallography of the catalyst is a crucial decision in designing a fuel cell. A lot of details have to be considered during the conception phase.

1.3.1 Platinum catalyst

The very first catalyst used and studied was pure platinum. Platinum has proven to be a reasonably good catalyst for the hydrogen/oxygen fuel cell. But using the same catalyst in a direct methanol fuel cell, Pt became poisoned by CO_{ad} species on its surface, thus greatly affecting the long term performances of the DMFCs.[14, 15] Thermodynamically, the MOR occurs at 0.016V. But this reaction is hindered by the CO poisoning resulting for intermediate species formation. The MOR onset is coupled with CO removal and the formation of hydroxyl on Pt sites, resulting in a greater overpotential. At higher potentials, the PtO formation limits the reaction. [21] Also, these authors discussed the fundamental difference between the usage of Pt smooth surface and Pt high surface area. According to the study of Jusys, Z. et al. on the MOR, the formation of formaldehyde

(H_2CO) and formic acid (HCOOH) are preferred in the first case, and the complete oxidation to CO_2 is dominant in the later one. We can make a correlation between the type of surface and the loading of Pt in electrode. According to Figure 1.1 below, using a loading of $2\mu g/cm^2$ yields formaldehyde that accounts for 65% of formed species, and with higher loading of $10\mu g/cm^2$ the main product is CO_2 (80% of formed species).

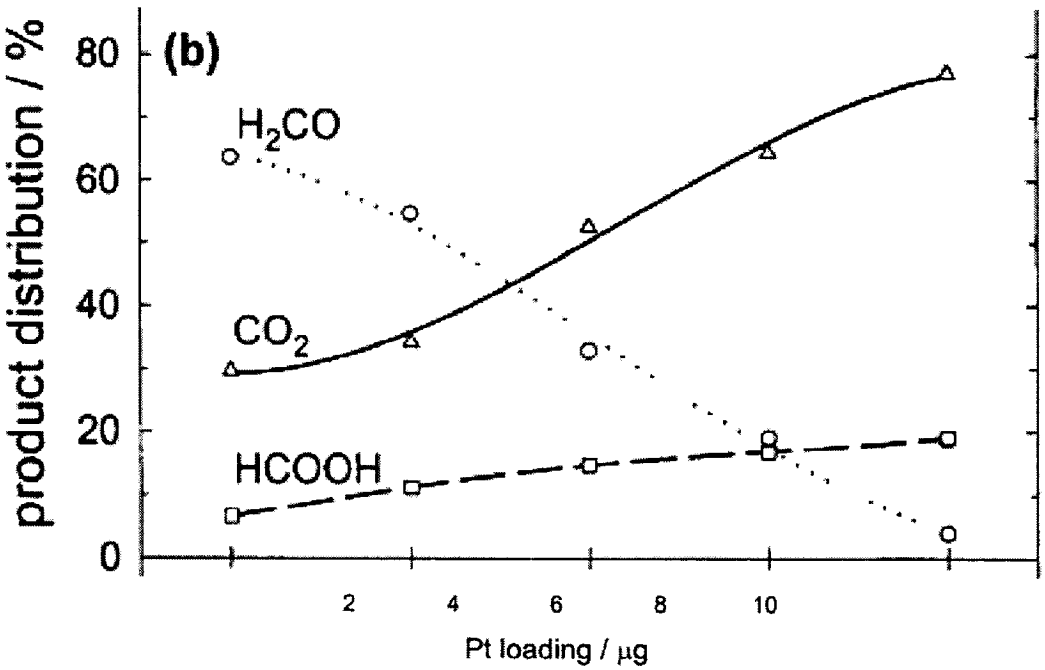

Figure 1.1: Product distribution for potentiostatic electrooxidation of methanol on Pt/Vulcan thin-film electrode in 0.5 M H2SO4 solution containing 0.1 M CH3OH at 0.61 V (data from Figure 6) as a function of Pt quantity (geometric area, 0.28 cm^2).

1.3.2 Pt-Ru catalyst

Since Pt is a costly precious metal, steps have been taken towards alloying Pt for the purpose of lowering its loading, and thus reducing the production costs for this MOR catalyst. The most popular approach is using Pt-Ru catalyst. A study by Vijayaraghavan, G. et al.[13] clearly showed the advantages of using such a catalyst instead of pure Pt. From their voltammetric study, on Pt/C the peak associated with CO_2 formation appeared around 0,8V vs. reference hydrogen electrode (RHE), and started to be important around 1,2V. For PtRu/C (30%Pt, 15%Ru) this band appeared strongly a 0,5V at 23°C, and at 60°C the peak drops to 0,30V. Clearly, from these results, we can conclude that PtRu/C is better adapted for the MOR. This bifunctional approach can be explained as using a second element (e.g. Ru) to help start initiate the oxidation of the CO and CHO molecules by activating water (forming OH species) at as low potential as possible with only Pt catalyst.[22, 25] The oxygenation species (Ru-OH) convert the CO (triple bond) to CO_2, and this intermediate step, being slow, determines the rate of the reaction.[24] But having an alloyed metal can lead to unexpected results like Piela, P. et al. showed in the article "*Ruthenium crossover in direct methanol fuel cell with Pt-Ru black anode*".[26] They first noticed that ruthenium had a tendency to cross through the Nafion® membrane and redeposit at the cathode. This yields a lower capacity to reduce the oxygen and to handle methanol crossover. And depending on different working conditions, the cell performances can be lower by 40mV to 200mV.

Even more advancement in MEA design allows the fuel cell to run better with less catalyst, oxygen and fuel. And a great improvement can be observed from results published in 1995 through 1999 (Figure 1.2).[27] To attain those results, they had to feed the fuel cell with high concentrated oxygen. The authors reported that with oxygen supplement a power output of 250mW/cm^2 can be measured, but only 100mW/cm^2 is obtained with lower oxygen content. This truly shows the need to design catalysts which can work in more standard conditions, without sacrificing the performances.

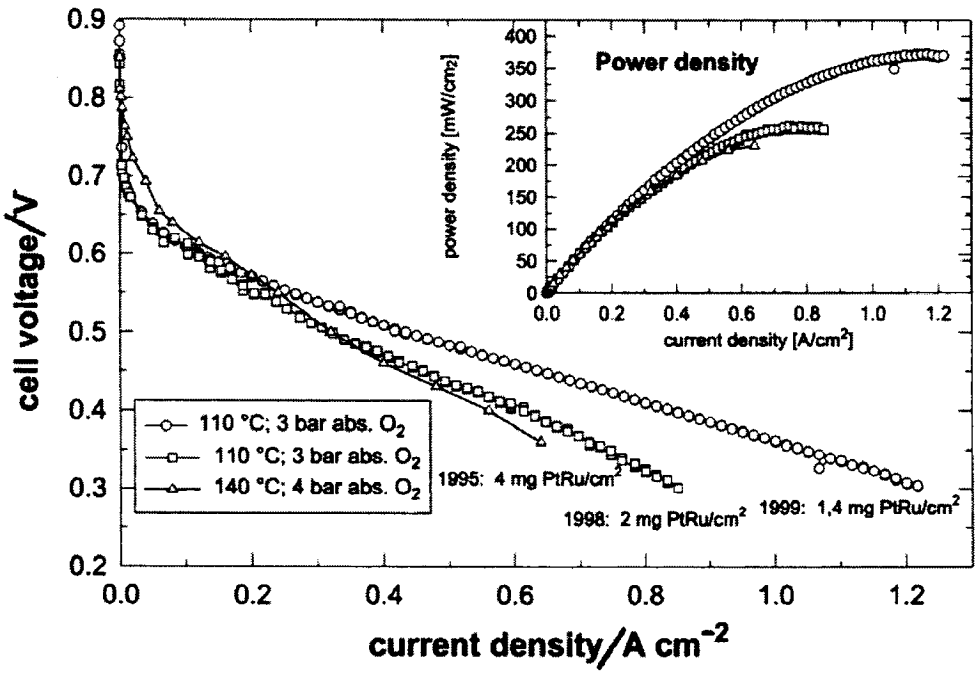

Figure 1.2: Voltage-current curves and power density plots (insert) of a 3cm² DMFC on oxygen operation.

One way to gain power is to better control the fabrication phase, resulting in a greater active surface area. It's one thing to obtain nanoscale particles, but it's much harder to obtain a normalized distribution of size the simplest way. In answer to this dilemma,

Coutanceau, C. et al. have proposed preparing Pt-Ru anodes by galvanostatic pulse electrodeposition.[23] Making variations of the ratio of metals in the solutions and changing the t_{off} (time off from 0,3s to 2,5s) with a t_{on} (time on) of 0,1s, they were able to draw conclusions to obtain certain catalyst composition at a certain particle size (Table 1.2). Results from the XRD show that this technique produces alloyed Pt-Ru catalyst.

Table 1.2: Electrodes preparation and characterization

Electrode	Pt/Ru atomic ratio in solution	t_{off} /s	Atomic ratio			Particle size /nm
			XRD	EDX	AAS	
PtRu 50-50	50/50	2.5	55/45	60/40	–	~7-8
PtRu 50-50	50/50	0.3	57/43	53/47	48/52	~5
PtRu 65-35	65/35	2.5	69/31	69/31	–	~7-8
PtRu 65-35	65/35	0.3	66/34	–	69/31	~5
PtRu 80-20	80/20	2.5	75/25	82/18	–	~7-8
PtRu 80-20	80/20	0.3	77/23	78/22	78/22	~5

Others have tried implementing the breakthrough of nanotechnology in the fabrication of catalysts. Using microwaves, almost perfectly spherical nanoparticles of Pt-Ru (4,5nm) have been synthesized. And after a heat treatment, great results have been obtained from this colloid catalyst.[28] While the synthesis of Pt-Ru/carbon fiber nanocomposites shows the importance of the carbon support lattice in obtaining a good catalyst performance.[29] Results prove that this catalysts, only containing 1,5mg/cm^2, can yield results equal to a catalyst with a loading of 2,7mg/cm^2 (Figure 1.3 a)). On the right side of this figure, a TEM micrograph shows the morphology of the herringbone GCNF (graphitic carbon nanofiber). It is also known that bulk and nano-scaled Pt-Ru produce different results because the bulk phase takes more time in converting CO to CO_2.[13]

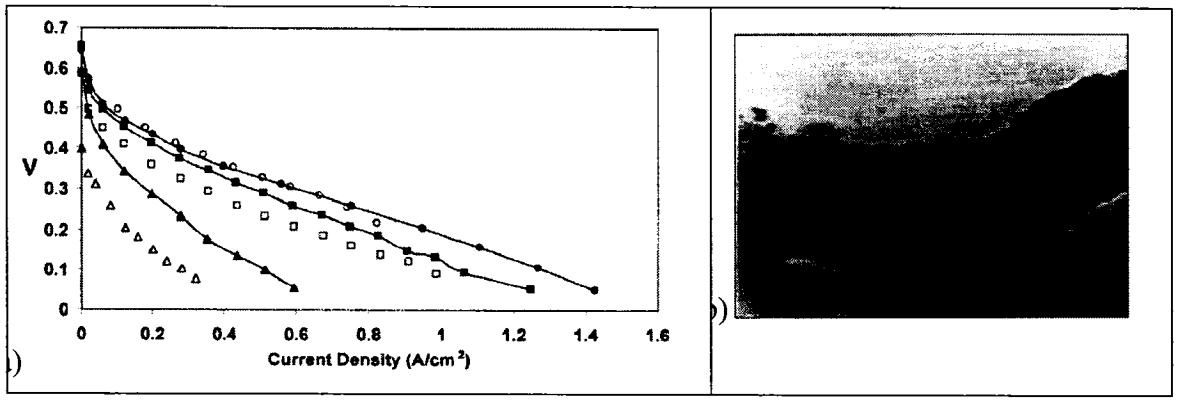

Figure 1.3: a) DMFC current density-voltage (V) curves comparing the performance of the herringbone GCNF (narrow) (connected data points) with that of an unsupported Pt-Ru colloid (unconnected data points) at anode catalyst loading of 2.7 mg total metal/cm2 (circles), 1.5 mg total metal/cm2 (squares), or 0.5 mg total metal/cm2 (triangles). b) bright-field TEM micrographs of the Pt-Ru/carbon fiber nanocomposites herringbone GCNF (narrow).

1.3.3 Binary and Multi-alloyed Pt bases catalyst

Over the years, the search for ever more performing catalysts has pushed scientists to consider using different alloys to reach their goals. But, as we have yet no solid theory which can help predict the best possible combination for a single fuel, the most common way to proceed is by trial and error. This method can be very time consuming. Luckily, novel methods have been developed to find the best matches in lesser time. One worth mentioning is a technique using a CCD (charge-couple device) camera with the help of quinine as a pH fluorescent indicator.[30] By using a matrix of different catalyst combination on a single plate, they are able to quickly find very active catalysts such as Pt_{90}/Sn_{10} and $Pt_{44}Ru_{41}Os_{10}Ir_5$. Also, the CCD camera is able to detect the poisoning

effect of the catalyst. Another research group talked about combining several known good catalysts and this has led to the finding of new promising catalysts. Comparing three catalysts, Pt/Ru(1:1), Pt/Ni(1:1), and Pt/Ru/Ni(5:4:1), they found out that the later one gave lowest onset potential and had a smaller activation energy for methanol oxidation. The better performance of this alloy can be attributed to change of the electronic of Pt by the presence of Ni.[31] Taking a step closer into comprehending the fundamental fuel and catalysts interactions, Yang, Y. et al. discussed the effect of the links between the alloyed metals.[32] With their phosphine linker and halide bridge between their metal centers, Ru/Pd and Ru/Pt complexes offer greater current densities than that of Ru mononuclear compound. As for the Ru/Au complex, it creates lower current densities because it possesses only a bidentate phosphine a dppm bridge between the Ru and Au centers.

All the above catalysts have the properties of working well in an acidic environment. It's worth mentioning that it is also possible to make the fuel cell work in an alkaline medium. Such an approach has a great advantage since the rate of reaction of methanol and oxygen is much higher in the alkaline medium than that in acidic one. Because of this, less expensive metals, such as iron and aluminum, can be considered for synthesizing the catalysts. With such catalysts in KOH support solution, a current density of $180A/m^2$ at 0,3V and $540A/m^2$ at 1.04V for Fe(III) and Al(III) respectively.[33] The downside of this medium is the inevitable carbonate and bicarbonate formation which lowers the concentrations of the electrolytes and affects the performance of the cell in time.

1.3.4 Catalysts for acetal oxidation

Another option to achieve higher performances would be to use a different kind of fuel. The acetals have been studied by few people even though they can theoretically produce more energy than methanol.[2-4] Since these are new fuels, the search for optimum catalysts has the start almost anew. The first steps to find the best catalysts have followed the previous research done on DMFCs. Out of several catalysts such as Pt/Ru, Pt/Sn, Pt-O_x, Pt-RuO_2 and Pt-MnO_2, they found that the best overall choice would be Pt/Sn. Finally, just to make a parallel between the methanol and methylal, it was found that using a $SeRe_2O_6$ catalysts could be used to make methylal from methanol in a single phase electrooxidation.[34]

1.4 Methanol oxidation in a DMFC

1.4.1 Methanol oxidation summary

As it is widely know, the overall reaction of methanol oxidation can be summarized in the following equations:

$$CH_3OH + H_2O \rightarrow CO_2 + 6\ H^+ + 6\ e^- \qquad (anode) \qquad (1.1)$$

$$3/2\ O_2 + 6\ H^+ + 6\ e^- \rightarrow 3\ H_2O \qquad (cathode) \qquad (1.2)$$

$$CH_3OH + 3/2\ O_2 \rightarrow CO_2 + 2\ H_2O \qquad (overall) \qquad (1.3)$$

But we have to keep in mind that those reactions do not take under consideration the formation of intermediates, which in the end determine the rate of the reaction of the MOR[19, 22]. Following the non-CO path, under low potential conditions, we can formulate that methanol can be oxidized into formaldehyde (Eq.1.4), and reacting with water at higher potentials, it further oxidizes into formic acid (Eq.1.5).[19] Finally, the formic acid can be oxidized to CO_2 (Eq.1.6).

$$CH_3OH \rightarrow HCHO + 2\,H^+ + 2\,e^- \quad (1.4)$$

$$HCHO + H_2O \rightarrow HCOOH + 2\,H^+ + 2\,e^- \quad (1.5)$$

$$HCOOH \rightarrow CO_2 + 2\,H^+ + 2\,e^- \quad (1.6)$$

In the presence of an acid catalyst, if we consider that water is absent from the system, the formaldehyde formed in equation 1.4 can then react with excess methanol to produce methylal (Eq. 1.7).

$$HCHO + 2\,CH_3OH \leftrightarrow H_2C(OCH_3)_2 + H_2O \quad (1.7)$$

As we can see, with water not being fed to the system, the complete oxidation of methanol into CO_2 can be very difficult.[22] In the end, the formation of CO_2 can be possible, but only because during the oxidation there is formation of water, which is crucial for having complete MOR.

The formation of formic acid also requires the presence of water (Eq. 1.8), and as for the formation of methylal, the formic acid is later oxidized into methylformate in presence of an acid catalysts (Eq.1.9).

$$CH_3OH + H_2O \rightarrow HCOOH + 4\ H^+ + 4\ e^- \quad (1.8)$$

$$HCOOH + CH_3OH \leftrightarrow HCOOCH_3 + H_2O \quad (1.9)$$

Still considering the non-CO path, with the help of SEIRAS (Surface-Enhanced Infrared Absorption Spectrosopy), it was proposed that there is formation of HCOO by chemisorptions on the Pt surface which then oxidize into CO_2 according to equations 1.10, 1.11, 1.12, and 1.13. This new species completes the list of the known products which includes formic acid, formaldehyde, methyl formate and dimethoxymethane that are produced at high current efficiencies.[20]

$$HCHO + H_2O \rightarrow H_2C(OH)_2 \quad (1.10)$$

$$H_2C(OH)_2 \rightarrow HCOO_{ad} + 3\ H^+ + 3\ e^- \quad (1.11)$$

Formate can be converted into CO_2 by decomposition

$$HCOO_{ad} \rightarrow CO_2 + H^+ + e^- \quad (1.12)$$

Or by reaction with OH_{ad}

$$HCOO_{ad} + OH_{ad} \rightarrow CO_2 + H_2O \quad (1.13)$$

Furthermore, it is also possible for methanol to form CO and CHO species during the MOR (Eq.1.14, Eq.1.15). With FTIR *in situ*, it was clearly shown that CO_{ad} is the major species observed on the surface after methanol oxidation. It is also said that CHO_{ad} is an instable product of the methanol adsorption according to the same study.[15] Moreover, the successive dehydrogenization steps towards the formation of CO species of the equation 1.14 can be better explained with Figure 1.4.[10]

$$CH_3OH \rightarrow CO + 4\,H^+ + 4\,e^- \qquad (1.14)$$

$$CH_3OH \rightarrow CHO + 3\,H^+ + 3\,e^- \qquad (1.15)$$

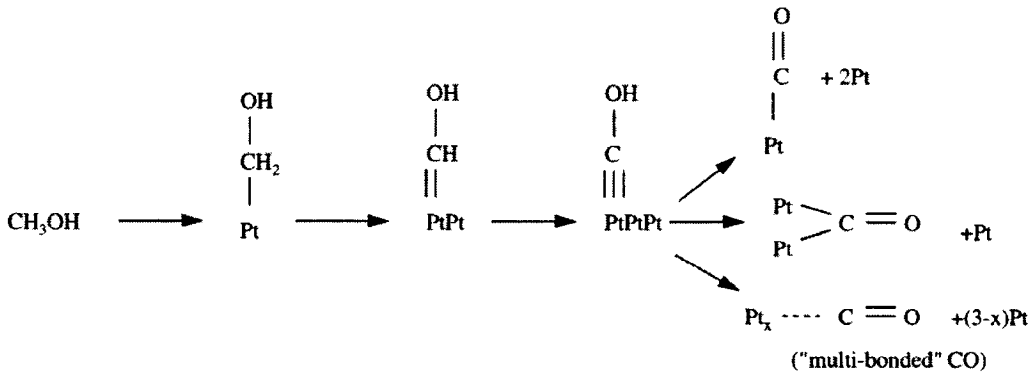

Figure 1.4: Scheme of the consecutive dissociative electrosorption of methanol at a Pt electrode.

While applying low potentials to the system, the CO will react with water in order to be converted into CO_2. And at higher potentials, with the presence of $Pt(OH)_{ad}$, the conversion can be made even faster.[35] Since CO and CHO species are strongly adsorbed on the Pt sites, we either need to apply a high potential in order to oxidize the carbon monoxide at a faster rate (Eq.1.16, Eq.1.17) or with the help of a binary alloy (i.e.,

Ru or RuO_2)[13] for the oxidation can also occur more easily (Eq.1.18, Eq.1.19). The higher the potential, the more CO_2 is formed on Pt-Ru/C catalyst.[19] Up to a certain point, the conversion of methanol to CO_2 can reach around the 100% mark, which is a lot better than the 80% or so obtained with only a Pt catalyst. This figure can be even lower in the instance that the applied potential is lower than 0,8V vs. RHE because the formation of formaldehyde is also going on.[36] The best ratio of Pt-Ru is 80% to 20% according to *in-situ* FTIR findings. This shows that four Pt sites for the dissociative adsorption of methanol and one Ru site for the water molecule activation are needed.[23] But according to earlier studies, it was established that this optimum ratio was settle at 50-50 Pt-Ru catalyst.[24]

$$Pt + H_2O \rightarrow Pt(OH)_{ad} + H^+ + e^- \quad (1.16)$$

$$Pt(OH)_{ad} + Pt(CO)_{ad} \rightarrow CO_2 + H^+ + e^- + 2\,Pt \quad (1.17)$$

$$Ru + H_2O \rightarrow Ru(OH)_{ad} + H^+ + e^- \quad (1.18)$$

$$Pt(CO)_{ad} + Ru(OH)_{ad} \rightarrow CO_2 + H^+ + e^- + Pt + Ru \quad (1.19)$$

Theoretically, the formation of CO_2 from MeOH (methanol) requires 6 electrons (see Eq.1.1). As stated above, in reality different oxidation paths exist during the MOR. Therefore, a third of the electrons are used for the formation of side products species such as formic acid and formaldehyde. Adding a 50% loss of theses species, the evaluated number of electrons needed climb to 14 instead of 6, thus reducing the efficiency of the reaction. This number correlates with the findings of Jusys, Z. et al.[15]

As Mukerjee, S. et al. demonstrated, with different alloyed metals the reaction mechanisms can vary.[25] For instance, if we take into account the Pt-Ru/C catalyst, as treated above, Ru oxy-hydroxides play a front role for oxidizing CO. But with Pt-Mo/C, at lower potentials Mo oxides act as the reaction inhibitor, and at higher potentials the apparition of Pt oxides (Pt-OH) is crucial for the CO oxidation. Choosing another alloy can also have an impact on the steady-state current densities of methanol oxidation. This value is reflected upon by the number of methanol molecules that reacts via per catalyst surface site per second. We refer to this as the turnover number (TON: molecule/s site). When adding a small fraction of nickel to the Pt-Ru/C, the activation energy is then lowered, and the TON is improved by almost 10%.[31]

The choice of the alloyed metal is not the only factor which can affect the outcome of the reaction. The loading of the catalyst also has a big influence on the MOR. With high catalyst loading of Pt-Ru, very high formation of CO_2 is measured via mass spectrometry. By reducing the catalyst loading, the CO_2 is then reduced because the MOR is incomplete. The lack of catalyst is reflected by the formation of intermediates, such as formaldehyde and formic acid.[21]

We have to be careful when the results are obtained in a controlled environment, because these results don't necessarily reflect the MOR that may exist in the realistic fuel cell operating condition and design.[21] Keeping this important fact in mind, Wasmus, S. et al. have compile a list of relative products at the anode under real operating

conditions.[22] They varied the water/MeOH ratio and the temperature, to see the relative effects on the product distribution. The results are presented in Table 1.3 below.

Table 1.3: Anode potentials and relative product distributions (in percent) measured during methanol oxidation in a DMFC being determined from galvanostatic step experiments. Electrolyte: PBI membrane doped with 500 m/o H_3PO_4. Anodes: Platinum-ruthenium (Pt-Ru) or platinum-black (Pt), 4mg/cm^2 each, feed rate adjusted by vacuum system of the MS (2-3 liquid ml/h). Cathode: platinum-ruthenium or platinum-black, 4mg/cm^2 each, 10 ml/min air. The error of the relative product distributions is ±7.5%.

H_2O/CH_3OH (mole ratio)	T (°C)	Relative product distribution						Anode potential (V) vs. RHE	
		CO_2		Methanaldi-methy-lacetal		Methylformate			
		Pt-Ru	Pt	Pt-Ru	Pt	Pt-Ru	Pt	Pt-Ru [a]	Pt [b]
4	150	96	88	0	1	4	11	0.42	0.44
	160	98	84	0	3	2	13	0.40	0.46
	170	99	92	0	0	1	9	0.39	0.46
	180	99	96	0	0	1	4	0.39	0.46
	190	98	97	0	0	2	3	0.38	0.46
2	150	91	77	2	6	7	17	0.45	0.45
	160	93	76	1	6	5	18	0.41	0.45
	170	96	84	1	4	4	13	0.40	0.46
	180	97	83	0	5	3	12	0.38	0.46
	190	98	91	0	2	2	8	0.38	0.46
1	150	79	50	7	23	14	27	0.45	0.45
	160	83	56	6	20	11	24	0.45	0.46
	170	88	63	4	18	8	20	0.44	0.46
	180	91	65	3	19	6	16	0.43	0.46
	190	93	78	3	12	4	11	0.42	0.46
0.5	150	60	33	19	40	21	27	0.47	0.48
	160	74	36	11	43	16	21	0.49	0.47
	170	73	43	13	39	14	18	0.48	0.48
	180	84	52	8	33	8	16	0.48	0.48
	190	85	57	8	30	8	13	0.47	0.48
0 (No water)	150	28	8	53	77	19	14	0.68	0.53
	160	17	12	71	74	12	15	0.54	0.53
	170	21	4	67	76	12	11	0.54	0.54
	180	26	18	64	73	10	9	0.55	0.56
	190	28	18	63	74	9	8	0.59	0.57

[a] At 300 mA/cm^2.
[b] At 150 mA/cm^2.

These results seem to be in accord with the findings that were discussed earlier. For both cases of catalysts, it seems that the increase of H_2O/CH_3OH raises the proportion of CO_2, indication to the point that the MOR is almost a 100% complete for Pt-Ru and up to 97% with Pt. But we can also clearly see that the increase of the temperature from 150°C to 190°C has a great impact. Its influence is even stronger when no water is present,

because it has a strong tendency to shift the reaction towards complete methanol oxidation into CO_2.

1.4.2 Methanol crossover

Crossover is defined as the passage of the fuel from the anode to the cathode. The presence of the fuel in the cathode is known to be detrimental to the fuel cell's power output. The crossover problem in the fuel cell has been noted in a lot of papers, and from their conclusions it ought to be considered when designing a fuel cell. According to Fick's Law, this problem is mainly due to the concentration differential of methanol that exists in the system. One might presume that reducing the intake concentration of methanol could solve this dilemma. But to a certain extent, we are faced with mass transport limitation at the anode. The optimum concentration needed is evaluated to be around 0,5M to 1M of methanol at 60°C.[37] At higher temperature, methanol turns into gas, resulting in higher crossover. The water flux in the membrane can also enhance the crossover of methanol by transporting it to the cathode,[12] so can a strong magnetic field between the dipoles.

Presently, Nafion® membranes are widely used for the study of methanol fuel cells. But it was found that the diffusion coefficient related to methanol crossover is in the order of 10^{-5} cm^2/s at room temperature.[38] Since the smallest presence of methanol in the cathode compartment can greatly hinder the overall efficiency of the fuel cell, novel routes have to be explored in order to reduce the crossover. It was reported that a new

membrane, called PBI (polybenzimidazole), can reduce by ten folds the crossover of methanol without sacrificing the good membrane conductivity.[22] The conventional method to determine the crossover is by detecting the CO_2 at the cathode exhaust.[39] But to be more accurate, one has to take into consideration that the anode formed CO_2 crosses over and can falsify the results.[37] In the electrochemistry lab at l'*École Polytechnique de Montréal*, Savadogo, O. et al. devised a new method to determine the crossover through the MEA (membrane electrolyte assembly) with cyclic voltammetry.[40]

1.5 Acetals

Having a greater energy density than methanol, the acetals are a new attractive way to fuel the direct oxidation fuel-cell (DOFC). Here are some numbers to support this argument : 4,89 Ah/mL for dimethoxymethane (DMM or methylal), 4,90 Ah/mL for trimethoxymethane (TMM), and 3,97 Ah/mL for methanol.[41] Even if the molecule has the advantage in terms of energy density, it doesn't necessarily imply that it is adequate for the fuel cell. One has to find a fuel that will also show good electrochemical properties, such as the acetals have proven to have. One advantage that's worth mentioning is a lack of any carbon-carbon links in the acetals molecules, making the oxidation to carbon dioxide a lot easier. Another reason why the acetals are more attractive than methanol depends on the size of its molecules. It is assumed that the crossover would be less in the case of the acetals because the molecules are bigger than those of the methanol. Since the molecules are bigger, the migration through the membrane would be more difficult to

achieve. Finally, comparing methanol and acetals, it is clearly shown that the later are less toxic to humans, making them a lot safer for usage in DOFCs.

The first kind of research in that new path was undertaken by NASA's Jet Propulsion laboratory. Their study revolved around dimethoxymethane (DMM), trimethoxymethane (TMM), and trioxane (1,3,5-trioane).[1] Their first findings showed that TMM and DMM had lower open-circuit potentials than methanol. This was explained by the fact that they possess more activated C-H bonds resulting in a higher coverage by adsorbed hydrogen atoms. Also, electrolysis of the acetals produces formic acid and formaldehyde which produce lower open-circuit potentials on Pt and Pt-Ru catalysts. And in comparing TMM and DMM, the second proved to be easier to be oxidized since its anodic potential was lower. Figure 1.5 shows the comparison of the anodic potential for both acetals on Pt-Ru and Pt-Sn catalysts.

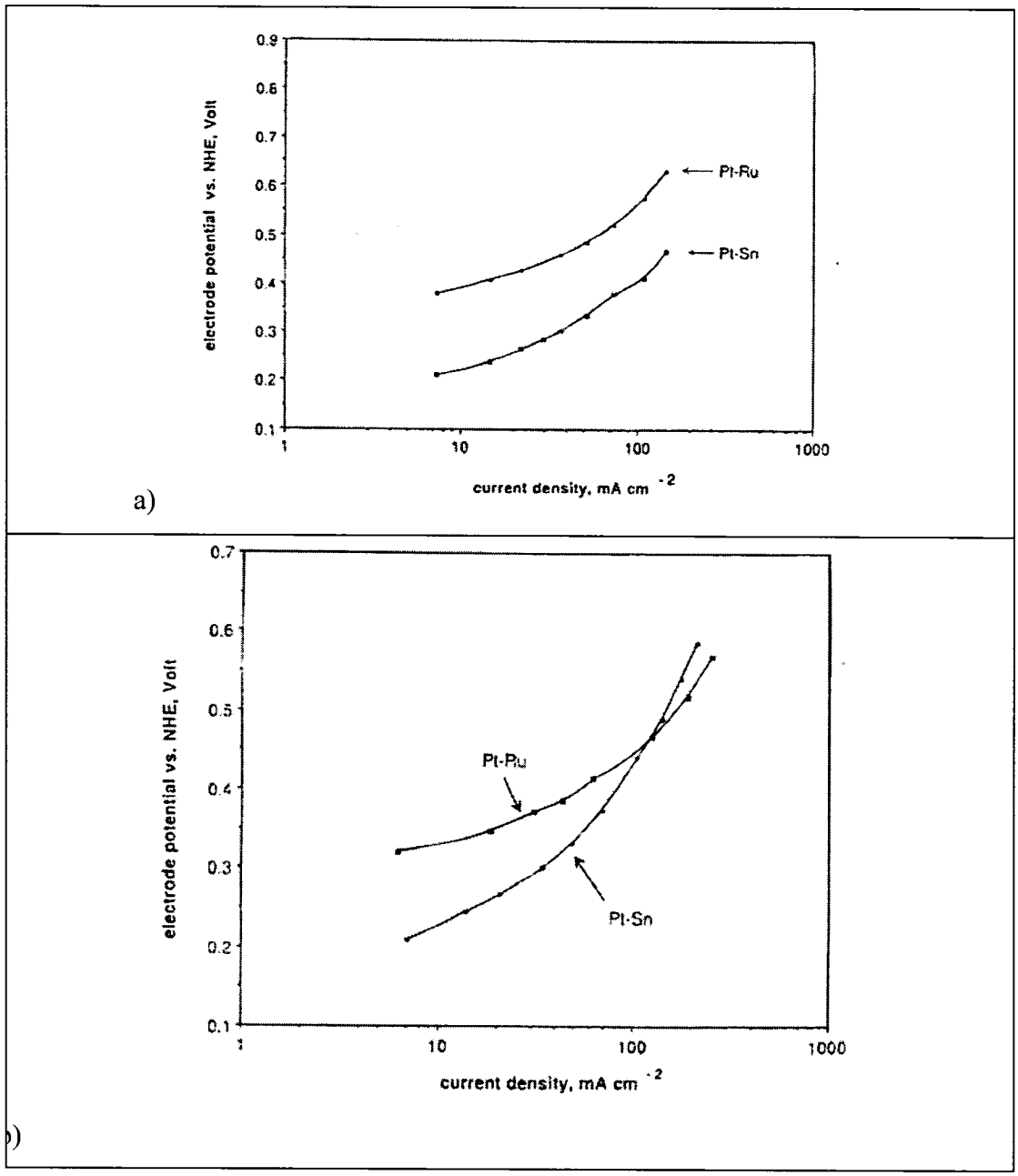

Figure 1.5: Steady-state galvanostatic polarization curves for oxidation of a) 1M DMM b) 1M TMM in 0.5M sulfuric acid at Pt-Ru and Pt-Sn(E-TEK) electrodes at 60°C.

Using gas chromatography, it was determined that the electrolysis products from DMM and TMM are methanol, formic acid and formaldehyde. In the cathode exhaust, it was

found that only methanol and CO_2 were the byproducts of the reactions, indicating that the formic acid and formaldehyde are oxidized a lot quicker than MeOH. Taking into consideration that the hydrolysis occurs, either in the acid support or at the acid membrane interface, the TMM oxidizes into formic acid and DMM into formaldehyde. In the end, each one is transformed into carbon dioxide.

Following the same steps, Savadogo and Yang started studying more closely the possibilities of using methylal, ethylal, and 1,3-dioxolane for direct acetal fuel cells.[2, 3] They showed again that methylal (DMM) was better suited than methanol because the anodic polarization curves were lower in the first case (Figure1.6).

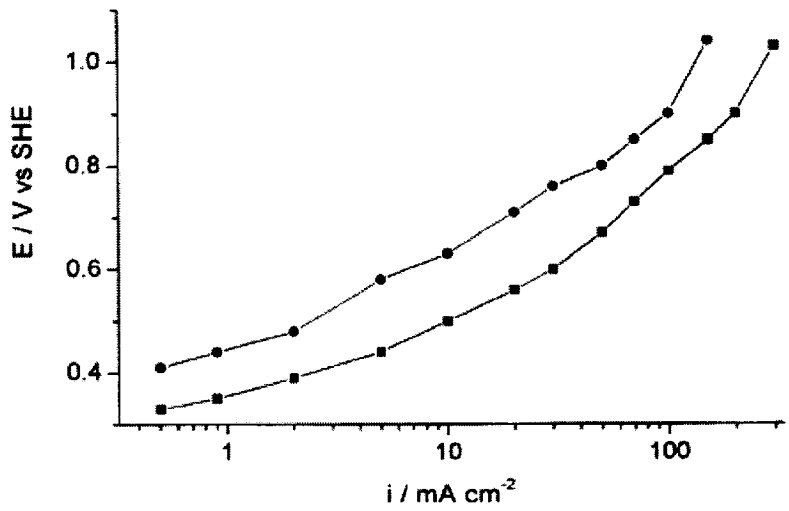

Figure 1.6: Quasi steady-state polarization curves for the direct electrooxidation of (▪) methylal (60°C) and (•) methanol (60°C) in 1 M H_2SO_4.[42]

Suspecting that hydrolysis was an intricate part of the complete oxidation process, they further investigated this phenomenon. They started by gathering data from the acetals manufacturer on the effect of pH level on the degree of hydrolysis (Table 1.4).[42]

Table 1.4: Percentage hydrolysis level variation with pH of acetals in H_2SO_4 during a 5 h period at 20°C.

Acetals/pH	0	1	3
Methylal	52%	4%	0%
Ethylal	33%	22%	0%
1,3-dioxolane	9%	0%	0%

From this, we can clearly see the drastic effect the pH can have on the fuels. It is without a doubt a factor that always has to be kept in mind during the study of direct acetals fuel cells. From now on, it would be appropriate to include the hydrolysis steps when stating the oxidation equations of the acetals. The equations for each acetal have been established as follows:

For methylal:

Hydrolysis: $$(CH_3O)_2CH_2 + H_2O \overset{H^+}{\leftrightarrow} CH_2O + 2CH_3OH \quad (1.20)$$

Electrooxidation: $$CH_2O + 2CH_3OH + 3H_2O \leftrightarrow 3CO_2 + 16H^+ + 16e^- \quad (1.21)$$

For ethylal:

Hydrolysis: $$(CH_3O)_2(CH_2)_3 + 3H_2O \overset{H^+}{\leftrightarrow} CH_2O + 4CH_3OH \quad (1.22)$$

Electrooxidation: $$CH_2O + 4CH_3OH + 5H_2O \leftrightarrow 5CO_2 + 28H^+ + 28e^- \quad (1.23)$$

For 1,3-dioxolane:

Hydrolysis: $$C_3H_6O_2 + 2H_2O \overset{H^+}{\leftrightarrow} HCOOH + 2CH_3OH \quad (1.24)$$

Electrooxidation: $$HCOOH + 2CH_3OH + 2H_2O \leftrightarrow 3CO_2 + 14H^+ + 14e^- \quad (1.25)$$

Over scoping their search for the best catalysts concerning acetals, 10%Pt-Sn was found to be better suited for ethylal and 10%Pt-Ru for methylal and 1,3-dioxolane. Overall, they obtained the highest current densities with ethylal. Trying to improve the performances even more, they used a sputtering technique that consists of depositing a small amount of a binary alloy on the Pt-Ru surface. In two cases, it was discovered that this approach could help attain higher current densities. The Figure 1.7 proves that sputtering Pt-Sn and Pt-Ru enhances the properties of the Pt-Ru catalyst.

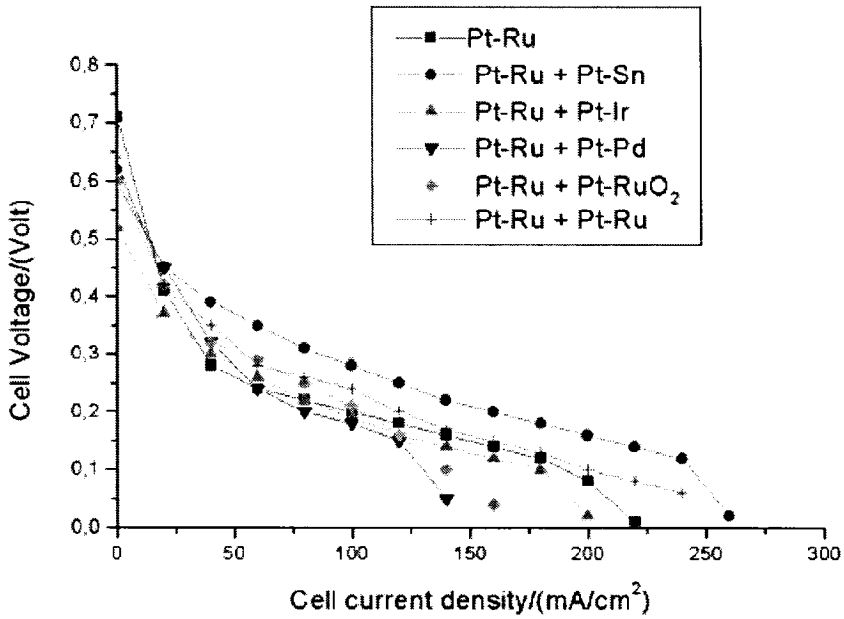

Figure 1.7: Polarization curves of Direct ethylal/O_2 PEMFC. T_{cell}: 90°C. Membrane: Nafion 117. Pressure: 1:1. Electrocatalyst loading of the cathode: 4mg/cm^2 Pt/C (60% Pt/C). Electrocatalyst loading of the anodes: 2mg/cm^2 on each of the various composite electrodes.

Recently, Wakabayashi, N. et al. have published about the effect of hydrolysis on the electrooxidation of DMM and TMM.[41] They methodically showed that DMM was not electrochemically active, but after hydrolysis to methanol and formaldehyde, the oxidation could occur. Figure 1.8 shows that no oxidation peaks are obtainable before hydrolysis, but afterwards, clear peaks appear because the hydrolysis products undergo oxidation.

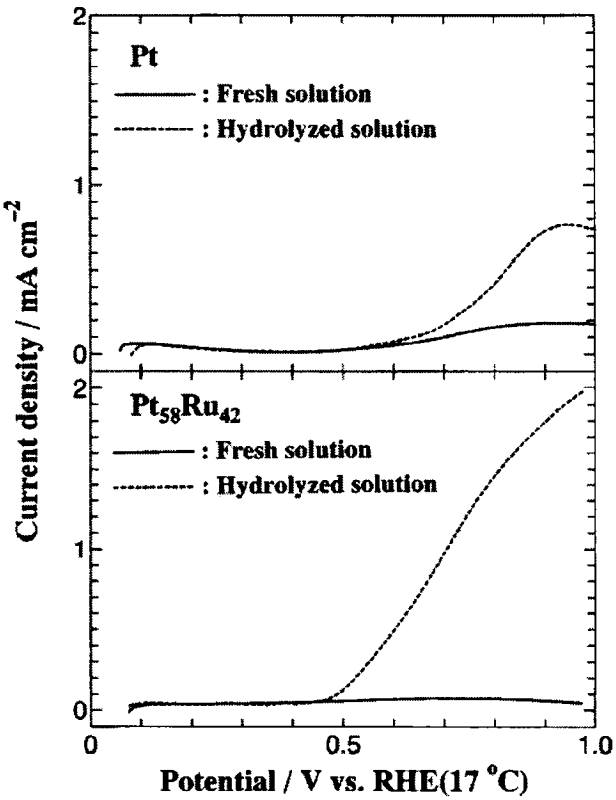

Figure 1.8: CVs obtained at 17°C at Pt and $Pt_{58}Ru_{42}$ electrodes in 0.27 M DMM + 0.1 M $HClO_4$ solution freshly prepared and after the hydrolysis treatment. DMM in the hydrolysis treated solution was completely hydrolyzed into 0.74M CH_3OH and 0.37 M HCHO. Scan rate was 20mV/s.

Thus, this article states that the hydrolysis can be activated by the pH, but also by heating the solution. This could also explain why the trioxane in Narayanan's work that couldn't yield good results until it was properly heated.[1]

CHAPTER 2

EXPERIMENTAL PROCEDURES

2.1 Experimental setup

The first apparatus used in this work is an electrochemical half-cell which will allow to perform cyclic voltammetry. During this research study a change of laboratory occurred, therefore two different half-cells were used. In view to get homogenous results from both Canada and Japan labs, a special attention was made to adjust the different parameters in order to achieve that goal.

First, we'll describe the half-cell used in "*l'École Polytechnique*" laboratory. It constituted of two identical glass compartments that were connected by a bridge of a small solid electrolyte membrane (Figure 2.1 a)). Such a configuration allows an excellent simulation of the fuel cell behavior. In each of those compartments, a 50 ml support solution can be contained. In the present case, the nature of the support electrolyte was a 0,5M sulfuric acid electrolyte. With Figure 2.1 b), we can notice that there are four openings on the top of each glass compartment. The first one is used for the gas entry, the second for the gas exit, the third for the reference electrode, and the fourth for the working electrode.

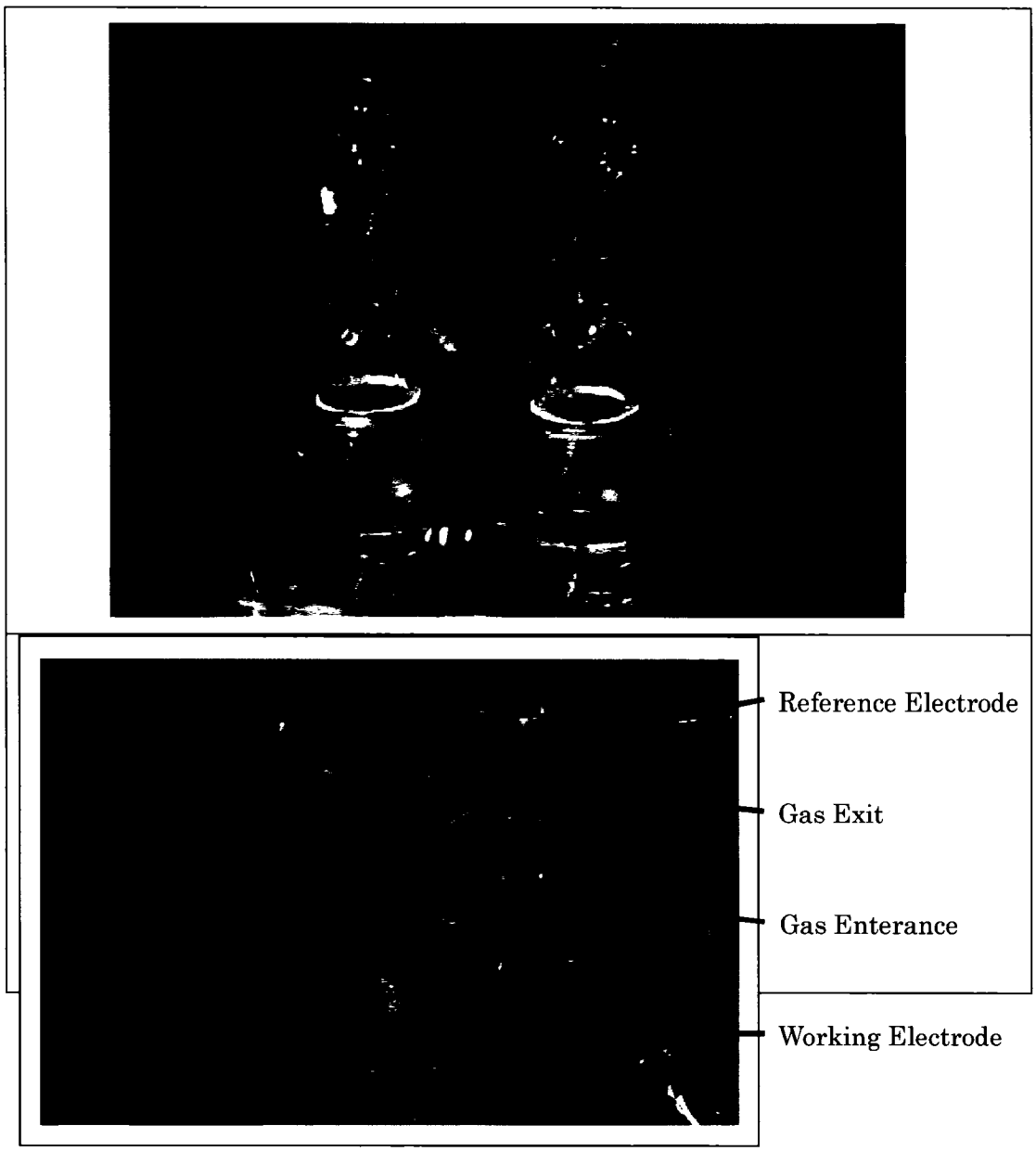

Figure 2.1: a) Electrochemical half-cell, b) Close up view of the openings on top of each glass compartment

The quality of the experiment depends on the air tightness of the whole system. The presence of only a few ppm of an undesired gas can greatly affect the results. Before every test, with only the support solution inserted, bubbling of nitrogen for an hour (at a

rate of one bubble per second) is required in order to see if the system is clean and ready for the cyclic voltammetry test. To do so, a reference cyclic voltammogram is necessary at this stage. Also, the reference CV is also useful for determining the active surface of the working electrode. Afterwards, to simulate the cathode compartment of the fuel cell, pure oxygen is bubbled for an hour in order to saturate the support solution. The gas exit is designed in such a manner that it lets the excess gas out of the system without letting any entry.

As mentioned above, we have an entry for the working platinum electrode. The platinum electrode of roughly 1 cm^2 that is plunged into the cell is attached by a platinum wire up to the exit. This permits us to plug the electrode to the potentiostat while ensuring the air tightness of the system. Finally, the Luggin bridge dips in the electrolyte as close as possible to the working electrode, if not an ohmic loss will be perceptible because of the electrolyte's resistance. The Luggin bridge serves as an ionic conductor which connects the working electrode and the reference through fritted glass (the reference is a Saturated Calomel Electrode (SCE)).

For the tests that we have to execute, the left compartment will contain the working electrode (WE) with the saturated calomel reference, and the right one will contain the counter electrode. In order to have a good sensitivity for collecting the current, the counter electrode surface has to be bigger (a large surface area, e.g. at least 100 times higher than those of the working electrode surface area) than that of the working electrode.

It is for that reason that the working electrode is a plate and that the counter electrode is a grid (which increases the surface area).

At Kyoto University, a single electrochemical glass cell was used for conducting the experiments (Figure 2.2). The cell contains a volume of 150 ml of ultra pure sulfuric acid 0,5M. There are two entrances for the gas, one above the solution, and one in the solution. With the use of valves, the rate flow of each line can be adjusted. Also, a gas exit gets rid of the excess gas. Integrated to the cell design, the reference electrode was connected by a bridge directly underneath the working electrode. The working electrode is made of a 6 mm diameter disk. For different purposes, the disk will be made either of pure platinum or glassy carbon as we will explain later on. Hung from a rotary machine in the center of the cell, it can be spun to reduce the effects of mass transport limitation. The spinning can be adjusted precisely according to the specific needs of the user. In the bottom of cell, a wire is looped several times so that it follows the contour of the cell. This counter electrode works efficiently because of its higher surface area compared to the small disk of the working electrode.

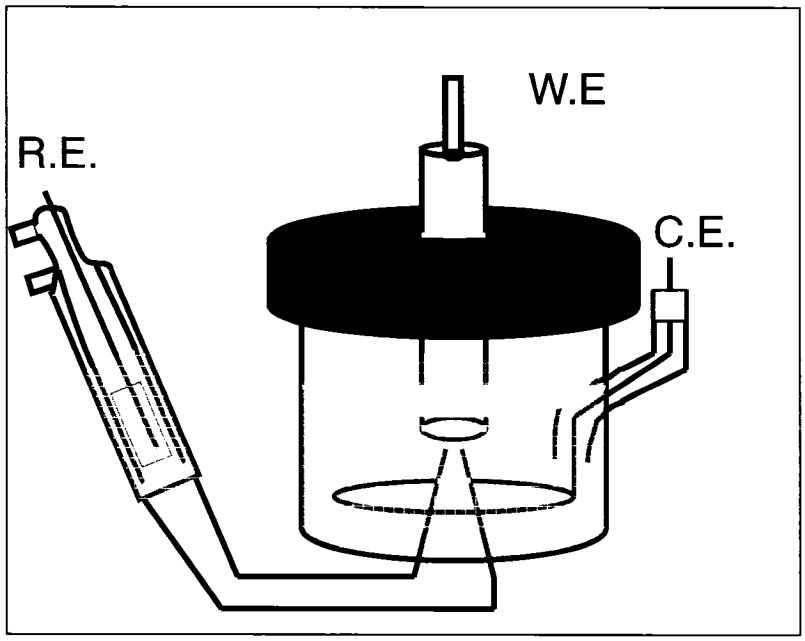

Figure 2.2: Single compartment electrochemical cell

2.2 Electrode fabrication

The usage of a pure platinum electrode as a working electrode can have its advantages when studying the oxidation reactions. But on the other hand, platinum is seldom used alone while preparing the catalyst. To simulate the reality of fuel cells more closely, we have to consider the working electrode catalysts which contain binary alloys too. In order to do so, we must start off by using a glassy carbon electrode. This 6mm diameter disk electrode will serve as a support surface and electric conductor for the desired catalysts. To fabricate such an electrode one needs to follow these steps:

1- Clean the surface of the glassy carbon electrode with a fine grained plastic polishing sheet. Beforehand, wet the surface of the sheet that has been deposited on a small glass piece.

2- Wash the electrode with water and ethanol.

3- Put the electrode in a glass recipient containing water for 30 minutes in the ultrasonic bath.

4- Insert the electrode in the dryer (Drying oven DO-300) for 15 minutes.

5- Let the electrode cool at room temperature. Be sure to protect the surface from impurities by putting the electrode under a glass container.

6- Prepare a solution of 1,2g/L concentration of platinum by mixing the desired catalyst with water. Also, we add liquid Nafion® to our mixture to achieve a 1% concentration. With this concentration, we will be able to achieve a 30µg of platinum when depositing 25µL of the solution on the surface of the glassy carbon electrode.

7- Stir the solution in an ultrasonic bath for an hour to obtain a homogenous mixture.

8- Apply 25µL of the solution on the surface of the cooled glassy carbon electrode.

9- Insert the electrode in the drying oven for 15 minutes.

10- Let the electrode cool down at ambient temperature.

11- Let everything dry overnight in a dust free environment.

All of the catalysts used in this project have been purchased at E-TEK™. Four different catalysts were chosen for this study: Pt/C, Pt-Ru/C, Pt-Sn/C, and Pt-Ir/C.

2.3 Cyclic voltammetry

Discovered and perfected only a few decades ago, the technique of cyclic voltammetry has proven to be indispensable for the fuel cell studies because it informs us about the essential electrochemical properties of the system. For example, from the obtained results, it is possible to extract information about:

-the oxidation and reduction potentials of the species in solution

-the number of electrons implicated in the reaction

-the reversibility of the system

-the electrochemical active surface of the electrode

-the diffusion and electron transfer coefficients

-the chemical reaction paths of the species

The working principal of CV is quite simple. The technique consists of applying a potential that we sweep back and forth between two different values at a constant rate. A cycle starts from the moment we apply the initial potential (E_1) up to the reversal point (E_2) and then return back to the initial potential (see Figure 2.3).

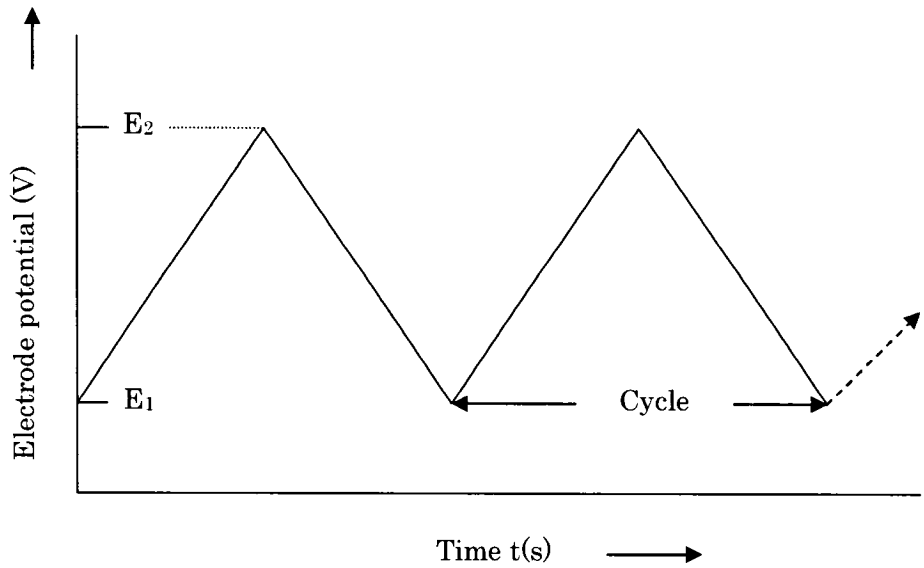

Figure 2.3: Illustration of the waveform of the cyclic voltammetry

The potentiostat, required for doing CV, acts as the regulator of the potential or the current depending on the users needs. Nowadays, the recording is all done by a computer program in order to simplify the procedures. The scheme presented in the Figure 2.4[43] shows the electrical equivalency of the system. The reference, which possesses a specific and constant potential, is thus needed to establish a basis for determining the applied potential. Without it, we can only apply a potential differential with the potentiostat. Knowing the exact applied potential is crucial to help determine the reactive species in the system. The working electrode is the surface which serves as the siege for the electron transfer reaction, so it is the heart of all the voltammetric systems. And the counter electrode assures the passage and the measuring of the current through the system.

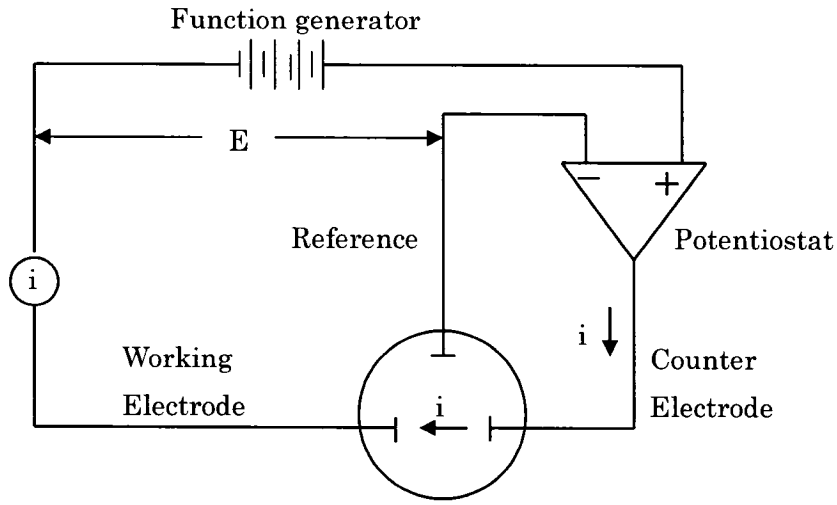

Figure 2.4: Scheme of the electric system for cyclic voltammetry

The measured current is the summation of the faradic and the capacitive currents[44]. The latter one exists because of the condenser that is represented by the interface between the electrode's surface and the solution layer next to it. But what matters more to us is the faradic current which results from the oxido-reduction of the elements at the working electrode's surface. This current is influenced by several factors:

-the rate of the mass transfer of the oxidized species from the solution towards the electrode (and vice-versa for a reduced specie)

-the rate of electron transfer at the electrode/solution interfaces

-the rate of the chemical reactions which precedes or follows the electrons transfer

The main interest of the cyclic voltammetry is to induce a reaction within the system in order to get a signal according to the present species. To do so, while sweeping the current positively, we force the system to consume the species near the electrode's surface. The reversal of the direction of the sweeping will then reduce the oxidized species. A

typical graph obtained in a sulfuric acid medium, which acts as an ionic conductor, is shown below in Figure 2.5[45].

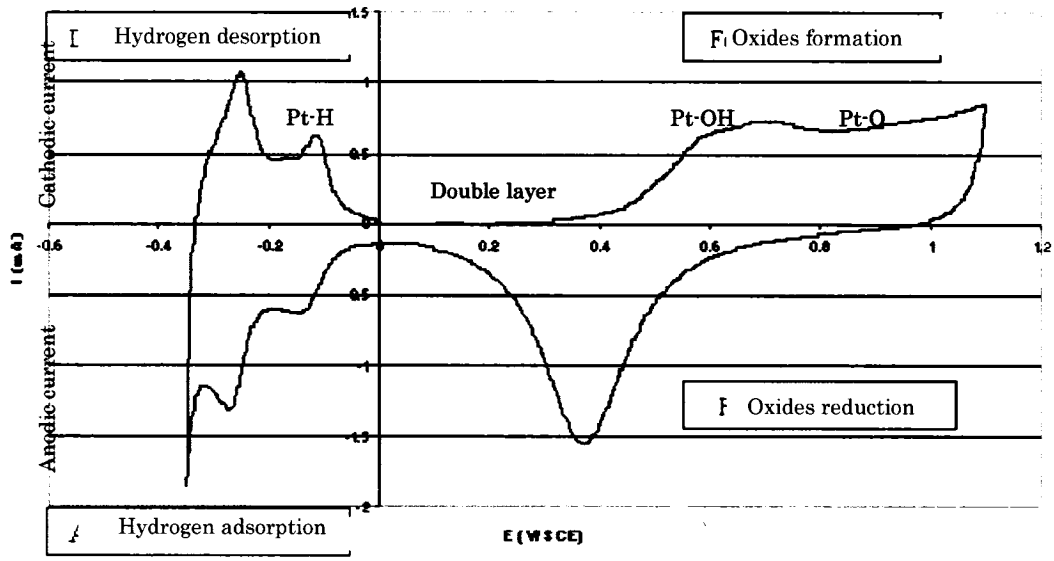

Figure 2.5: Reference voltammogram in 0,5M H_2SO_4 on pure platinum (ambient temperature, nitrogen purged, sweep rate of 50mV/s).

By convention, we establish the positive current to be that of the cathodic current, and the negative of the anodic current. Therefore, a positive signal indicates the oxidation of the species. Looking at the above graph, we observe that the hydrogen region is typical to that of the polycrystalline platinum electrode. As mentioned in Vielstich's work[43], we observe a convolution of three peaks that corresponds to the 110, 100 and 111 surfaces of platinum. By measuring the adsorption and desorption area of the hydrogen region and correlating it to the reported value of 210μC/cm^2[46], we are able to determine the real surface area of the working electrode. Also, between the regions where hydrogen is

adsorbed and Pt-O/Pt-OH are formed, we can observe a central zoned known as the double layer which originates from the capacitive current.

Coupling the data obtained with CVs with others, such a high performance liquid chromatography and mass spectrometry, we will be able to further evaluate the nature of the produced species during the reduction of the fuel.

2.4 High Performance Liquid Chromatography (HPLC)

Back in the late 60's and early 70's, a new technique for determining species was being developed. The high performance liquid chromatography has since then found a niche in such fields as pharmaceuticals, biotechnology, environmental, polymer and food industries.

Over the years, the HPLC has become the method of choice for the analysis of a wide range of compounds. It is stated that one of its main advantage over gas chromatography is that the analyzed species are not required to be volatile. Hence, it is possible to analyze macromolecules with the HPLC[47].

To begin an HPLC test, the user has to inject a certain amount of the liquid sample into a small opening. The liquid is then incorporated into the mobile phase that passes through a column packed with small sized particles (called stationary phase). The stationary

phase acts as a separator for the different compounds of the sample. This phenomenon is possible because of the different degrees of retention of each component in the column. The partitioning between the liquid mobile phase and the stationary phase determines the extent to which a component is slowed in the column. The different mobility of each component results in different exit times, thus partitioning the species. At the exit, a detector signals the presence of compounds different than the transport phase. Nowadays, the results are posted on a computer screen showing the peaks relative to the specific retention times (the difference of time between the injection and the exit) (Figure 2.6). For a qualitative test, one must match the retention times of know compounds with the ones obtained during the test. But to further the analysis, one can also quantify the species with the help of calibrated graphs previously obtained. A simple method to determine the concentration is to measure the heights of the peaks, but over time, this may not be the most accurate option. By comparing the surface area of the desired peak, it is then possible to determine the concentration of the compound even more precisely. This later option is relatively easy to follow since the computer automatically makes those measuring.

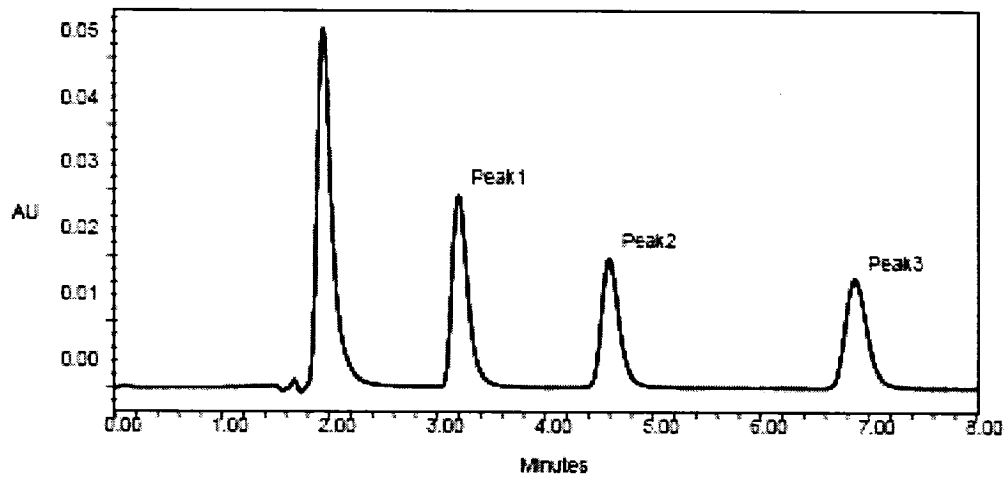

Figure 2.6: Example of a HPLC graph with several compounds

As it may now be obvious, the HPLC is most easily used when targeted compounds are known. In the instance that no or not all compounds have been identified, a combination of HPLC and mass spectroscopy is generally the best option to overcome this specific problem. By analyzing the exiting compounds of the HPLC with a mass spectrometer, we can therefore make the technique even more precise and useful. Since such a combination of machines is relatively costly, it is also typical to perform almost the same test using both machines separately. When doing so, one has to be careful with the data obtained with mass spectroscopy. Since sometimes the overlapping of components can occur, results obtained can be misleading.

The analysis in the work will be made with an HPLC system composed of a pump (L-7100, Hitachi Ltd.), an oven (L-7300 Hitachi Ltd.), two columns (C610-S, Hitachi Ltd., and inertsil ODS3, GL Sciences) and a UV detector (L-7405, Hitachi Ltd.). Also, it is worth mentioning that the wavelength of the UV spectrum used in this analysis was

established at 210nm. To analyze the electrolyte solution, we will inject a 10μL sample into the HPLC system (the sample is diluted 10 times in ultra pure water).

2.5 Mass spectrometry

After injecting the sample into the mass spectrometer, it is vaporized and then ionized using a beam of electrons (source: American Society for Mass Spectrometry, http://www.asms.org/whatisms/page_index.html). The obtained cations are separated from the anions and neutral species via an ion focusing lens (Figure 2.7)[48].

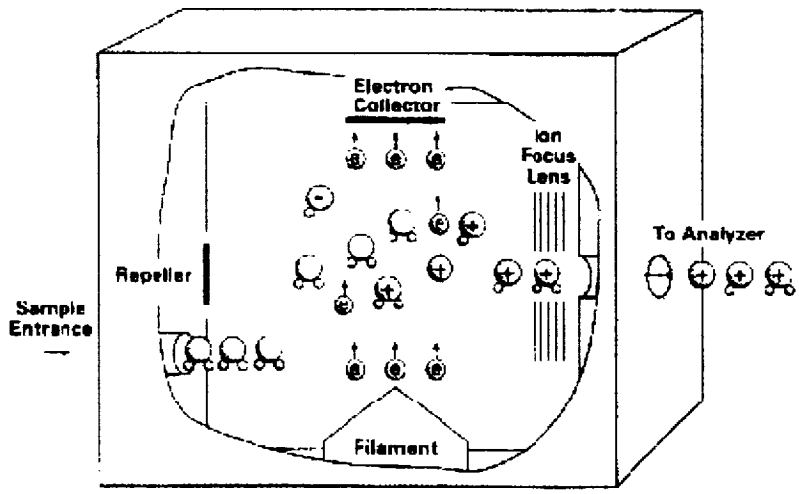

Figure 2.7: The workings of an electron ionizing source in a mass spectrometer

In the analyzer, the cations are then sorted according to their mass-to-charge ratio (m/z). The most widely used analyzers are magnetic sectors, quadrupole mass filters, quadrupole ion traps, Fourier transform ion cyclotron resonance spectrometers, and time-of-flight

mass analyzers. The inner workings of the magnetic sectors analyzer results on bending the trajectory of the cations by applying a magnetic field in a semi-circular chamber. At the end of this path, depending on the magnetic fields intensity, specific ions pass through a slit and are then detected according to their m/z ratio (Figure 2.8)[48].

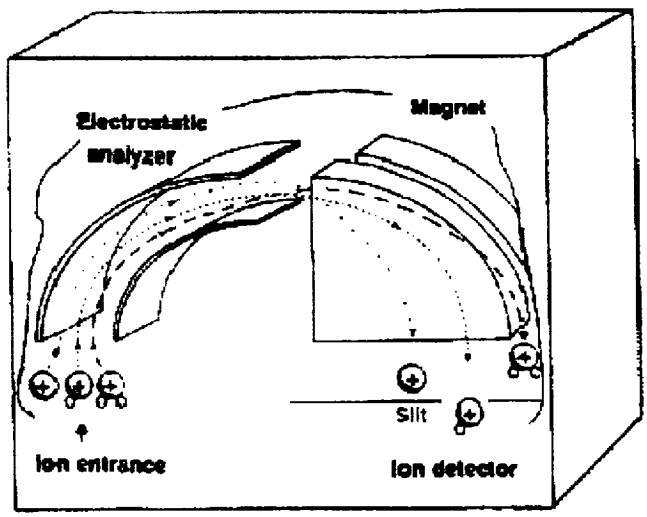

Figure 2.8: Schematics of the magnetic sectors analyzer.

Finally, the detector counts the specific ions, and sends this information to a computer. The final results are presented on a mass spectrum that consists of a histogram that classifies the ions by there specific m/z, and also it shows their relative intensities (Figure 2.9)[48]. To show the precision of such a device, with the latest technology advancements, a high resolution mass spectrometer is able to differentiate the carbon monoxide (CO, m/z 27,995) from nitrogen (N_2, m/z 28,006).

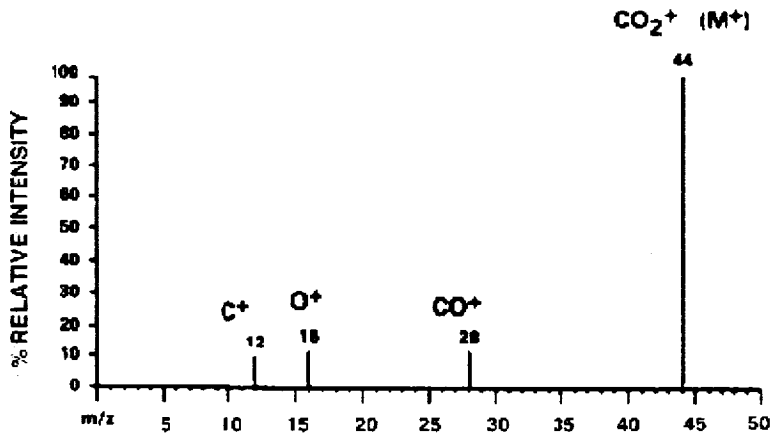

Figure 2.9: Example of a mass spectrum for carbon dioxide

With the mass spectrum, it is then possible for the user to determine the nature of the compounds in the sample. In some cases, the researcher does not only want to know the nature of the species, but he may also want to measure its quantity. To be able to quantify the sample's compounds, calibrations can be done either with external or internal samples. For external samples, it is required to produce MS spectrums for desired products at different concentrations. Since a direct correlation between the height of the peak and the concentration can be established, the measuring can be done without a lot of complications. The internal sample technique consists of adding the isotope of the compound that we wish to study. Knowing the isotopes concentration, the concentration of the unknown compound can be determined by comparing the height of the peaks. The mass spectrometer is very useful for measuring such concentrations because it is

remarkably sensitive. We can therefore obtain results in terms of ppm or even ppb for certain species.

At Kyoto University's laboratory, the mass spectrometer used is a JEOL MS Route JMS-600W from the JEOL company. According to the manufacturer, the sensitivity of the MS can detect 0,03ng of methyl stearate (m/z = 298) with a signal-to-noise ration of 10. Also, the software MSroute ver.1.8.00 was used during this research for storing the data in the computer.

For each MS test, we inject 0,4mL of the sample solution in the inlet using a syringe (the sample is diluted 5 times in ultra pure water). Once in this compartment, we have to open a small window in order to control the flow rate of the sample to the MS. During this step, we must be careful to open the window wide enough to get a clear signal for the detection of products, but not too much as to lose the vacuum in the ionic chamber.

According to the "principles of instrumental analysis" handbook, the quantitative analyses can be very accurate.[49] Using simple aqueous standards, they show that a log/log plot of concentration vs. ion count shows linearity. Therefore, using this technique, we will establish calibration curves (for concentrations of 10mM and 30mM) for methanol, methylal, ethylal, 1,3-dioxolane, formic acid, formaldehyde, and methyl format. Also, a spectrum of sulfuric acid will be obtained since the support solution is of the same nature, and we want to make sure that it doesn't interfere with our products analysis.

2.6 Experimental procedures

The primary steps to be taken in this project are to gather cyclic voltammograms of all the fuels with and without saturation of oxygen. On the first hand, by comparing both CV graphs for the same fuel, we can observe if the presence of the fuel has an effect on the kinetics of the oxygen reaction in the cathode compartment. Also, with the CVs, we can evaluate the potentials of the oxidation peaks for each fuel. Knowing the range of those peaks, we can therefore focus our attention on studying precisely the potentials at which the poisoning effects can be observed. Another important value that we can obtain from such plots is the oxygen reduction reaction onset potential. This value is found where the current density is nil during the negative sweep. To have a broader understanding of the effects of fuels and catalysts on the ORR, we chose to make tests for each combination of fuel (methylal, ethylal, 1,3-dioxolane and methanol) and catalyst (Pt, Pt/C, PtRu/C and PtIr/C).

From then on, we started looking into the factors that might influence the nature of the products at the cathode. For methanol, methylal, ethylal, and 1,3-dioxolane we performed a chronoamperometry test for each of these fuels during 6 hours (21 600 sec). Before launching such tests with acetals, after injecting the fuel in the cell, we waited 30 minutes to let the hydrolysis take effect. By not having done so, no oxidation peaks could have been observed initially. At the same time, this helps to simulate the real conditions of the acidic fuel cell's environment more closely.

Wanting to learn more about the nature of the species produced during the potentiostat tests of the cathode, we are going to use in parallel the HPLC and the mass spectrometer. Before starting such tests, we needed to calibrate each machine to be able to identify the different species and measure their concentrations. For the HPLC, we performed the calibration for probable products of the reaction for concentrations of 10mM and 30mM. The targeted species were as follows: methanol, ethylal, methylal, 1,3-dioxolane, formic acid and formaldehyde. And for the mass spectrometer, it was decided to calibrate the MS for the same products, adding also methyl format to the list. The concentrations for calibrating the MS were the same as the ones established for the HPLC. With theses calibrations at our disposal, during the poisoning experiment, we could perform the two tests using a sample taken from the electrochemical cell. The samples were taken directly underneath the working electrodes surface using a syringe. This precaution insured us that the sample taken from the cell would accurately represent the system at that precise moment.

The products analysis was done under the following conditions. For each of our four main fuels, we used two different potentials: 0,65V/RHE and 0,90V/RHE. The choice of those two potentials has been made to simulate, in the first case, the cathodic potential that corresponds to 100mA/cm^2, and in the second case, the open circuit potential of the fuel cell's cathode. Both theses results were based on the average results obtained in Yanick Cyr's memoir[4]. The samples were taken after roughly 3 hours (10 000 sec).

And finally, to determine the influence of the nature of the catalyst, we performed the tests using four types of catalysts: Pt/C, Pt-Ru/C, Pt-Ir/C, and Pt-Sn/C. To make this series of tests more easily understandable, the working conditions are resumed in the following table.

Table 2.1: Parameters studied during the poisoning tests at room temperature, to observe the produced species via HPLC and mass spectrometry

Fuel (0,5M)	Potential (V/RHE)	Catalyst	Time (sec)
Methanol	0,65	Pt(5%)/C	10 000
Methylal	0,90	Pt-Ru(10%)/C (1:1)	
Ethylal		Pt-Ir(10%)/C (4:1)	
1,3-Dioxolane		Pt-Sn(10%)/C (4:1)	

It was noticed that with these fabricated electrodes, there was a tendency that bubbles would accumulate on the rough surface (compared with pure platinum), making the results not perfectly reliable throughout the tests. Rotating the electrode at a speed of 700 rpm helped to prevent this problem from further occurring during the course of our experiments when using home made electrodes.

CHAPTER 3

RESULTS AND DISCUSSION

3.1 Effect of the fuel on the oxygen reduction reaction (ORR) of Pt based catalyst

3.1.1 Pt bulk catalyst

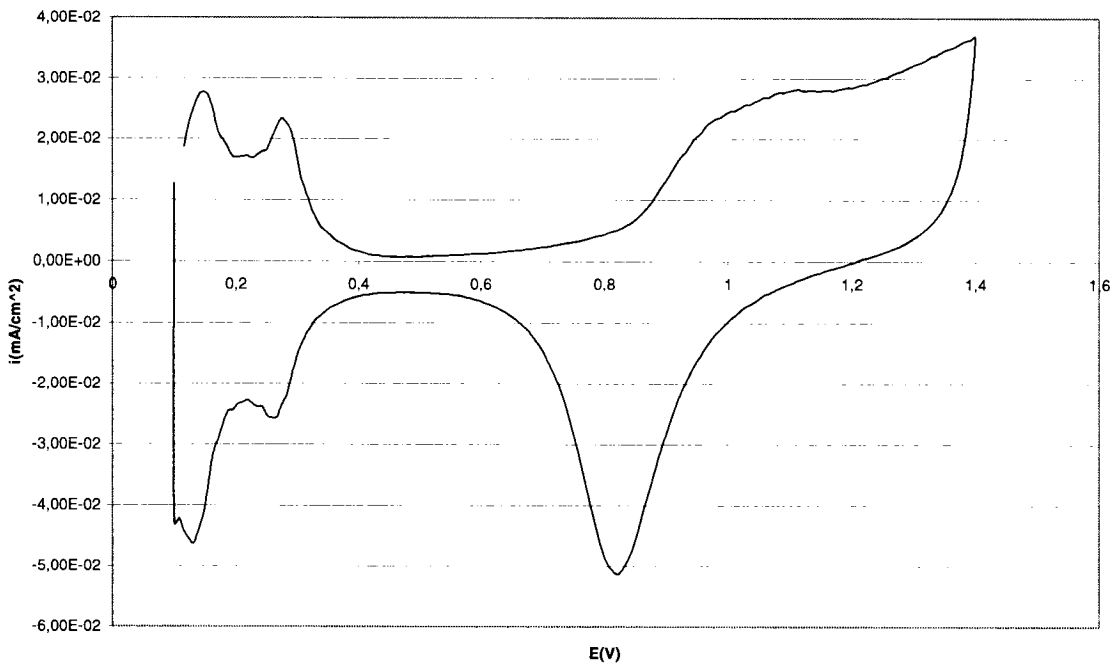

Figure 3.1: CV in 0,5M H_2SO_4 on bulk Pt (ambient temperature, nitrogen saturated / 60 minutes bubbling, sweep rate of 50mV/s)

Figure 3.1 shows the typical cyclic voltammogram obtained on pure platinum with an electrolyte of 0,5M H_2SO_4 in a nitrogen saturated atmosphere. Below 0,40V the adsorption and desorption of hydrogen occurs. The formation of oxides is indicated by

the positive currents above 0,80V. As for the oxygen reduction, it is represented by the negative peak at 0,80V. Also, a double layer effect is visible between 0,40V and 0,60V. These results are in agreement with those obtained classically in the literature.

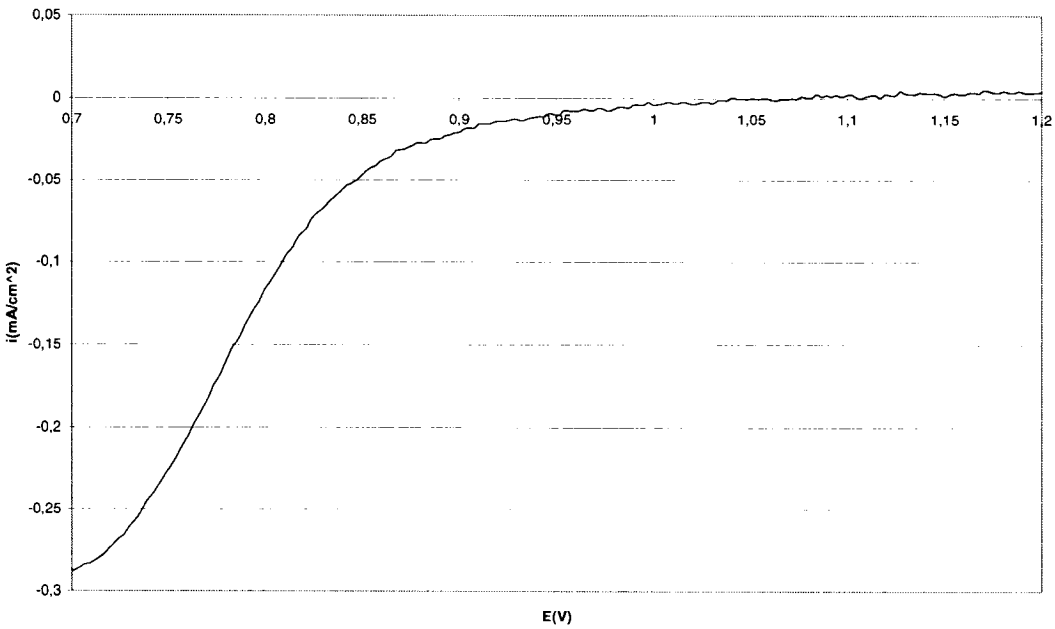

Figure 3.2: CV in 0,5M H_2SO_4 on bulk Pt (ambient temperature, oxygen saturated / 60 minutes bubbling, sweep rate of 50mV/s)

If we saturate the electrolyte with oxygen instead of nitrogen, we obtain the CV in Figure 3.2. Therefore, the oxygen reduction reaction (ORR) becomes the predominant reaction. During the decreasing of the potential, we see that the onset potential of the ORR is 1.05V. The current densities start to stabilize around 0,70V in this case. But since the ORR is a very slow reaction, it is important to analyze with sweep rates such as 5mV/sec instead of 50mV/sec. Figure 3.3 is the CV taken at 5mV/sec. In such conditions we can evaluate the ORR more precisely. We can see that the onset potential is 1,00V and the current

density plateau starts at 0,78V. Comparing both figures, we come to the conclusion that the sweeping rate has a great influence on the study of the ORR. The 50mV/sec CVs will be used at the oxidation peaks of the fuels. As for the 5mV/sec CVs they will be used for the study of the ORR in presence of different fuels and catalysts.

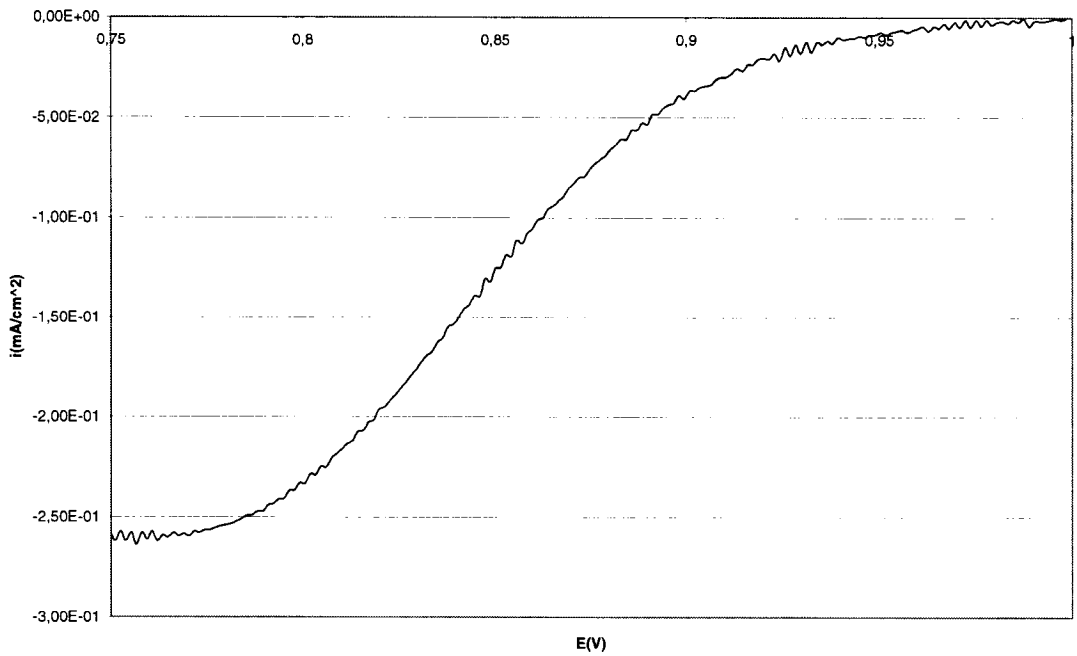

Figure 3.3: CV in 0,5M H_2SO_4 on bulk Pt (ambient temperature, oxygen saturated / 60 minutes bubbling, sweep rate of 5mV/s)

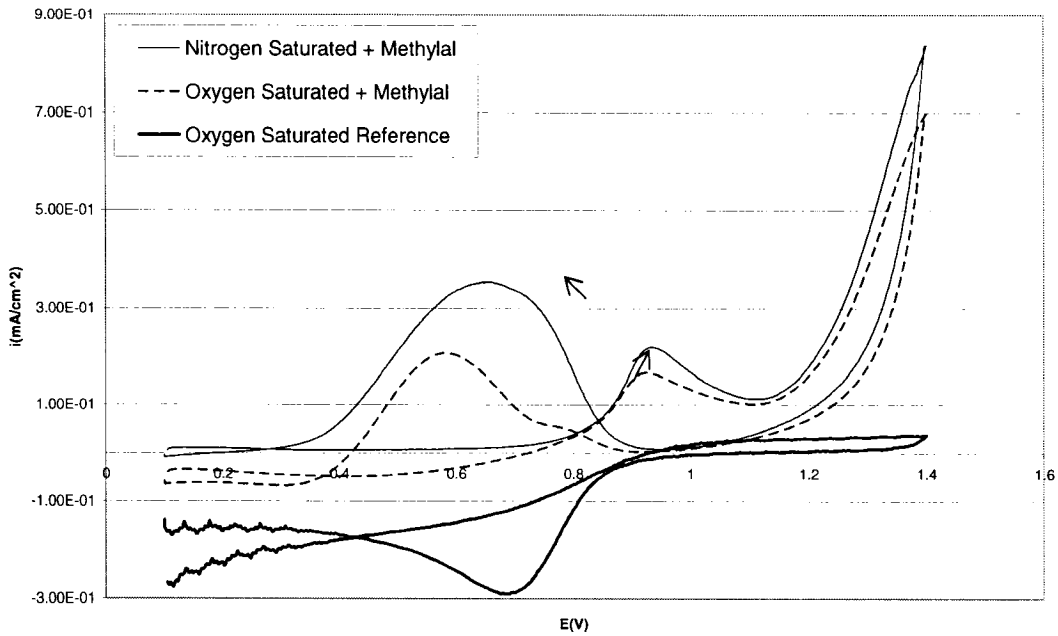

Figure 3.4: CV in 0,5M H_2SO_4 on bulk Pt (ambient temperature, nitrogen or oxygen saturated / 60 minutes bubbling, sweep rate of 50mV/s) with 0,5M methylal

Figure 3.4 helps to establish the effect of methylal on the ORR. We clearly see that when adding methylal to an oxygen saturated electrolyte, the oxidation of methylal is to still occurring over the ORR. The onset potential of the ORR drops to around 0,41V compared to 0,9V. The oxidation current of the ORR is roughly $1/10^{th}$ in scale with methylal. The nitrogen saturated curves helps us see the competitiveness between the oxidation of methylal and the ORR. Without oxygen in the solution, the oxidation peaks of methylal are higher.

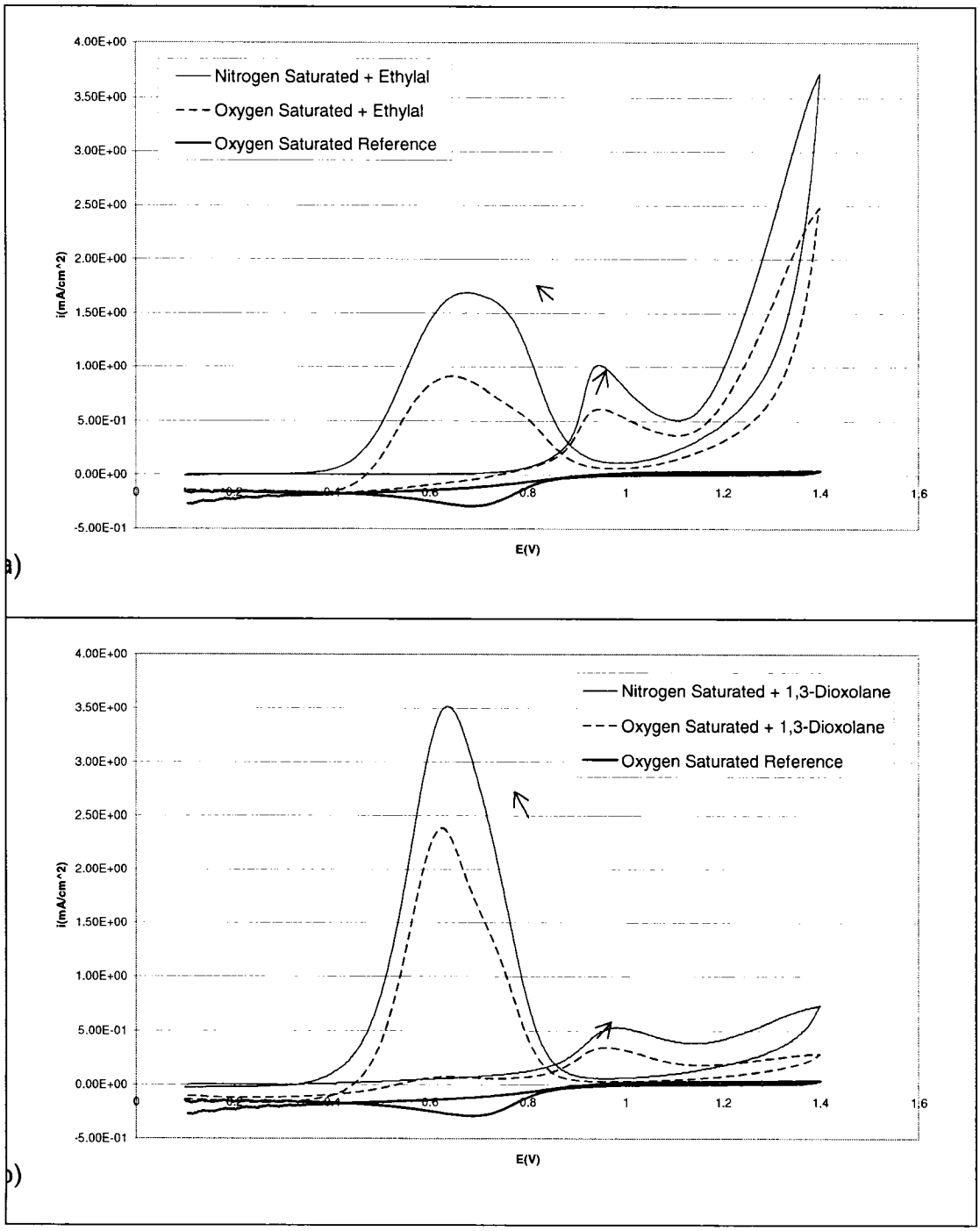
4.00E+00
3.50E+00
3.00E+00
2.50E+00
2.00E+00
1.50E+00
1.00E+00
5.00E-01
0.00E+00
-5.00E-01
i(mA/cm^2)
Nitrogen Saturated + Ethylal
Oxygen Saturated + Ethylal
Oxygen Saturated Reference
0
0.2
0.4
0.6
0.8
1
1.2
1.4
1.6
E(V)
a)
Nitrogen Saturated + 1,3-Dioxolane
Oxygen Saturated + 1,3-Dioxolane
Oxygen Saturated Reference
b)

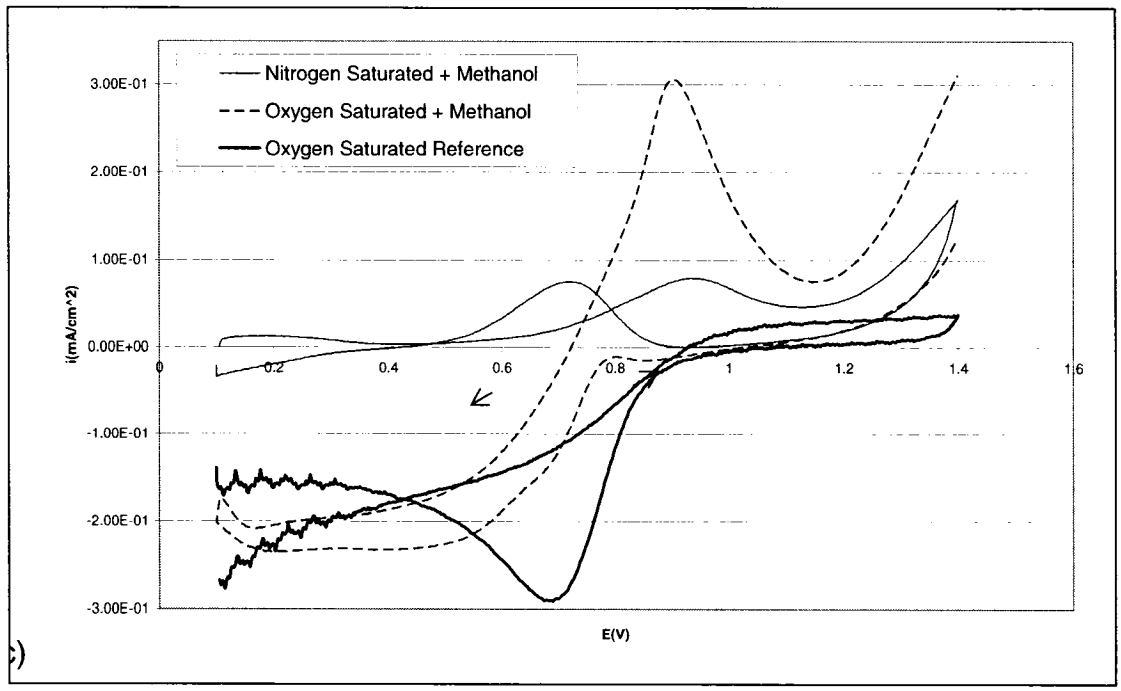

Figure 3.5: CV in 0,5M H_2SO_4 on bulk Pt (ambient temperature, nitrogen or oxygen saturated / 60 minutes bubbling, sweep rate of 50mV/s) with 0,5M a) ethylal, b) 1,3-dioxolane, c) methanol

Figure 3.5 shows the CVs for ethylal, 1,3-dioxolane and methanol. The effect of ethylal is somewhat similar to methylal. The oxidation of ethylal makes the onset potential of the ORR drop to 0,47V. But the current density of the ORR is near those of the levels obtained from working electrodes used as the reference for the study. When 1,3-dioxolane is used as a fuel, a bigger oxidation peak during the negative scan is obtained, when compared to those obtained with the methylal fuel. But again, the onset potential for the ORR is 0,44V. Methanol doesn't oxidize too much during the negative scan. Therefore the onset potential of the ORR with methanol is slightly below 0,70V.

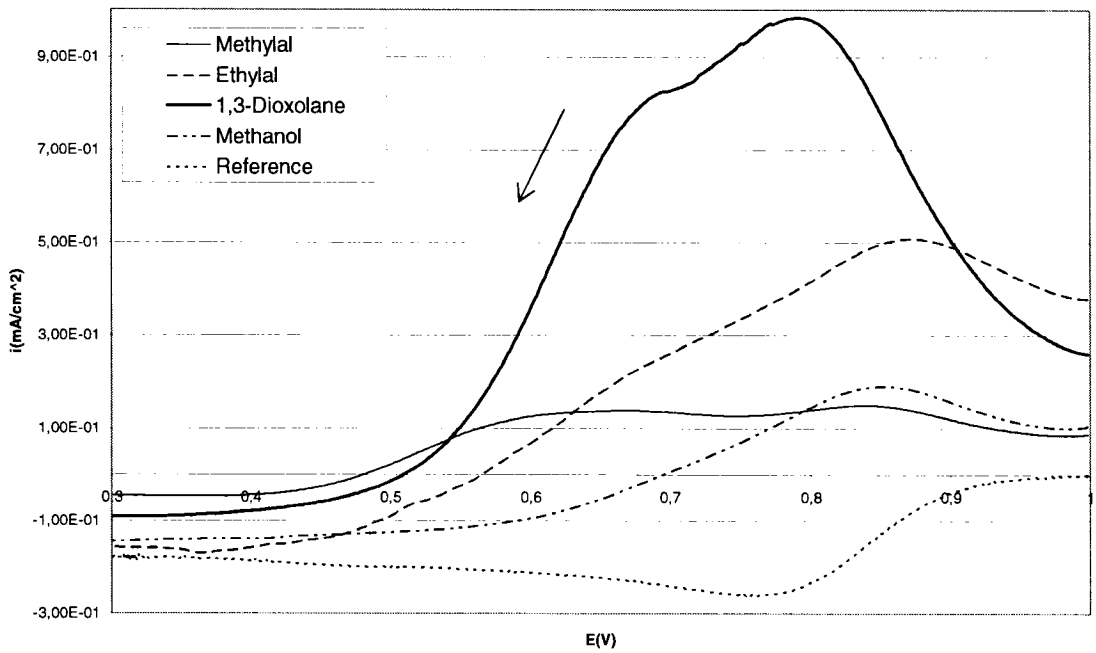

Figure 3.6: CV in 0,5M H_2SO_4 on bulk Pt (ambient temperature, oxygen saturated / 60 minutes bubbling, sweep rate of 5mV/s) with 0,5M for methylal, ethylal, 1,3-dioxolane and methanol

At slower sweeping rate (Figure 3.6), we observe that 1,3-dioxolane seems to generate the highest oxidation peaks, followed by ethylal, methanol, and methylal. We also find that the presence of 1,3-dioxolane makes the onset potential of the ORR shift to 0,51V. Furthermore, we have ethylal with an onset potential of the ORR at 0,56V, and methanol at 0,69V. We see that the greater the oxidation peak is, the greater the onset potential of the ORR is shifted negatively. But methylal seems to be a special case. Even though his oxidation peak is the lowest, it is the fuel that affects the most the onset potential of the ORR since it is lowered to 0,48V. In this case, methylal seems to have a broader oxidation peak. When compared, it looks as if methanol is the least harmful fuel for the ORR.

3.1.2 Pt/C based catalyst

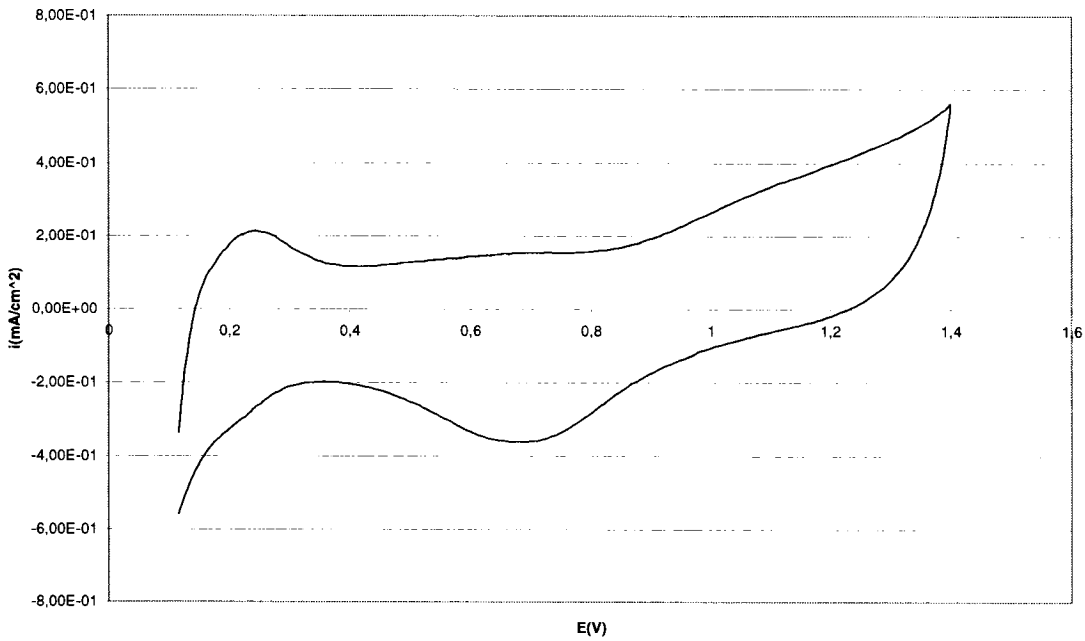

Figure 3.7: CV in 0,5M H_2SO_4 on Pt/C (ambient temperature, nitrogen saturated / 60 minutes bubbling, sweep rate of 50mV/s)

Figure 3.7 represents the reference CV on a Pt/C based catalyst in the absence of the oxygen. When Compared to the CV on pure platinum (Figure 3.1), the first notable difference is the less defined peaks. The hydrogen desorption with Pt/C based catalyst doesn't present two well defined peaks. The oxidation reduction peak is also less sharp and broader than with Pt electrode. Finally, the double layer effect is stronger with a Pt/C based catalyst.

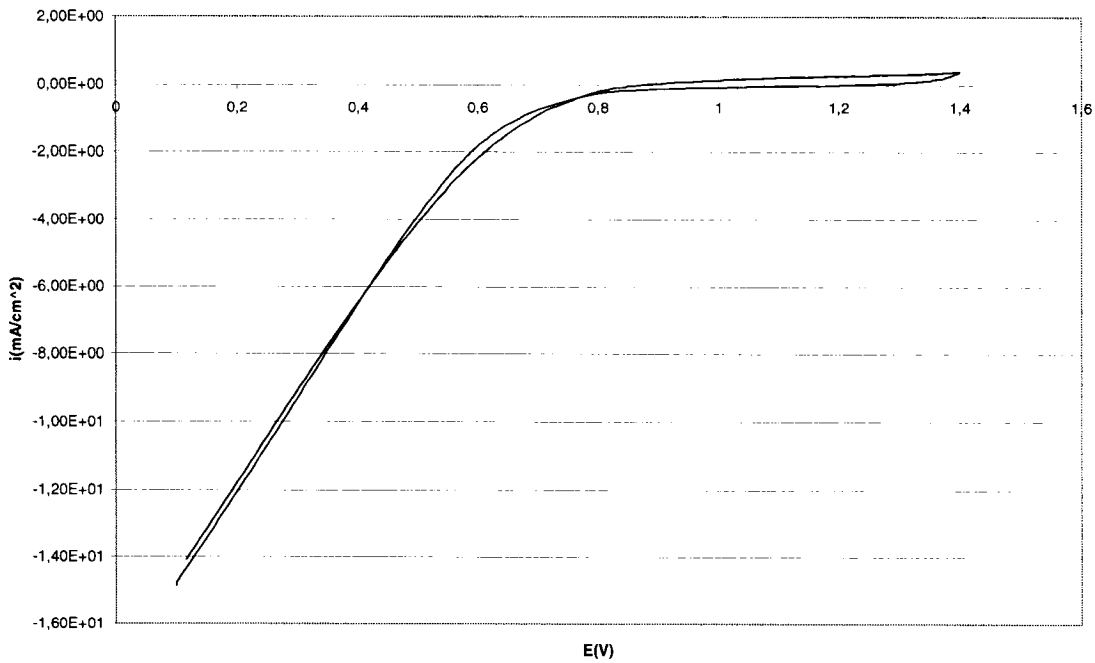

Figure 3.8: CV in 0,5M H_2SO_4 on Pt/C (ambient temperature, oxygen saturated / 60 minutes bubbling, sweep rate of 50mV/s)

The aspect of Figure 3.8 is different than that of Figure 3.2. On a Pt/C based catalyst, the ORR seems to start also slightly above 1,00V. When, compared to pure Pt electrode, there is no current density plateau starting around 0,75V. It seems that the current lowers slightly up to 0,60V. After that point, current density follows a downward linear path. It seems that the porous nature of this catalyst helps counter the mass transport limits of the oxygen.

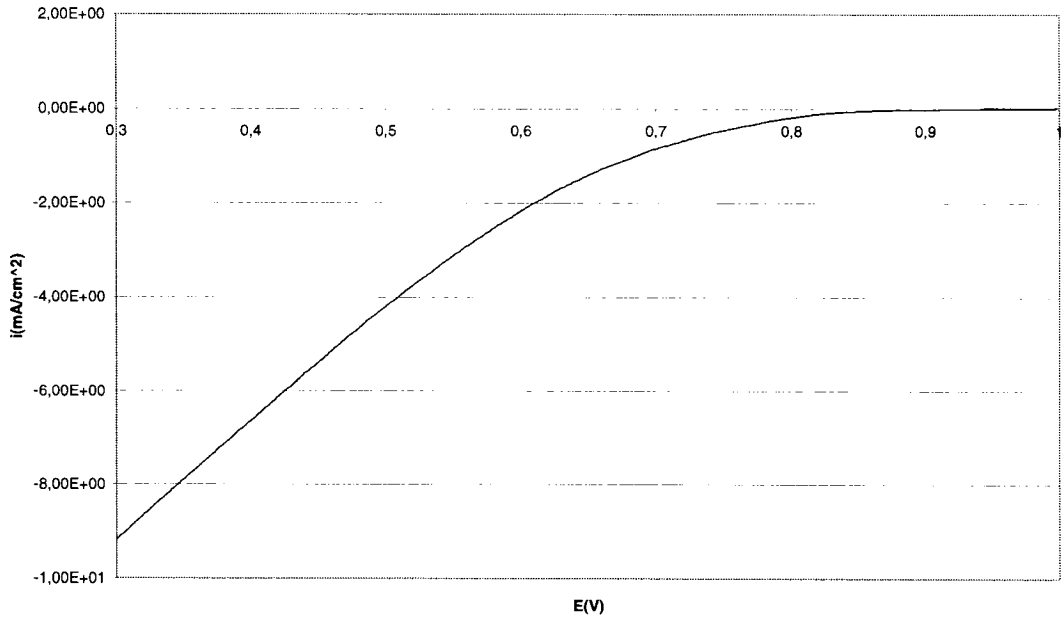

Figure 3.9: CV in 0,5M H_2SO_4 on Pt/C (ambient temperature, oxygen saturated / 60 minutes bubbling, sweep rate of 5mV/s)

Figure 3.9 indicates that the onset potential of the ORR on Pt/C is 0,91V, which is 0,09V lower than with a Pt plate electrode. Again, the linear decrease of the current density is seen on this figure. Even though no plateaus are reached, the current densities for the ORR are 40 times greater on Pt/C based catalysts at 0,30V. This teaches us that the nature of the Pt/C catalysts is more favorable to the yielding of higher currents, even if the onset potential of the ORR is slightly shifted to lower potentials.

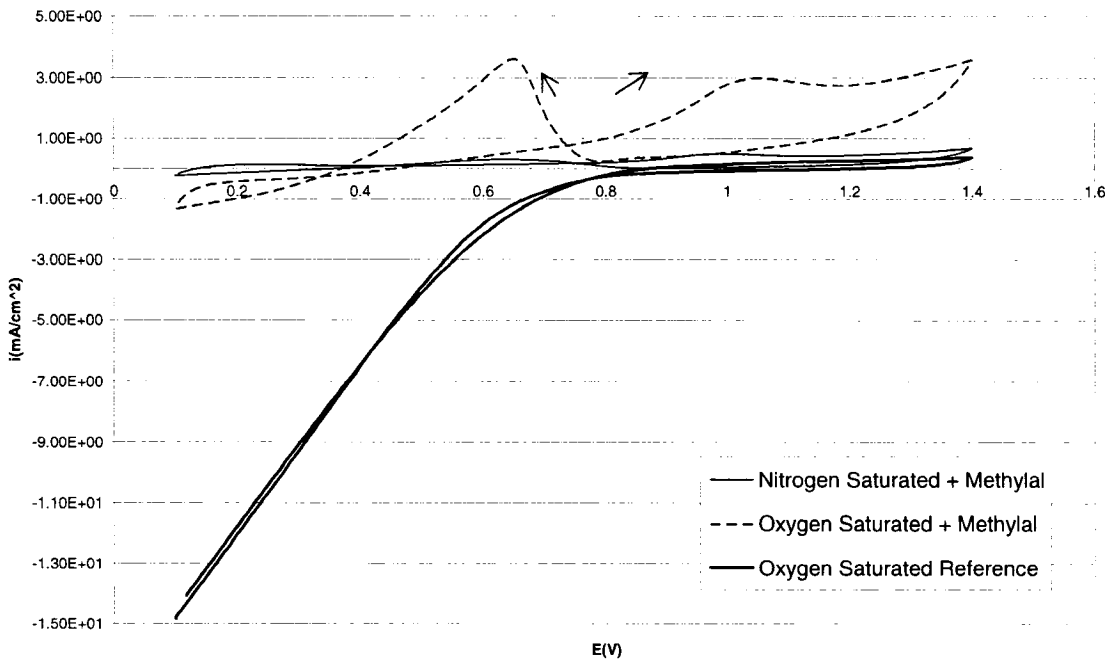

Figure 3.10: CV in 0,5M H_2SO_4 on Pt/C (ambient temperature, nitrogen or oxygen saturated / 60 minutes bubbling, sweep rate of 50mV/s) with 0,5M methylal

With the Figure 3.10, it can be observed that methylal still hinders the ORR. In the present case, the onset potential for the ORR is evaluated at 0.36V compared to 0.41V with the Pt electrode. Also, the current density for the ORR is almost 15 times lower in the presence of methylal. Another noticeable difference is that the oxidation peaks of methylal decreases in the absence of oxygen. This is the opposite effect observed on the platinum electrode.

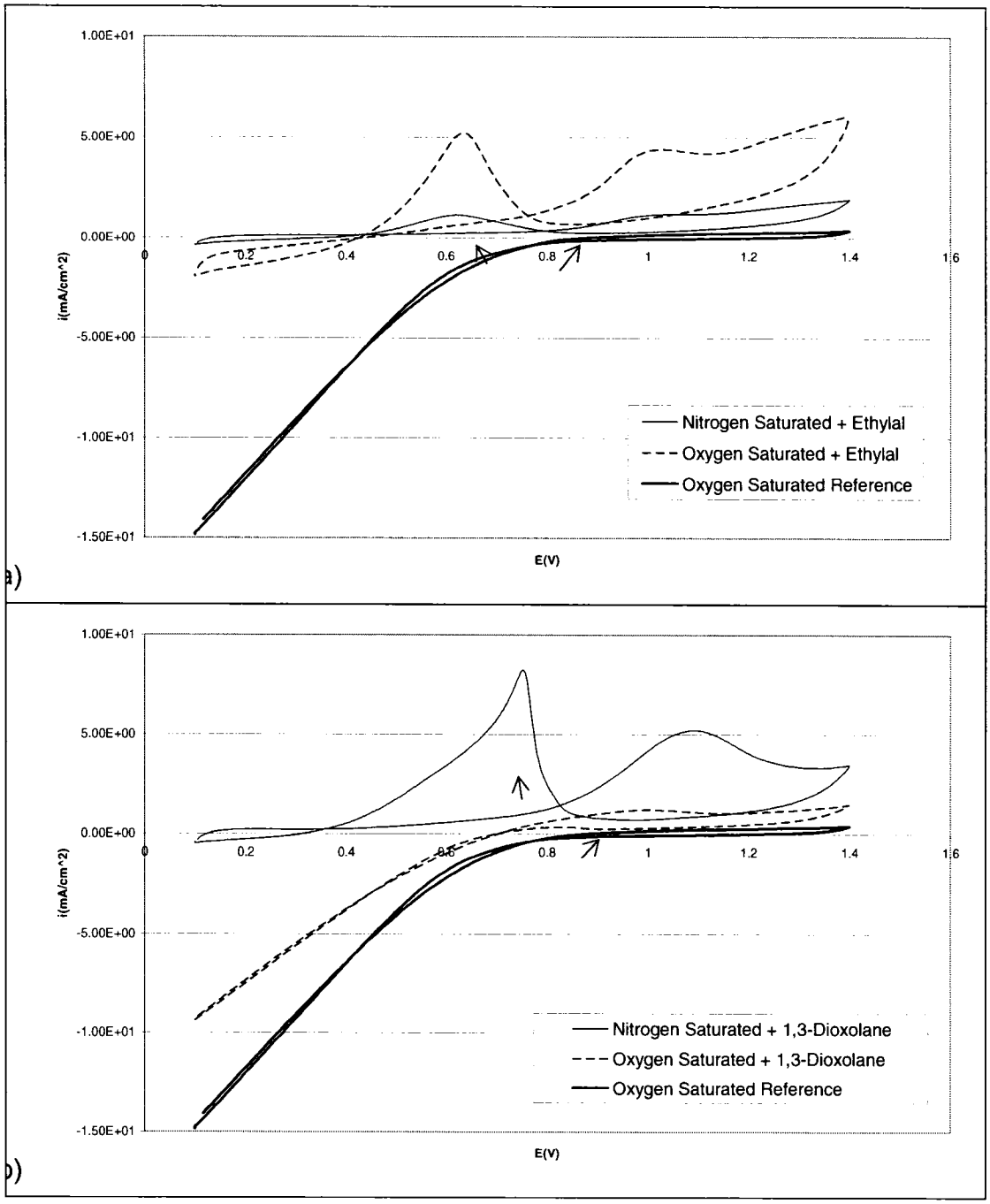
1.00E+01
5.00E+00
0.00E+00
-5.00E+00
-1.00E+01
-1.50E+01
i(mA/cm^2)
0
0.2
0.4
0.6
0.8
1
1.2
1.4
1.6
E(V)
Nitrogen Saturated + Ethylal
Oxygen Saturated + Ethylal
Oxygen Saturated Reference
a)
1.00E+01
5.00E+00
0.00E+00
-5.00E+00
-1.00E+01
-1.50E+01
i(mA/cm^2)
0
0.2
0.4
0.6
0.8
1
1.2
1.4
1.6
E(V)
Nitrogen Saturated + 1,3-Dioxolane
Oxygen Saturated + 1,3-Dioxolane
Oxygen Saturated Reference
b)

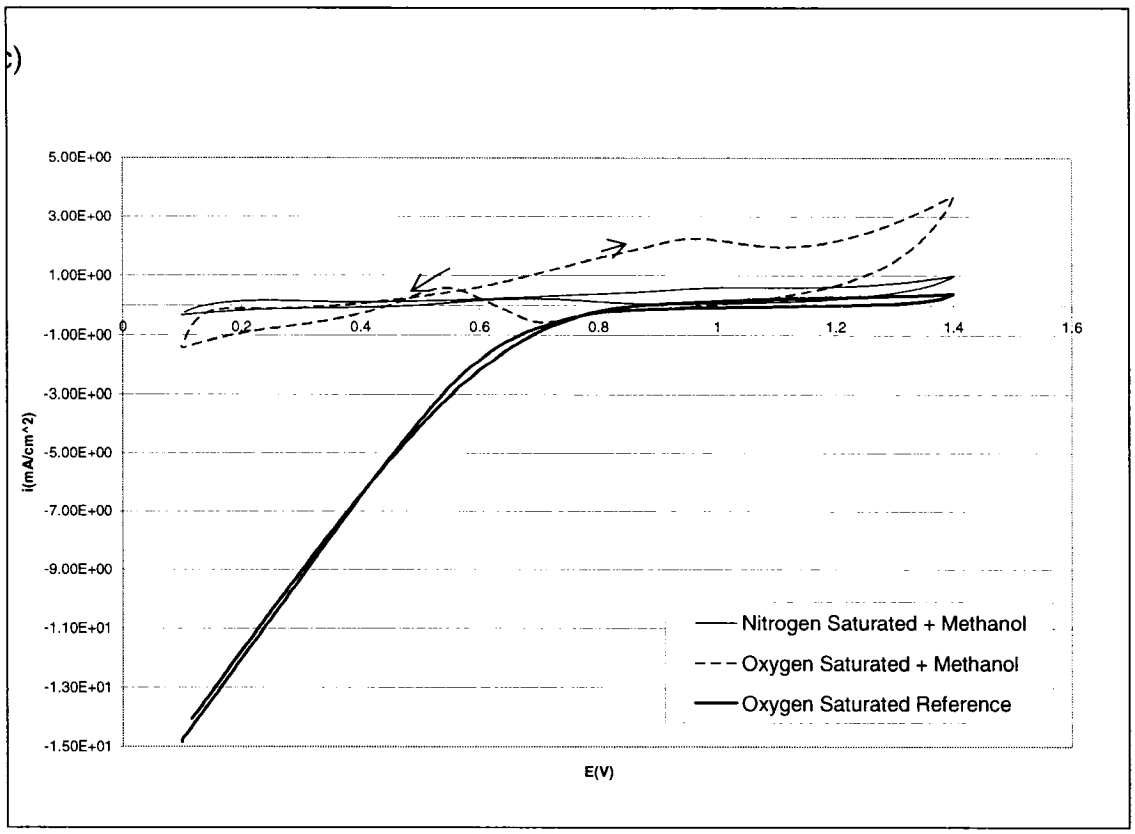

Figure 3.11: CV in 0,5M H_2SO_4 on Pt/C (ambient temperature, nitrogen or oxygen saturated / 60 minutes bubbling, sweep rate of 50mV/s) with 0,5M a) ethylal, b) 1,3-dioxolane, c) methanol

Looking at Figure 3.11 a), we see that ethylal has almost the same effects as methylal has on the ORR. With ethylal, the onset potential of the ORR is now at 0,42V on Pt/C based catalysts, instead of 0,46V on platinum. Methanol shows similar properties. But with 1,3-dioxolane on the Pt/C based catalyst, the presence of oxygen lowers the oxidation peaks. This explains why 1,3-dioxolane is the only fuel that shows an onset potential of the ORR as high as 0,69V.

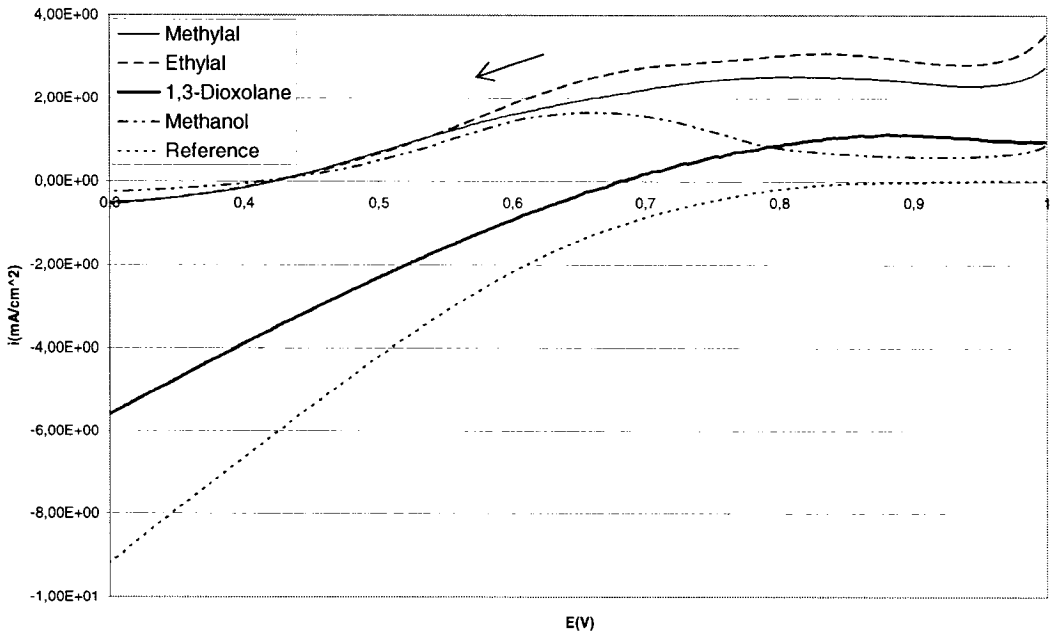

Figure 3.12: CV in 0,5M H_2SO_4 on Pt/C (ambient temperature, oxygen saturated / 60 minutes bubbling, sweep rate of 5mV/s) with 0,5M methylal, ethylal, 1,3-dioxolane and methanol

Table 3.1: Onset Potential of the ORR for each fuels on a Pt/C based catalyst

Fuel	Onset Potential (E/RHE)
Methylal	0,423
Ethylal	0,423
1,3-Dioxolane	0,680
Methanol	0,413

With more precision, Figure 3.12 gives us a more insightful view of the ORR with the fuels on a Pt/C based catalyst. It seems that with methylal, ethylal and methanol the onset potential of the ORR is around 0,42V. With ethylal we observe the highest oxidation peak, followed closely by methylal and methanol. The methanol peak is also at

a lower potential than the first two. As for 1,3-dioxolane, it seems that it is the fuel that allows for a better reduction of oxygen since the onset potential is evaluated at 0,68V.

If we compare these results with the ones obtained on a platinum catalyst, we clearly see that we have worst performances with methylal, ethylal and methanol in presence of oxygen. It is with methanol that the drop of performance is the most noticeable. But with 1,3-dioxolane, the ORR is favored on a Pt/C based catalyst. For now, we can conclude that 1,3-dioxolane is the least harmful to the ORR when using a Pt/C electrode.

3.2 Effect of the fuel on the oxygen reduction reaction (ORR) of binary alloyed Pt based catalyst

3.2.1 PtRu/C based catalyst

Figure 3.13 below shows the reference curves with the saturation of nitrogen and oxygen on a PtRu/C based catalyst. At first glance, the nitrogen reference is similar to the one obtained for the Pt/C based catalyst (Figure 3.7). We can also notice that the difference resides in the fact that the peaks are flatter with the PtRu/C based catalyst. Moving on to the oxygen saturated reference, we see that with oxygen the CV shows a bigger double layer affect. The graph looks almost as if there were a resistance in the system since the curve is inclined.

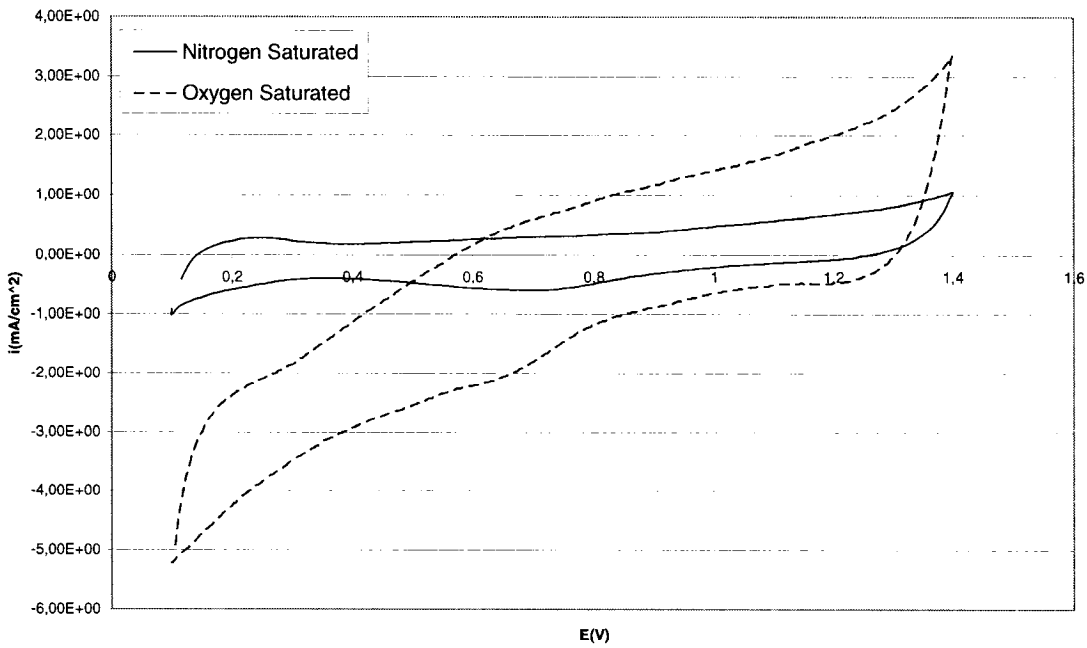

Figure 3.13: CV in 0,5M H_2SO_4 on PtRu/C (ambient temperature, nitrogen or oxygen saturated / 60 minutes bubbling, sweep rate of 50mV/s)

When scanning at 5mV/sec, we obtain the figure 3.14 with the PtRu/C based catalyst. In this case, we now find a more similar plot compared with the Pt/C based catalyst in Figure 3.9. Even more surprising is the onset potential for PtRu/C is evaluated at 0,97V which is higher than the 0,91V obtained with Pt/C and close to the 1,00V found on the bulk Pt electrode. Another notable difference with the Pt/C based catalyst is that for PtRu/C catalyst the current density seems to stabilize around 0,80V. After that point, the current density decreases linearly just like the Pt/C based catalyst. At 0,30V, the current density for PtRu/C based catalyst is 3 times less than that of the Pt/C catalyst.

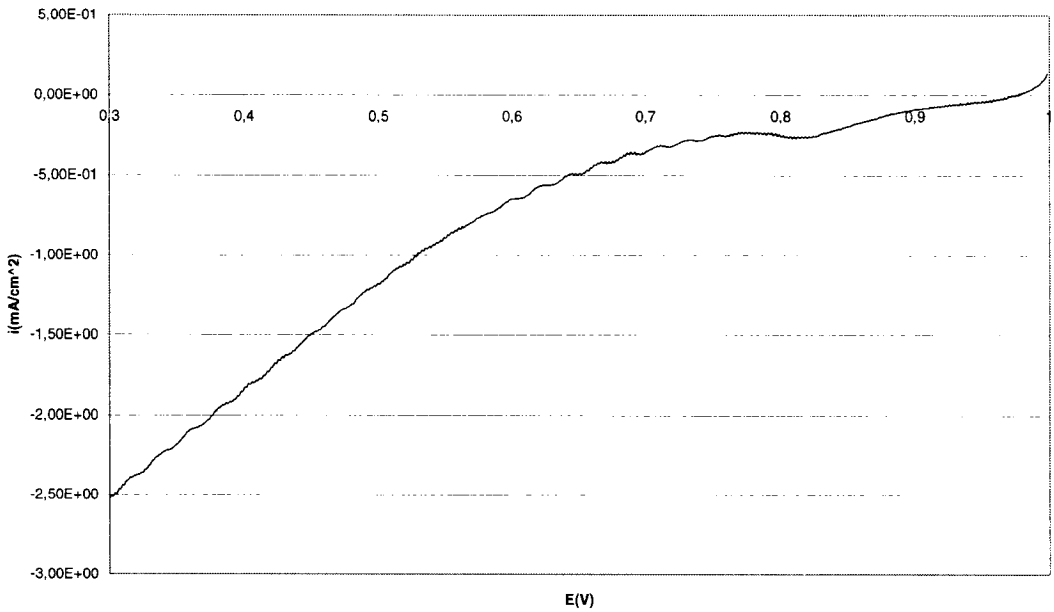

Figure 3.14: CV in 0,5M H_2SO_4 on PtRu/C (ambient temperature, oxygen saturated / 60 minutes bubbling, sweep rate of 5mV/s)

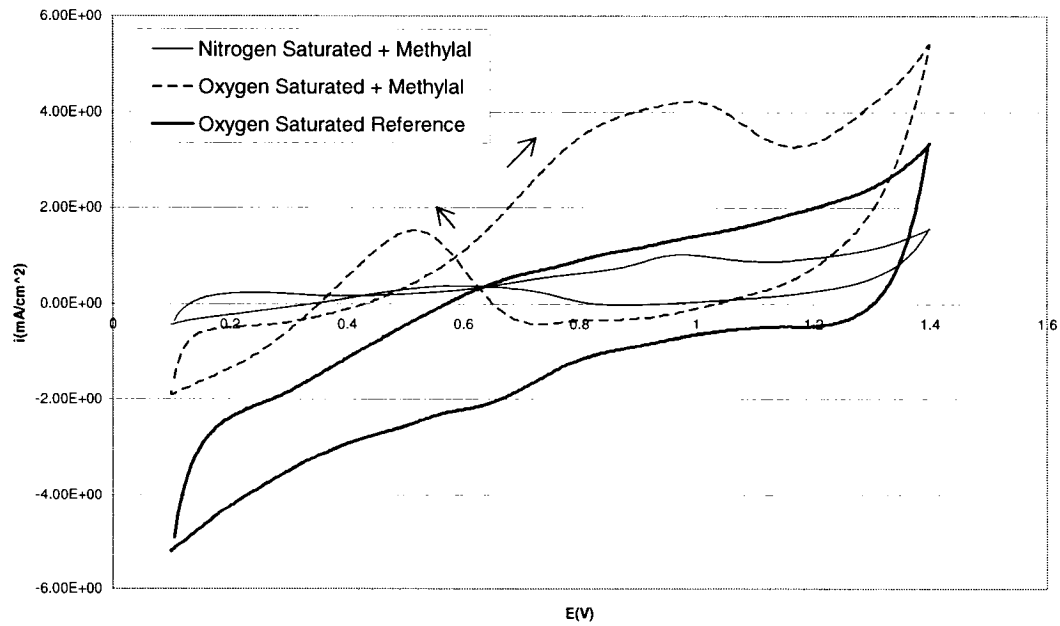

Figure 3.15: CV in 0,5M H_2SO_4 on PtRu/C (ambient temperature, nitrogen or oxygen saturated / 60 minutes bubbling, sweep rate of 50mV/s) with 0,5M methylal

Figure 3.15 shows that methylal has higher oxidation peaks in the presence of oxygen, just like on Pt/C. We have a negative current between for 1,00V and 0,65V when in presence of oxygen. But more likely, the onset potential of the ORR is 0,35V. Compared to Pt/C based catalyst, the oxidation peaks of methylal are located at lower potentials and are a bit broader.

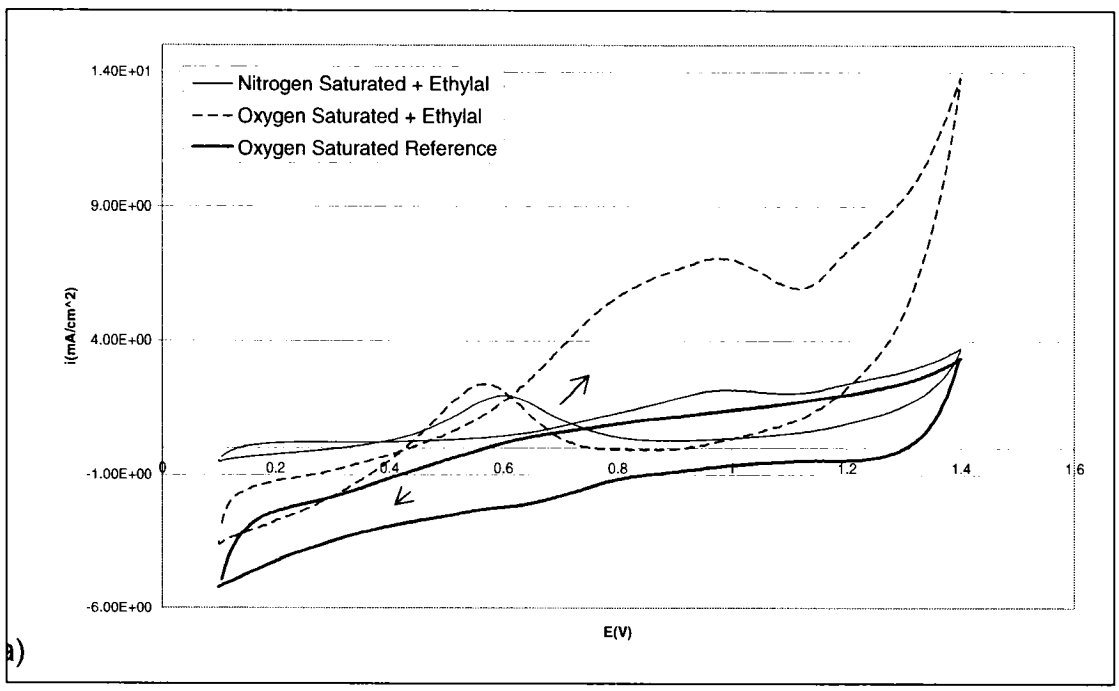

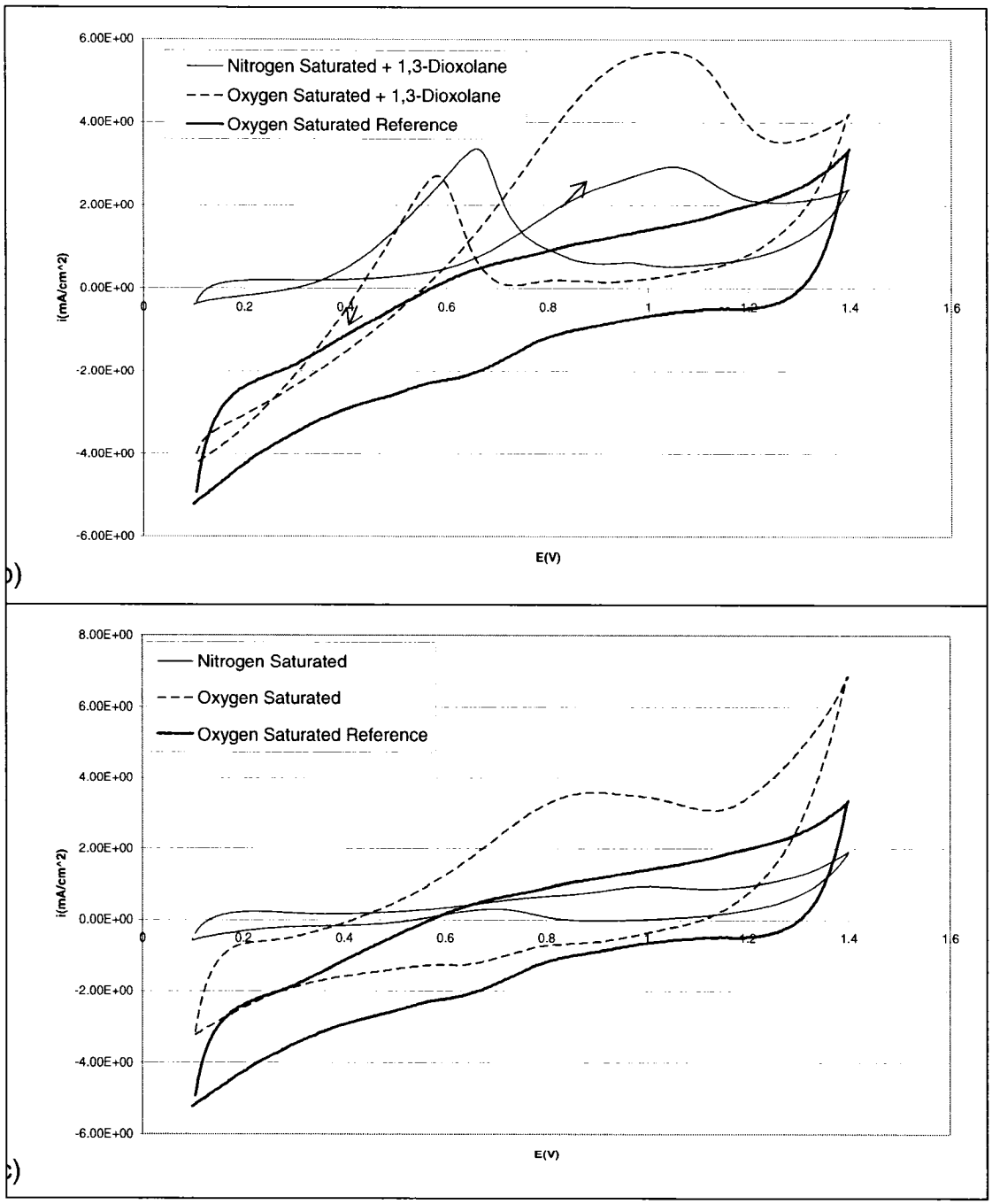

Figure 3.16: CV in 0,5M H_2SO_4 on PtRu/C (ambient temperature, nitrogen or oxygen saturated / 60 minutes bubbling, sweep rate of 50mV/s) with 0,5M a) ethylal, b) 1,3-dioxolane, c) methanol

By comparing Figure 3.16 to Figure 3.11 we can immediately see that the PtRu/C based catalyst seems to diminish the oxidation peaks during the negative scanning. Again we find the peaks are broader and shifted to lower potentials for all the fuels tested.

More interestingly, Figure 3.17 shows us to which extent the PtRu/C based catalyst has an effect on the ORR with the fuels. First, we can see that ethylal and 1,3-dioxolane show similar high and broad oxidation peaks. Methylal seems not to show any clear peaks, but only one slow decreasing slope. Methanol has the smallest oxidation peak. As for the observables peaks, they are all located around 0,75V. Compared to the Pt/C based catalyst, methanol peaks are found at a higher potential and the acetals at a lower potential. More importantly, we find that with methanol in solution, the onset potential for the ORR is the highest at 0,54V. The acetals offer onset potentials in the range of 0,40V to 0,50V. We find that for 1,3-dioxolane, ethylal and methylal, their onset potentials for the ORR are respectively 0,47V, 0,42V and 0,41V. When looking at the current densities at 0,30V, we find that methylal has the lowest oxidation current followed by methanol and ethylal. 1,3-dioxolane has the closest reduction current compared to the reference plot. With either methylal or ethylal, we can observe that the onset potentials for the ORR are the same when using Pt/C and PtRu/C based catalysts. But as for 1,3-dioxolane there is a sharp drop when using PtRu/C catalyst and methanol shows a higher ORR onset potential with this same catalyst.

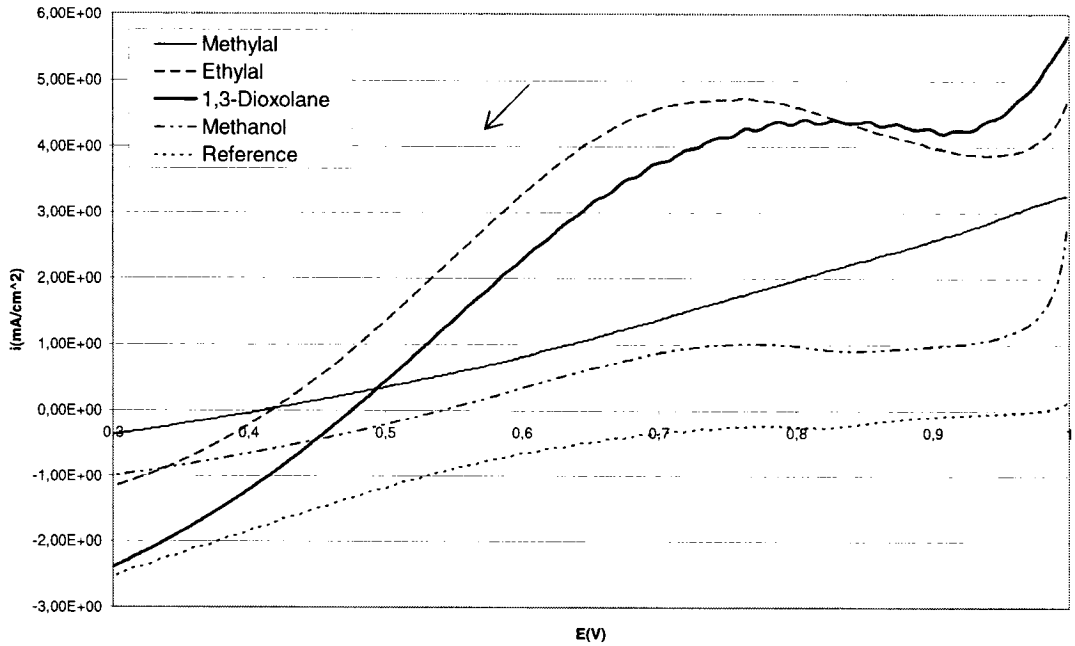

Figure 3.17: CV in 0,5M H_2SO_4 on PtRu/C (ambient temperature, oxygen saturated / 60 minutes bubbling, sweep rate of 5mV/s) with 0,5M methylal, ethylal, 1,3-dioxolane and methanol

Table 3.2: Onset Potential of the ORR for each fuels on a PtRu/C based catalyst

Fuel	Onset Potential (E/RHE)
Methylal	0,412
Ethylal	0,417
1,3-Dioxolane	0,476
Methanol	0,542

3.2.2 PtIr/C based catalyst

The PtIr/C based catalyst shows more defined peaks when in a nitrogen atmosphere compared to both Pt/C and PtRu/C catalysts. Figure 3.18 also shows that under an

oxygen saturated atmosphere, we still can see the ORR effect on the catalyst. But with the difference with other catalysts, it seems in this case that above 0,80V the effect of oxygen is barely noticeable. But lower than this potential, the plot seems to bend towards negatives currents. We can still perceive the oxygen reduction peak on the 'oxygen saturated' plot.

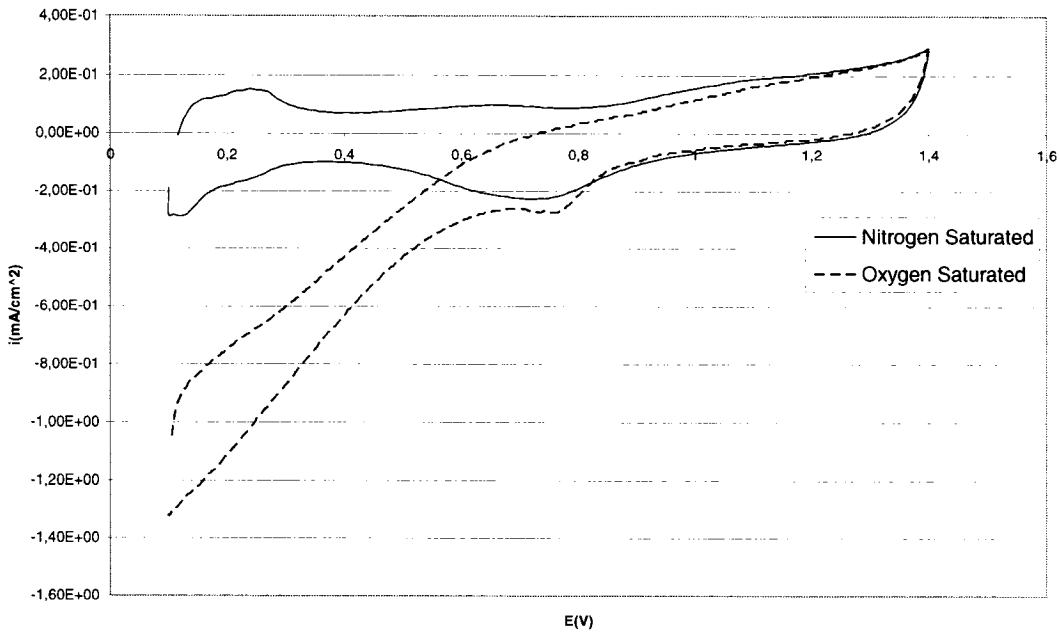

Figure 3.18: CV in 0,5M H_2SO_4 on PtIr/C (ambient temperature, nitrogen or oxygen saturated / 60 minutes bubbling, sweep rate of 50mV/s)

Figure 3.19 shows that on a PtIr/C based catalysts, the oxidation current looks somewhat like the curve obtained between 0,75V and 1,00V on pure platinum. The plot follows sort of an 'S' shaped path starting 0,97V until reaching 0,75V. But in contradiction with the Pt electrode, we find that the oxidation current further drops in a linear way. This drop is again explained by the porous nature of the PtIr/C based catalyst.

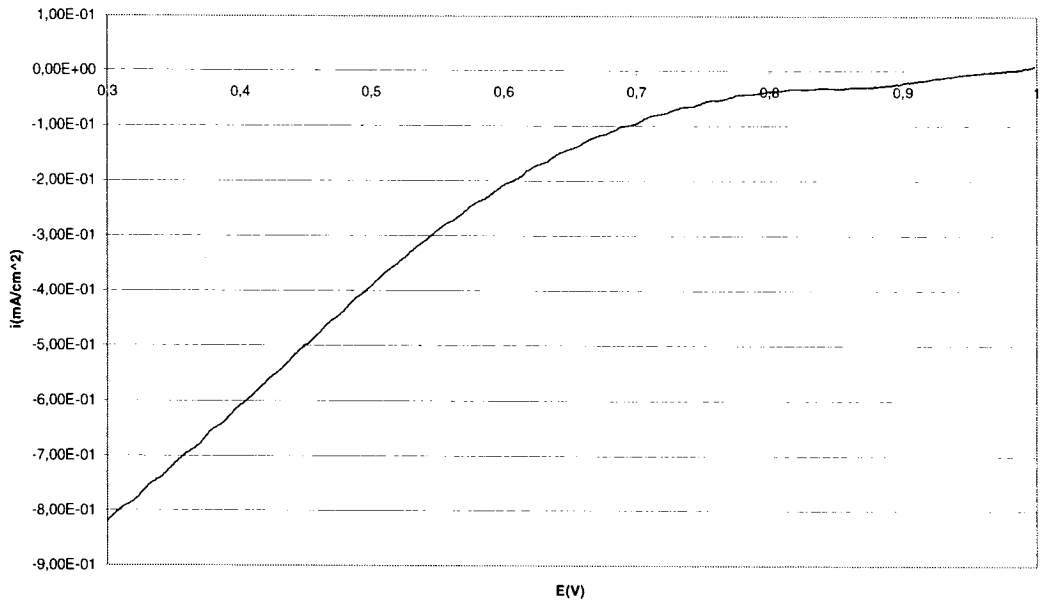

Figure 3.19: CV in 0,5M H_2SO_4 on PtIr/C (ambient temperature, oxygen saturated / 60 minutes bubbling, sweep rate of 5mV/s)

By adding methylal in the electrolyte (Figure 3.20) in an oxygen saturated atmosphere, the negative oxidation peak is a lot weaker and shifted to higher potentials compared to a nitrogen saturated atmosphere. But with methylal a higher oxidation peak is observed in the positive scan when oxygen is present. Looking at lower potentials, we see that the presence of methylal provokes a slight drop in the reduction current.

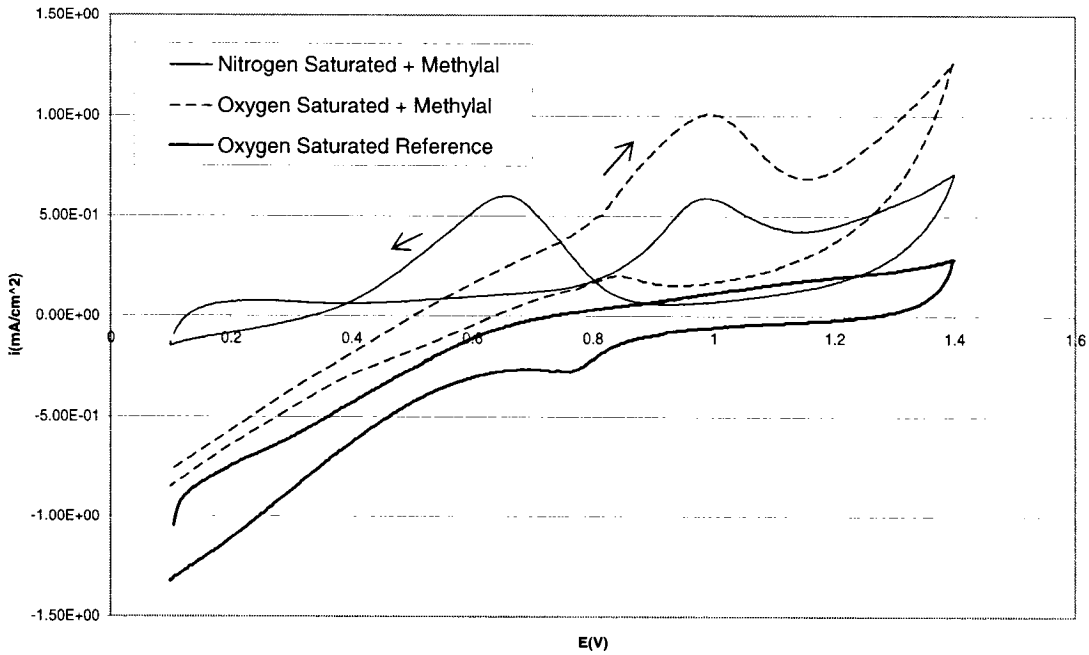

Figure 3.20: CV in 0,5M H_2SO_4 on PtIr/C (ambient temperature, nitrogen or oxygen saturated / 60 minutes bubbling, sweep rate of 50mV/s) with 0,5M methylal

Testing the three other fuels on the PtIr/C based catalyst, we obtain Figure 3.21 below. At first glance, we immediately see that oxygen has a positive oxidizing effect on ethylal just like methylal. But with 1,3-dioxolane and methanol, the presence of oxygen generates the opposite effect. Both ethylal and 1,3-dioxolane have relatively high oxidation currents during the negative scan. In comparison, methanol has a smaller oxidation peak. This explains why with methanol we seem to obtain a higher onset potential for the ORR. Regardless of this advantage, methanol seems to be more harmful to the reduction process when reaching lower potentials. As for ethylal, those currents a slightly above those of the reference plot. And 1,3-dioxolane generates a current similar to the oxygen saturated reference on the PtIr/C based catalyst.

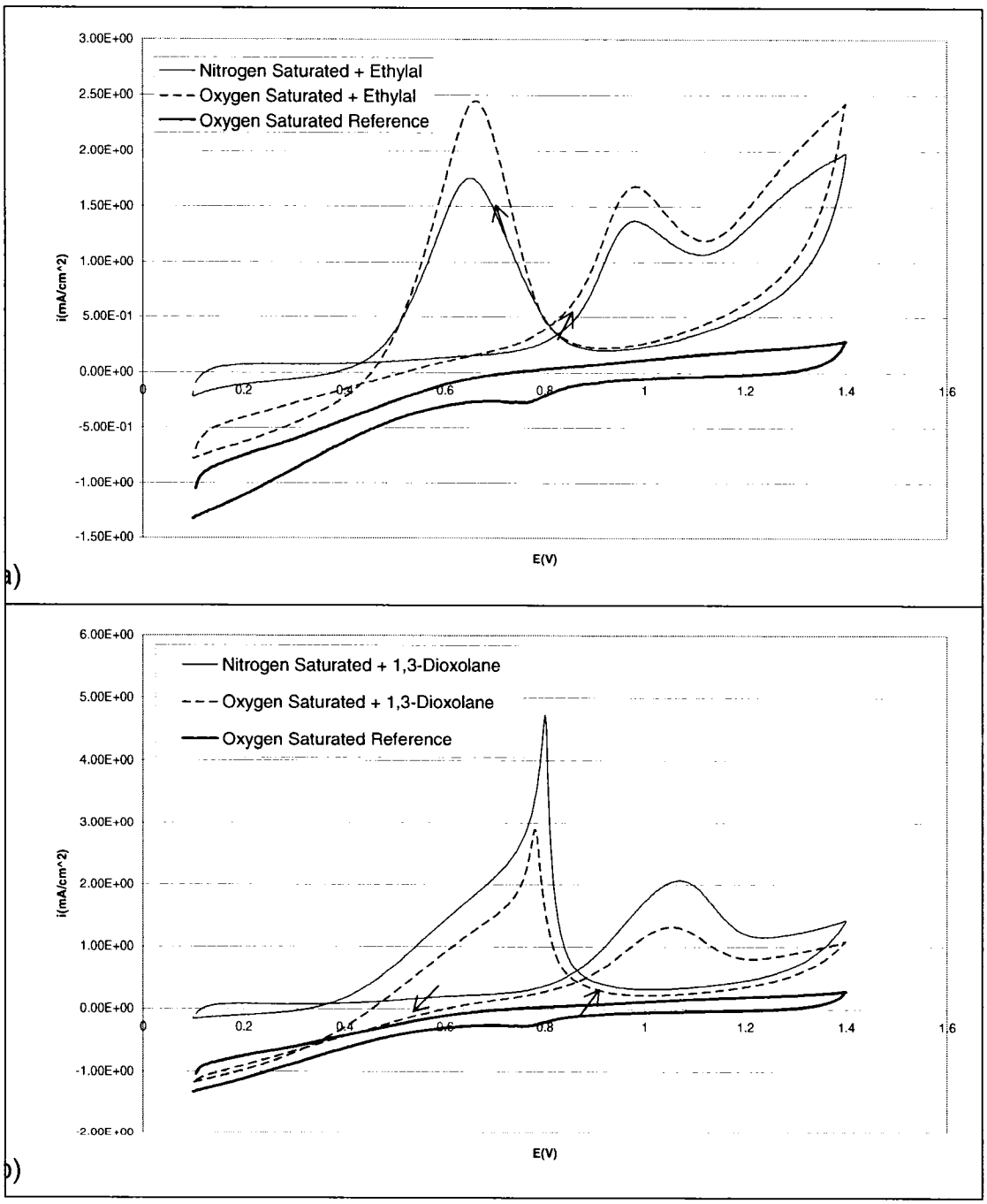
Nitrogen Saturated + Ethylal
Oxygen Saturated + Ethylal
Oxygen Saturated Reference
i(mA/cm^2)
E(V)
Nitrogen Saturated + 1,3-Dioxolane
Oxygen Saturated + 1,3-Dioxolane
Oxygen Saturated Reference
i(mA/cm^2)
E(V)

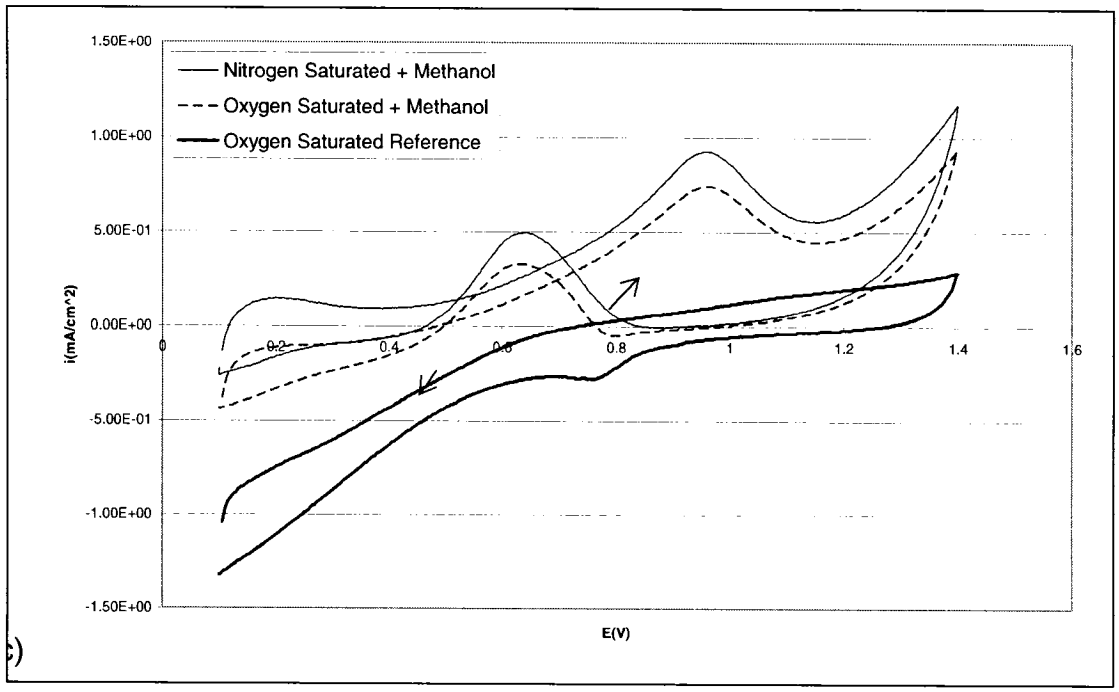

Figure 3.21: CV in 0,5M H_2SO_4 on PtIr/C (ambient temperature, nitrogen or oxygen saturated / 60 minutes bubbling, sweep rate of 50mV/s) with 0,5M a) ethylal, b) 1,3-dioxolane, c) methanol

With more precision, Figure 3.22 helps us compare the effects of the fuels on the ORR with a PtIr/C based catalyst. With the presence of ethylal we observe the highest and broadest oxidation peak among all fuels. At higher potentials, we find that methylal and 1,3-dioxolane have similar peak heights. Around 0,80V, we have the smallest oxidation peak associated in presence of methanol. The same order doesn't apply to the onset potentials for the ORR. In fact, we find that in decreasing order we have methylal, methanol, 1,3-dioxolane and ethylal with 0,69V, 0,55V, 0,52V and 0,47V respectively. As for the reduction currents at 0,30V we find that methylal and 1,3-dioxolane finish close to the reference plot. After this follows the ethylal and finally the methanol plot. From

the present observations, we can see that the PtIr/C based catalyst favors the ORR most when in the presence of methylal.

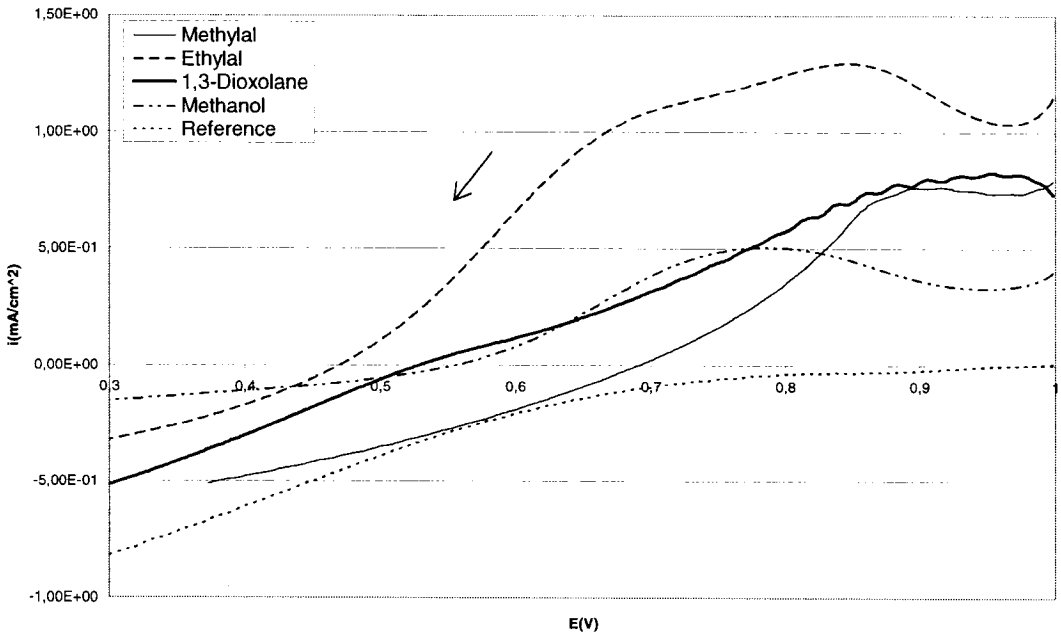

Figure 3.22: CV in 0,5M H_2SO_4 on PtIr/C (ambient temperature, oxygen saturated / 60 minutes bubbling, sweep rate of 5mV/s) with 0,5M methylal, ethylal, 1,3-dioxolane and methanol

Table 3.3: Onset Potential of the ORR for each fuels on a PtIr/C based catalyst

Fuel	Onset Potential (E/RHE)
Methylal	0,692
Ethylal	0,471
1,3-Dioxolane	0,530
Methanol	0,556

Let us summarize the effects of the catalysts on the ORR in the presence of different fuels. First, on the pure platinum catalyst the ORR was the best in presence of methanol. But as we changed to a Pt/C based catalyst, the ORR was best with 1,3-dioxolane. The other three fuels all posted similar lower ORR onset potentials. On the PtRu/C based catalyst, the advantage went again to methanol, followed by 1,3-dioxolane and ethylal and methylal finished last. With the PtIr/C based catalyst, the ORR onset potential was the highest in the presence of methylal. Methanol came in second place, while 1,3-dioxolane and ethylal took third and fourth places.

3.3 Volcano effect on the ORR of a binary alloyed Pt based catalyst

When plotting the current densities of the oxidation peak in the presence of the fuels against the ΔR (the radii difference, in Angstrom, between the alloyed metals' compared to Pt) we obtain Figure 3.23 below. From such plots, we can immediately see that a volcano effect is present in such a case. When connecting the data for each different fuel, we obtain parabolas with similar features. If we follow such a pattern, we could suggest that metal alloys with ΔR of 3Å would yield the lowest oxidation peaks for fuels in presence of oxygen. To summarize this test, we can say that a PtIr/C based catalyst gives the lowest oxidation peaks.

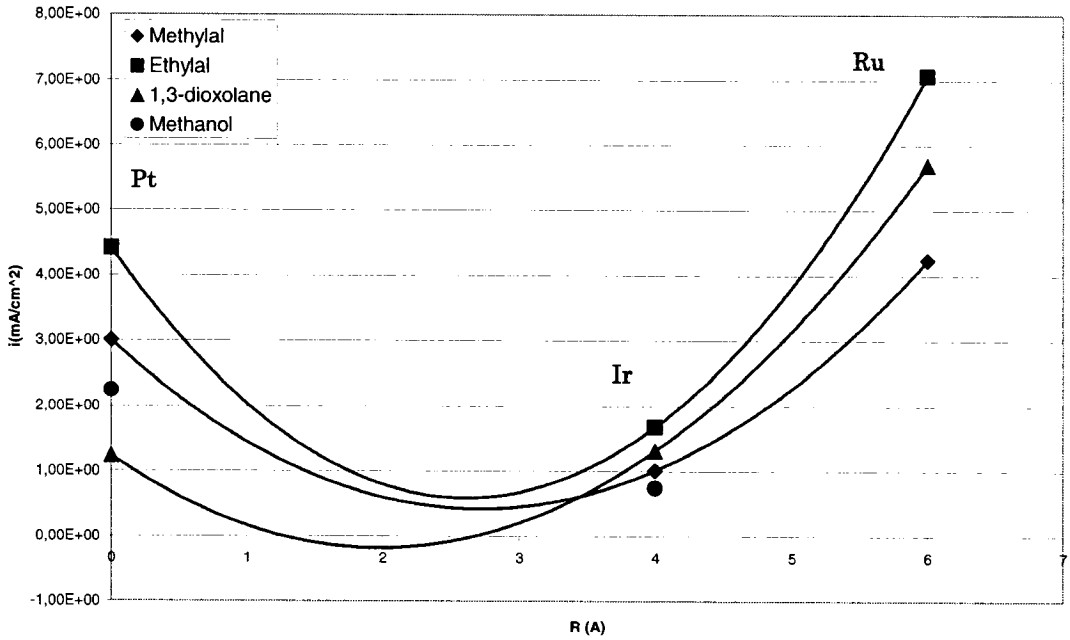

Figure 3.23: Current intensity of the oxidation peak against ΔR with methylal, ethylal, 1,3-dioxolane,and methanol in 0,5M H_2SO_4 (ambient temperature, oxygen saturated / 60 minutes bubbling, sweep rate of 50mV/s)

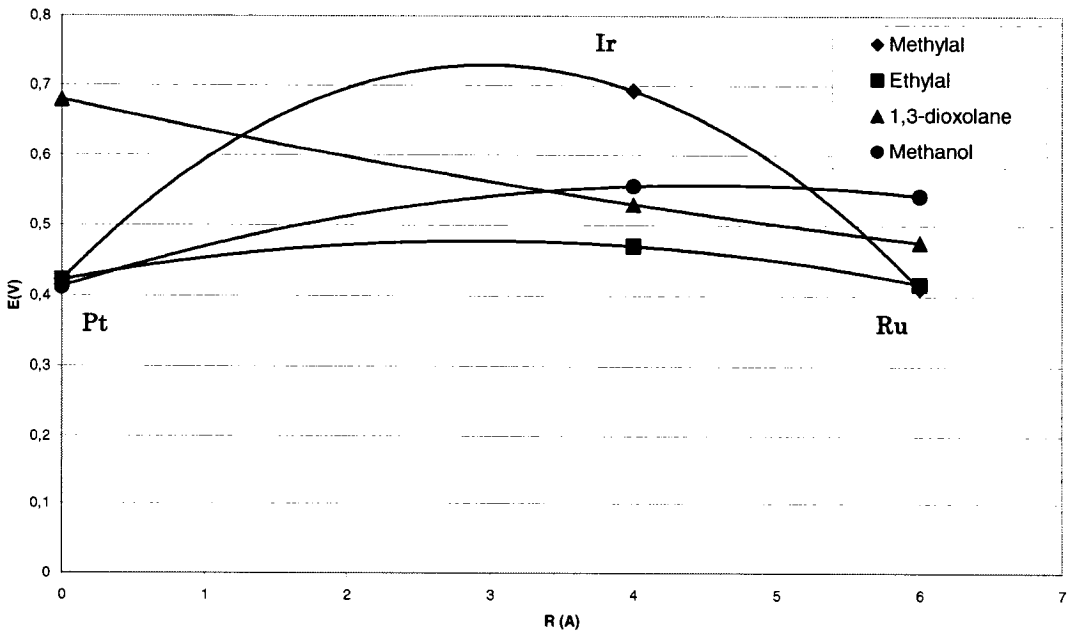

Figure 3.24: Onset potential of the ORR against ΔR with methylal, ethylal, 1,3-dioxolane,and methanol in 0,5M H_2SO_4 (ambient temperature, oxygen saturated / 60 minutes bubbling, sweep rate of 5mV/s)

By looking at Figure 3.24, again we see an overall volcano phenomenon when looking at the ORR onset potential against ΔR. First, this is the most perceptible when using methylal. Ethylal also shows a maximum when using an Ir alloy. As for methanol, since the PtIr/C and PtRu/C have almost the same ORR onset potentials, we see a milder volcano effect. 1,3-dioxolane is the exception to the rule since the bigger the ΔR is, the lower is the ORR onset potential.

Figure 3.25 demonstrates a more erratic volcano behavior. This present graphic compares the current density at 0,4V against ΔR. 1,3-dioxolane seems to show the lowest reduction current densities when using Ir as an alloy. But for all other fuels, it looks as if the Pt/C based catalyst yields the least negative current densities. As for methanol, the curve follows a slight downward pattern. When using ethylal, the current densities are somewhat similar on all catalysts tested. Also, methylal shows the opposite volcano effect compared to 1,3-dioxolane, since its parabola is opened towards the negative axis, meaning that the highest reduction current densities are measured on the PtIr/C based catalyst.

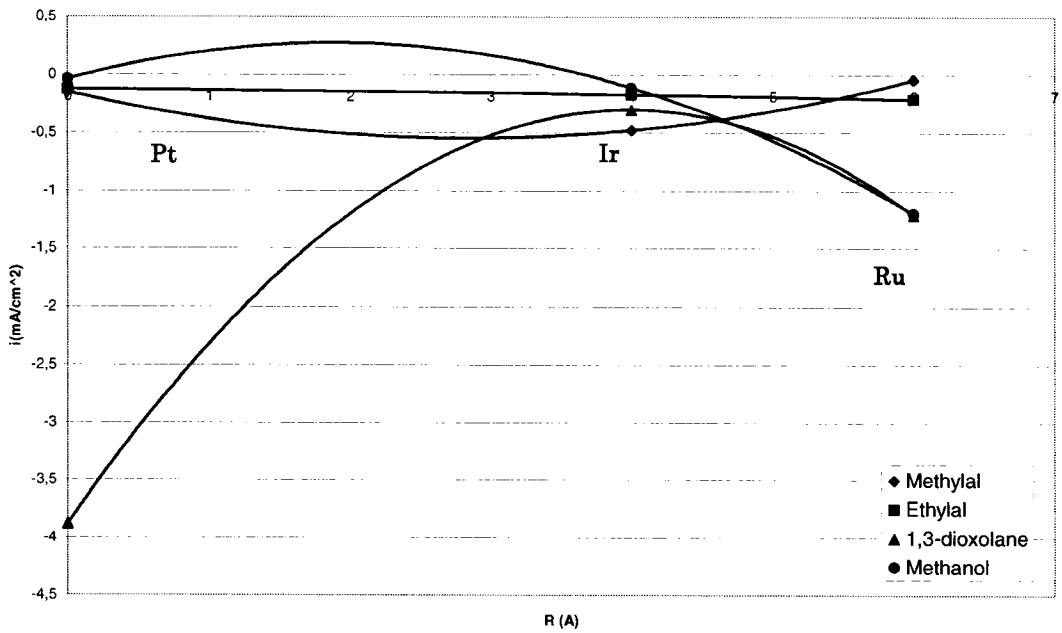

Figure 3.25: Reduction current at 0.4V against ΔR with methylal, ethylal, 1,3-dioxolane,and methanol in 0,5M H_2SO_4 (ambient temperature, oxygen saturated / 60 minutes bubbling, sweep rate of 5mV/s)

Finally, Figure 3.26 shows us the current densities at 0,6V against ΔR. In contradiction with the previous graph, it seems that a volcano effect is visible for acetals. Methylal and ethylal both have shown minimums in the vicinity of the Iridium radii. This conclusion is not actually true with 1,3-dioxolane, since its lowest point is observed for the Pt/C based catalyst. Still, all three acetals show distinct parabolas. As for methanol, like in Figure 3.25, the plot follows a negative leaner path.

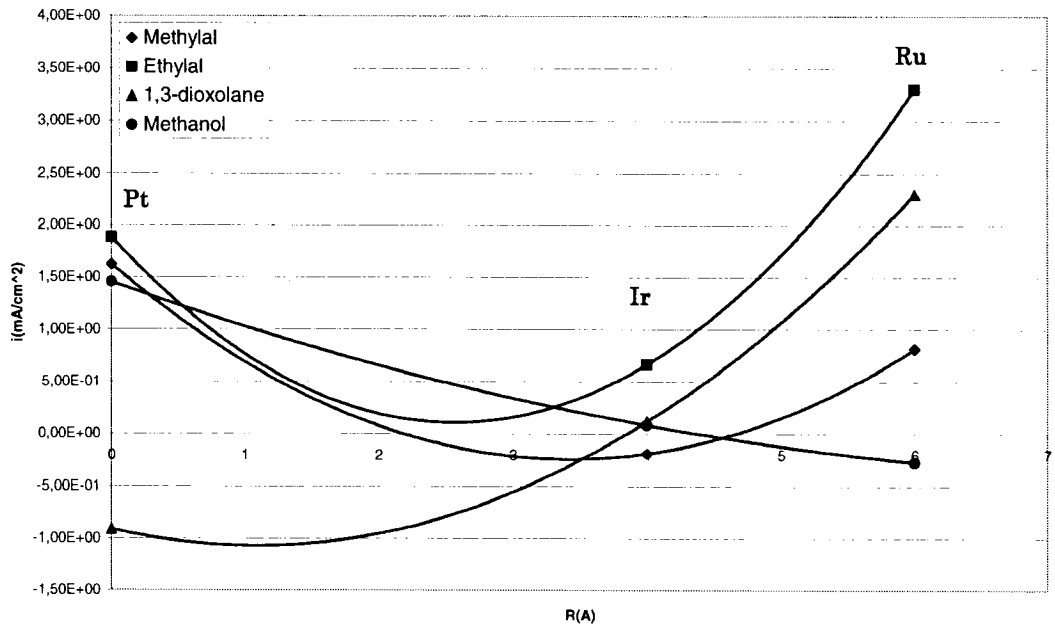

Figure 3.26: Reduction current at 0.6V against ΔR with methylal, ethylal, 1,3-dioxolane,and methanol in 0,5M H_2SO_4 (ambient temperature, oxygen saturated / 60 minutes bubbling, sweep rate of 5mV/s)

Keeping in mind all the facts we obtained by the study of the volcano effect on the ORR, we would tend to say that an Ir alloy seems to facilitate the ORR in the presence of acetals. When comparing the volcano plots of the acetals, the 1,3-dioxolane curves seemed to be the most different of the all. With methanol, we may conclude that Ruthenium is the best choice since the behavior followed a more linear path in the plots shown above.

3.4 Correlation between the performance of the catalyst and the reaction products

3.4.1 Pt/C based catalyst

In Figure 3.27 we observe the products obtained on a Pt/C based catalyst after applying a potential of 0,90V during 10 000 sec. First, we see that no fuels were completely

consumed after that period of time. Methylal was the least consumed, followed by 1,3-dioxolane, ethylal and methanol. The main reaction product found in the electrolyte was formaldehyde. Such a product is to be expected since formaldehyde is an intermediate product in the complete oxidation reaction path of acetals. This same order is found when we look at the concentrations of formaldehyde detected. It seems that the Pt/C based catalyst oxidizes acetals and formaldehyde at similar rates. Methanol doesn't show any presence of formaldehyde during this test.

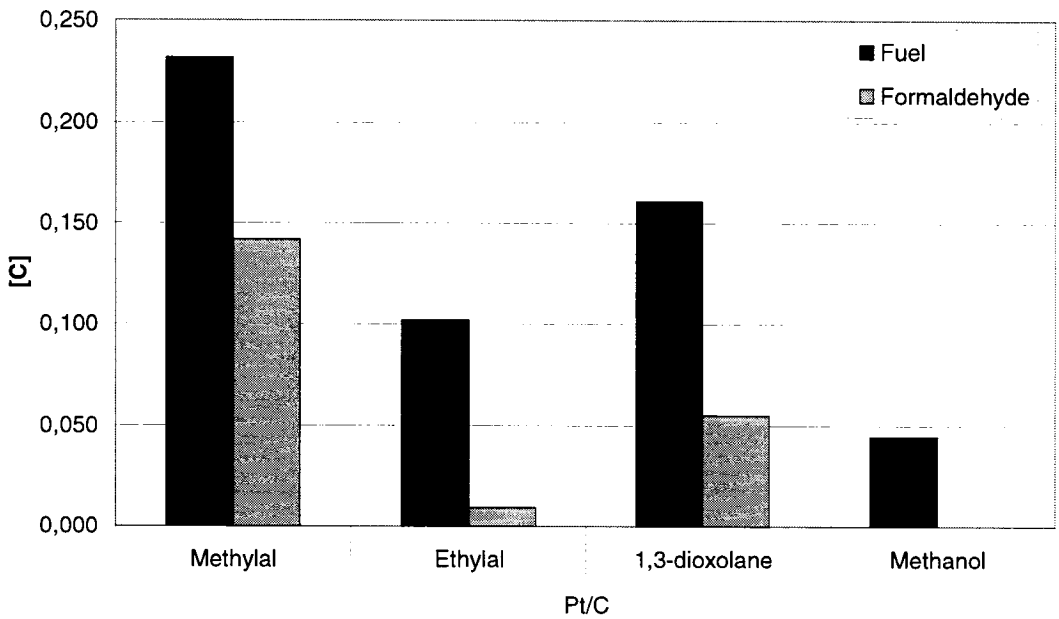

Figure 3.27: Products detected on Pt/C with an applied potential of 0,90V during 10 000 sec, for methylal, ethylal, 1,3-dioxolane, and methanol (oxygen saturated / 60 min bubbling)

3.4.2 PtRu/C based catalyst

For the same kind of tests, we replaced the catalyst by a PtRu/C based one, and we obtained Figure 3.28. Again we observe that the catalyst doesn't have the same effect on each of the fuels. It seems that the PtRu/C based catalyst consumes methylal the most, followed by methanol, 1,3-dioxolane and ethylal. Compared to the Pt/C base catalyst, this time we find that formaldehyde is detected with all four fuels. In addition, with 1,3-dioxolane we also observe a small presence of formic acid. Formic acid is around $1/10^{th}$ of the concentration of formaldehyde detected on the PtRu/C based catalyst. We find that the most formaldehyde detected is with methylal, then 1,3-dioxolane, methanol and ethylal. With the present catalyst, it seems like we detect more intermediate products when using methylal. It looks as if methylal is consumed faster than formaldehyde. But if we look at ethylal, it seems that the opposite phenomenon occurs.

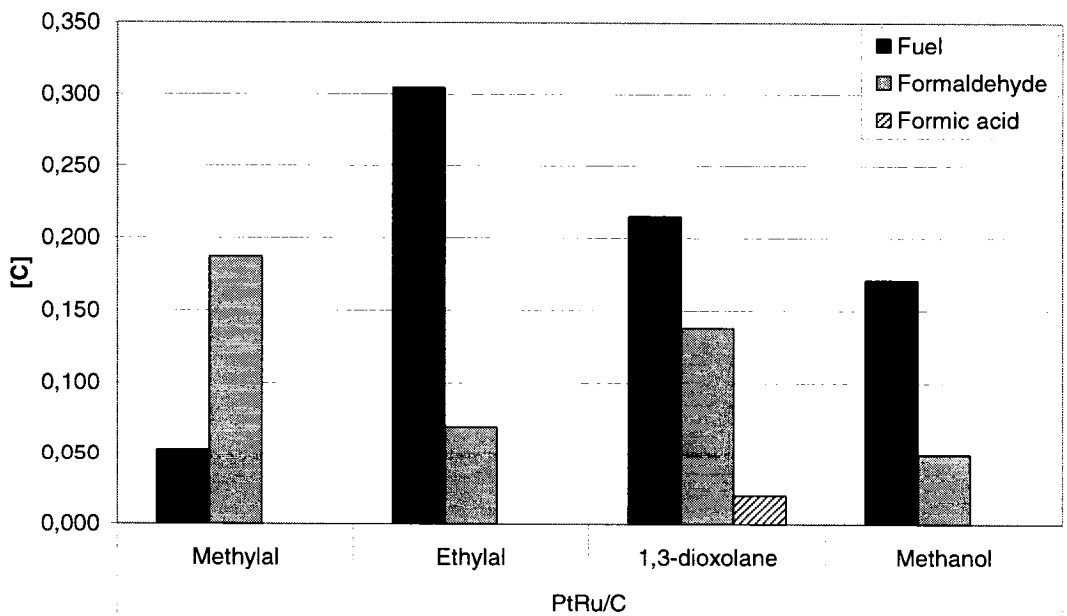

Figure 3.28: Products detected on PtRu/C with an applied potential of 0,90V during 10 000 sec, for methylal, ethylal, 1,3-dioxolane, and methanol (oxygen saturated / 60 min bubbling)

3.4.3 PtIr/C based catalyst

In Figure 3.29, we can observe the concentration of products found on the PtIr/C based catalyst. If we are careful enough, we tend to see that the Ir alloy seems to have a similar effect on the products as the Ru alloy does. By putting both Figures 3.28 and 3.29 side by side, we clearly see their resemblance. A few differences can be noticed. With methylal, the presence of formaldehyde is less perceivable. As for 1,3-dioxolane, formic acid is detected in greater concentrations. Still, we have more formaldehyde than formic acid, but the difference between those two is less than what we obtained on the PtRu/C based catalyst.

When comparing the fuel concentrations with those of the PtRu/C based catalyst, we see that those of ethylal and 1,3-dioxolane are higher on the PtIr/C catalyst. Methanol has the exact same concentration on both catalysts. Ethylal is more consumed on the PtIr/C based catalyst. As for the intermediate products, there are more of them with ethylal and 1,3-dioxlane when using the PtIr/C based catalyst. Methylal and methanol show lower concentrations of intermediates on this same catalyst compared to the PtRu/C based catalyst.

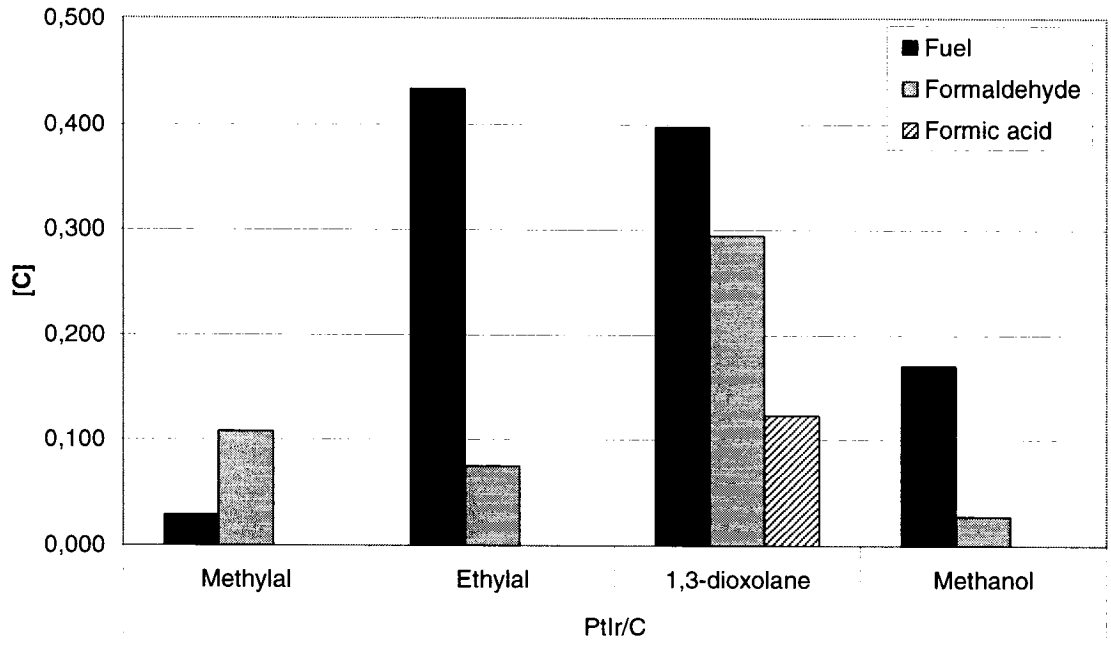

Figure 3.29: Products detected on PtIr/C with an applied potential of 0,90V during 10 000 sec, for methylal, ethylal, 1,3-dioxolane, and methanol (oxygen saturated / 60 min bubbling)

3.4.4 PtSn/C based catalyst

The concentrations of products from the PtSn/C based catalyst were collected and plotted in Figure 3.30. It clearly appears on this figure that ethylal is the least compatible with the catalyst since it is less consumed compared to the other fuels. With a concentration half of ethylal, we have methanol that comes in second place. Following this, we have 1,3-dioxolane and methylal with a concentration of around 0,100 molar. As for the concentration of formaldehyde, we have almost identical values with ethylal and 1,3-dioxolane. With methylal and methanol, we detected less formaldehyde. Finally,

we notice again the presence of formic acid with the usage of 1,3-dioxolane as a fuel on the PtSn/C based catalyst. Its concentration is closer to the value obtain on the PtRu/C catalyst than that of the PtIr/C based catalyst.

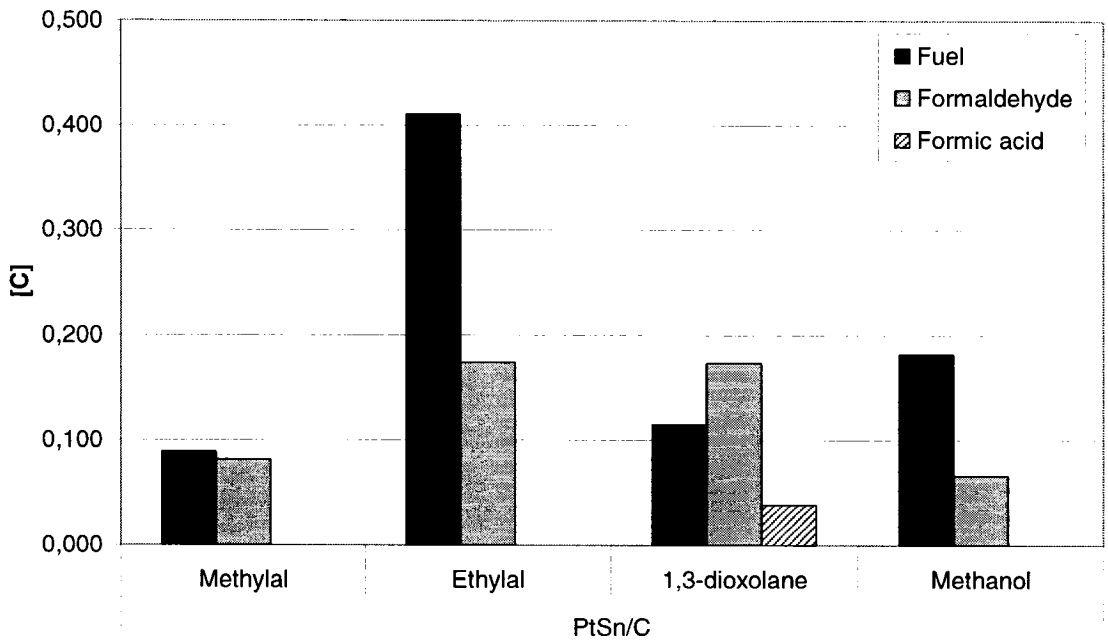

Figure 3.30: Products detected on PtSn/C with an applied potential of 0,90V during 10 000 sec, for methylal, ethylal, 1,3-dioxolane, and methanol (oxygen saturated / 60 min bubbling)

3.4.5 Effect of the catalyst on each fuel

Previously we have separately discussed the effects of the catalysts on the fuels. In order to better compare this influence we have plotted Figure 3.31. This last figure is the equivalent of figures 3.27 to 3.30, but they are classified according to the fuels. All bar charts have identical scales to enable us to make more precise comparisons between each fuel in the presence of oxygen.

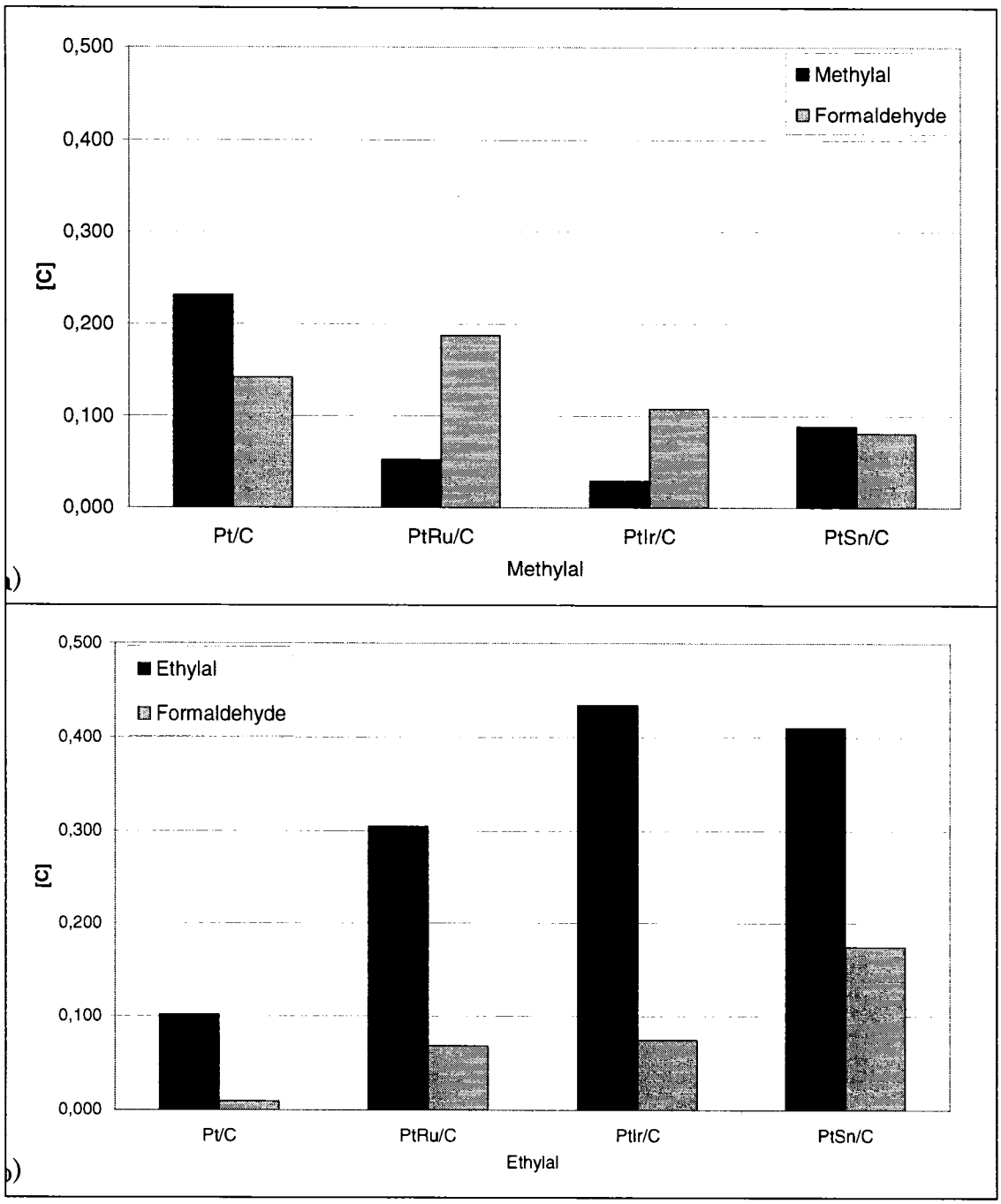
0,500
0,400
0,300
0,200
0,100
0,000
[C]
Methylal
Formaldehyde
Pt/C
PtRu/C
PtIr/C
PtSn/C
Methylal
a)
0,500
0,400
0,300
0,200
0,100
0,000
[C]
Ethylal
Formaldehyde
Pt/C
PtRu/C
PtIr/C
PtSn/C
Ethylal
b)

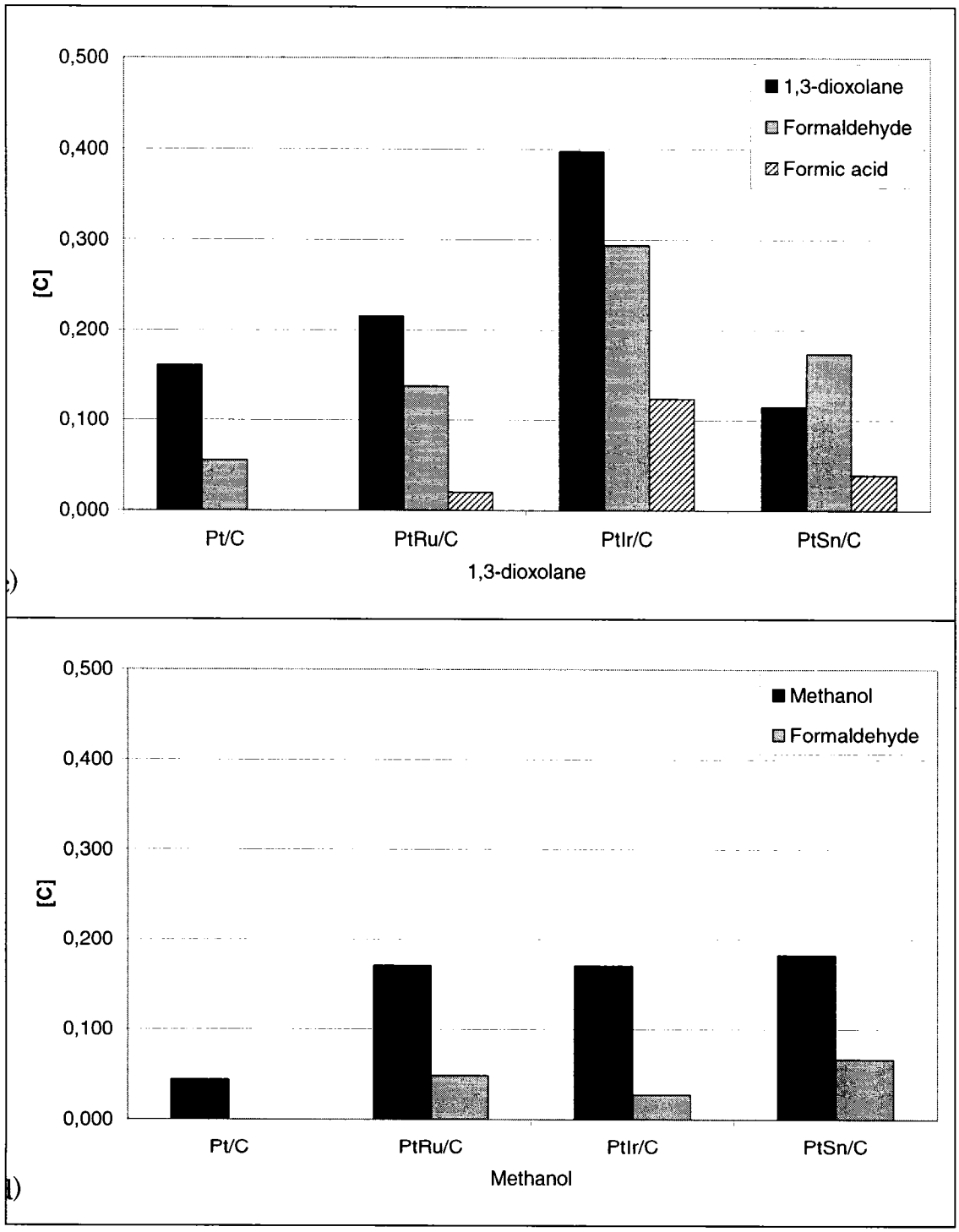

Figure 3.31: Products detected on different Pt based catalysts with an applied potential of 0,90V during 10 000 sec, (oxygen saturated / 60 min bubbling) for a) methylal, b) ethylal, c) 1,3-dioxolane, and d) methanol

We will begin by looking at the methylal case. At first glance, we see that on the Pt/C based catalyst, we obtain twice as much methylal as obtained on the alloyed catalysts. On alloyed catalyst, the consumption of methylal is the fastest on the PtIr/C, followed by the PtRu/C and PtSn/C. The concentration of formaldehyde detected decreases starting with the PtRu/C, Pt/C, PtIr/C and PtSn/C based catalysts. In the case of PtRu/C and PtIr/C catalyst, we find a higher concentration of formaldehyde than methylal. From such results we could conclude that when using methylal as a fuel, the Pt/C based catalyst would be the best choice for the cathode electrode since it minimizes the consumption of the fuel after its crossover.

While observing Figure 3.31 b), we can clearly see that the alloyed catalysts seem to consume less ethylal. The concentrations levels are three times that of Pt/C on the PtRu/C. This ratio jumps to four times when we compare Pt/C to PtSn/C and PtIr/C based catalysts. In the case of formaldehyde, the highest concentrations detected were on the PtSn/C based catalyst. In the middle, we seem to have equal amounts for PtRu/C and PtIr/C catalyst, and the lowest on the Pt/C based catalyst. Therefore we could say that the PtIr/C based catalyst would be our best choice to maximize the ORR since it oxidizes the least amount of ethylal. But we should also consider the PtSn/C based catalyst as a valid choice since its fuel concentration is just a bit lower than that of the PtIr/C. Also, it seems that the intermediate product, formaldehyde, is even less consumed on the PtSn/C based catalyst.

The consumption of 1,3-dioxolane appears to be favored the most on the PtSn/C based catalyst. We find increasing concentrations of 1,3-dioxolane when using Pt/C, then PtRu/C and then PtIr/C. In addition to the formaldehyde, formic acid is the second intermediate product detected when using binary alloyed catalysts. It seems that the PtIr/C based catalyst consumes the least amount of intermediate products. This tendency decreases when switching to PtSn/C, then PtRu/C and finally Pt/C catalysts. In the light of those results, it looks as if the PtIr/C based catalyst is the best choice to minimize the crossover effects on the ORR when using 1,3-dioxolane as the fuel.

The final fuel studied is methanol. On the Pt/C based catalyst, the detection of the fuel is the lowest among all catalyst. Also, on this same catalyst, we did not detect any other products during this test. When using binary alloyed catalysts, we detect formaldehyde in addition to the methanol. Curiously, it seems that the nature of binary alloyed catalyst doesn't seem to alter the oxidation process of the fuel too much since all three catalysts have a similar concentration of methanol and formaldehyde. In general we can say that for PtRu/C, PtIr/C and PtSn/C we have a ratio of 3.5:1 between methanol and formaldehyde. This phenomenon is somewhat different that what we can observe with all acetals. It would look as the usage of an alloyed catalyst should be favored to the Pt/C based catalyst if in the case of methanol crossover if we desire to have a better cathodic performance.

CONCLUSION

This work was the study of the effect of acetals on the cathode behavior of Direct Acetals Polymer Electrolyte Fuel Cells (DAPEFC). Methanol was used throughout this research as a benchmark. The research was done in two different laboratories. The first part of these studies conducted at l'École Polytechnique de Montréal was focused on the determination of the electrochemical responses of cell fed by the various fuels with and without alcohols using cyclic voltammograms. The effect of the acetals on the electrochemical response was determined. Tests were done on methylal, ethylal, 1,3-dioxolane and methanol all at 0.5M concentration. The catalysts used were based on Pt, Pt/C, PtRu/C and PtIr/C. The second part was conducted at the University of Kyoto and the tests focused were analyzing the electrochemical products of all four fuels on the following catalysts: Pt/C, PtRu/C, PtIr/C and PtSn/C.

The CV tests started with the bulk platinum electrode. From then on, we discussed the typical reference CVs with a sulfuric acid electrolyte in the presence and in the absence of oxygen. In the presence of oxygen, we detected the oxygen reduction reaction (ORR) during the negative scanning starting at a potential of 1.00V/RHE.

According to the cyclic voltamogramme, the ORR onset potential was greatly hindered with the presence of any fuels. On pure platinum the ORR potential is measured at 1,00V/RHE. When measuring all the combinations of fuel/catalysts, it was found that

the combinations that yielded the lowest drops of potentials were: 0,69V for methanol on Pt/C, 0,54V for methanol on PtRu/C, and 0,70V for methylal on PtIr/C.

It was shown that the variation of the current oxidation peak (at given potential) with the difference between the radius of the alloying element and those of Pt (ΔR) is a volcano plot. The lowest oxidation peak current was obtained when ΔR is close to 3Å; e.g. for PtIr/C based catalyst. This corresponds to a situation where the fuel crossover has less effect on the ORR response. Similar conclusion was drawn when the variation of the ORR onset potential with ΔR which shows a volcano shape. A highest onset potential was obtained for ΔR close to 3Å (e.g. Cr, Rh). An exception to this observation was noticed with 1,3-dioxolane because it was with ΔR close to 0Å that we obtained the highest onset potentials.

The analysis of the oxidation reaction products of the electrochemical reactions performed with each of the acetals showed that formaldehyde was produced in the cell when using carbon based electrode for each of the catalysts. Moreover, with 1,3-dioxolane, the presence of formic acid was detected when binary alloy catalysts were used. In the case of the methanol reaction on Pt/C base catalyst, in the presence of oxygen, no intermediate products were detected. For the other catalyst, formaldehyde was produced. In all the cases, it seemed that it was less susceptible to reduce oxygen in the presence of ethylal or 1,3-dioxolane on the PtIr/C based catalyst. In the case of methylal, it was shown that the ORR activity is less reduced when Pt/C was used as a catalyst. If methanol was used as a

fuel, the ORR is reduced when one of the three binary alloyed catalysts compared with the Pt/C.

Based on the results obtained in this work, the following recommendations can be suggested:

i) Further studies should focus on coupling the mass spectrometer and HPLC with the half cell in order to better quantify and detect the products in the electrolyte. By using Differential Electrochemical Mass Spectrometry, the detection of the gaseous products will be possible.

ii) It would also be advisable to have an automatic sampler which would forward the liquid to the HPLC, thus permitting faster analysis.

iii) The FTIR could also prove to be useful in confirming the results obtained with the MS, and also give us an insight into the type of species adsorbed at the catalyst's surface.

iv) If we are to find optimized cathodic catalysts, tests parameters should also include deferent operating temperatures, fuel concentrations, and electrolyte pH (acidic and alkaline).

v) The catalysts compositions should also be investigated by changing both the platinum's and binary alloy's concentrations. Also, catalyst with multiple binary alloys should be investigated.

vi) Finally, tests should be conducted in a working fuel cell in order to evaluate the effects of these ameliorations at the cathode.

REFERENCES

1. Narayanan, S.R., et al., *Direct electro-oxidation of dimethoxymethane, trimethoxymethane, and trioxane and their application in fuel cells.* Journal of the Electrochemical Society, 1997. **144**(12): p. 4195-4201.
2. Savadogo, O. and X. Yang, *Electrooxidation of acetals for direct hydrocarbon fuel cell applications.* Journal of Applied Electrochemistry, 2001. **31**(7): p. 787-792.
3. Savadogo, O. and X. Yang, *Development of Pt-Alloy and Pt-Metal Oxide Mixed Anodes f or Direct Acetal/Oxygen Polymer Electrolyte Membrane Fuel Cell (DAPEMFC).* Journal of New Materials for Electrochemical Systems, 2002. **5**: p. 9-13.
4. Cyr, Y., *Mise au point d'une pile a combustible a consommation directe d'acetals liquides*, in *Genie Metallurgique.* 2004, Universite de Montreal, Ecole Poytechnique de Montreal: Montreal. p. 135.
5. Vielstich, W., A. Lamm, and H.A. Gasteiger, *Handbook of Fuel Cells.* Vol. Volume 1 Fundamentals and Survey of Systems. 2003: John Wiley & Sons Ltd. 449.
6. Schoenbein, C.F., Schweiz. Ges., 1838. **82**.
7. Schoenbein, C.F., Compte Rendu Hebdomadaire des affaires de l'Academie de la Science, 1838. **7**: p. 741.
8. Grove, W.R., Philosophy Magasine, 1839. **14**: p. 127.
9. Grove, W.R., Phil. Transactions (I), 1845: p. 127.
10. Wasmus, S. and A. Kuver, *Methanol oxidation and direct methanol fuel cells: a selective review.* Journal of Electroanalytical Chemistry, 1998. **461**: p. 14-31.
11. Lin, W.-F., J.-T. Wang, and R.F. Savinell, *On-line FTIR spectroscopic investigations of methanol oxidation in a direct methanol fuel cell.* Journal of the Electrochemical Society, 1997. **144**(6): p. 1917-1922.
12. Meier, F., et al., *Analysis of Direct Methanol Fuel Cell (DMFC)-Performance via FTIR Spectroscopy of Cathode Exhaust.* Fuel Cells, 2003. **3**(4): p. 161-168.
13. Vijayaraghavan, G., L. Gao, and C. Korzeniewski, *Methanol electrochemistry at carbon-supported Pt and PtRu fuel cell catalysts: Voltammetric and in situ infrared spectroscopic measurements at 23 and 60 °C.* Langmuir, 2003. **19**(6): p. 2333-2337.
14. Fan, Q., et al., *In situ FTIR-diffuse reflection spectroscopy of the anode surface in a direct methanol/oxygen fuel cell.* Journal of the Electrochemical Society, 1996. **143**(2): p. L21-L23.

15. Jusys, Z. and R.J. Behm, *Methanol oxidation on a carbon-supported Pt fuel cell catalyst - A kinetic and mechanistic study by differential electrochemical mass spectrometry.* Journal of Physical Chemistry B, 2001. **105**(44): p. 10874-10883.
16. Wallington, T.J., et al., *Atmospheric chemistry of dimethoxymethane (CH3OCH2OCH3): Kinetics and mechanism of its reaction with OH radicals and fate of the alkoxy radicals CH3OCHO(•)OCH3 and CH3OCH2OCH2O(•).* Journal of Physical Chemistry A, 1997. **101**(29): p. 5302-5308.
17. Venkatesan, V., et al., *Conformations of dimethoxymethane: matrix isolation infrared and ab initio studies.* Spectrochimica Acta Part A: Molecular and Biomolecular Spectroscopy, 2002. **58**(3): p. 467-478.
18. Sauer, C.G., et al., *Atmospheric chemistry of 1,3-dioxolane: Kinetic, mechanistic, and modeling study of OH radical initiated oxidation.* Journal of Physical Chemistry A, 1999. **103**(30): p. 5959-5966.
19. Fan, Q., C. Pu, and E.S. Smotkin, *In situ Fourier transform infrared-diffuse reflection spectroscopy of direct methanol fuel cell anodes and cathodes.* Journal of the Electrochemical Society, 1996. **143**(10): p. 3053-3057.
20. Miki, A., et al., *Surface-enhanced infrared study of catalytic electrooxidation of formaldehyde, methyl formate, and dimethoxymethane on platinum electrodes in acidic solution.* Journal of Electroanalytical Chemistry, 2004. **563**(1): p. 23-31.
21. Jusys, Z., J. Kaiser, and R.J. Behm, *Methanol electrooxidation over Pt/C fuel cell. Catalysts: Dependence of product yields on catalyst loading.* Langmuir, 2003. **19**(17): p. 6759-6769.
22. Wasmus, S., J.-T. Wang, and R.F. Savinell, *Real-time mass spectrometric investigation of the methanol oxidation in a direct methanol fuel cell.* Journal of the Electrochemical Society, 1995. **142**(11): p. 3825-3833.
23. Coutanceau, C., et al., *Preparation of Pt-Ru bimetallic anodes by galvanostatic pulse electrodeposition: Characterization and application to the direct methanol fuel cell.* Journal of Applied Electrochemistry, 2004. **34**(1): p. 61-66.
24. Rolison, D.R., P.L. Hagans, and K.E.L. Swider, Jeffrey W., *Role of hydrous ruthenium oxide in Pt-Ru direct methanol fuel cell anode electrocatalysts: The importance of mixed electron/proton conductivity.* Langmuir, 1999. **15**(3): p. 774-779.

25. Mukerjee, S. and R.C. Urian, *Bifunctionality in Pt alloy nanocluster electrocatalysts for enhanced methanol oxidation and CO tolerance in PEM fuel cells: Electrochemical and in situ synchrotron spectroscopy.* Electrochimica Acta, 2002. **47**(19): p. 3219-3231.
26. Piela, P., et al., *Ruthenium Crossover in Direct Methanol Fuel Cell with Pt-Ru Black Anode.* Journal of The Electrochemical Society, 2004. **151**(12): p. A2053-A2059.
27. Baldauf, M. and W. Preidel, *Experimental results on the direct electrochemical oxidation of methanol in PEM fuel cells.* Journal of Applied Electrochemistry, 2001. **31**(7): p. 781-786.
28. Liu, Z., et al., *Nanosized Pt and PtRu colloids as precursors for direct methanol fuel cell catalysts.* Journal of Materials Chemistry, 2003. **13**(12): p. 3049-3052.
29. Steigerwalt, E.S., G.A. Deluga, and C.M. Lukehart, *Pt-Ru/carbon fiber nanocomposites: Synthesis, characterization, and performance as anode catalysts of direct methanol fuel cells. A search for exceptional performance.* Journal of Physical Chemistry B, 2002. **106**(4): p. 760-766.
30. Gruber, K., et al., *Optical Measurements of Platinum Based Electrocatalysts for the Electrooxidation of Methanol.* Fuel Cells, 2003. **3**(1-2): p. 3-7.
31. Choi, J.-H., et al., *Methanol oxidation on Pt/Ru, Pt/Ni, and Pt/Ru/Ni anode electrocatalysts at different temperatures for DMFCs.* Journal of the Electrochemical Society, 2003. **150**(7): p. A973-A978.
32. Yang Y and M.-W. L, *Electrochemical oxidation of methanol using dppm-bridged Ru/Pd, Ru/Pt and Ru/Au catalysts.* DALTON TRANSACTIONS, 2004. **15**: p. 2352-2356.
33. Verma, L.K., *Studies on methanol fuel cell.* Journal of Power Sources, 2000. **86**(1-2): p. 464-468.
34. Yuan, Y. and Y. Iwasawa, *Performance and characterization of supported rhenium oxide catalysts for selective oxidation of methanol to methylal.* Journal of Physical Chemistry B, 2002. **106**(17): p. 4441-4449.
35. Schell, M., *Mechanistic and fuel-cell implications of a tristable response in the electrochemical oxidation of methanol.* Journal of Electroanalytical Chemistry, 1998. **457**(1-2): p. 221-228.
36. Gao, L., H. Huang, and C. Korzeniewski, *The efficiency of methanol conversion to CO2 on thin films of Pt and PtRu fuel cell catalysts.* Electrochimica Acta, 2004. **49**(8): p. 1281-1287.

37. Jiang, R. and D. Chu, *Comparative studies of methanol crossover and cell performance for a DMFC.* Journal of the Electrochemical Society, 2004. **151**(1): p. A69-A76.
38. Heinzel, A. and V.M. Barragan, *A review of the state-of-the-art of the methanol crossover in direct methanol fuel cells.* Journal of Power Sources, 1999. **84**: p. 70-74.
39. Jiang, R. and D. Chu, *CO2 crossover through a nafion membrane in a direct methanol fuel cell.* Electrochemical and Solid-State Letters, 2002. **5**(7): p. A156-A159.
40. Longtin, G., et al. *Determination of methanol cross-over through MEA by cyclic voltammetry.* in *Fifth International Symposium on New Materials for Electrochemical Systems.* 2003. Montreal.
41. Wakabayashi, N., et al., *Characterization of Methoxy Fuels for Direct Oxidation-Type Fuel Cell.* Journal of the Electrochemical Society, 2004. **151**(10): p. A1636-A1640.
42. Beaujean, M., *Technical report.* 1995, Lambiotte et Cie.
43. Vielstich, W., *Handbook of Fuel Cells: Fundamentals Technology and Applications, Volume 2 Electrocatalysis*, ed. W. Vielstich, A. Lamm, and H.A. Gasteiger. 2003.
44. Wojciechowski, K., *Introduction aux travaux pratiques de voltamétrie.* 2004, University of Geneva. Consulté le 8 janvier 2006, tiré de http://www.unige.ch/cabe/wojciechowski/TP_VOLTA_05_06.pdf
45. Longtin, G., *Étude du comportement du méthanol dans la pile à combustible méthanol/oxygène*, in *Génie des matériaux.* 2002, École Polytechnique de Montréal: Montreal.
46. Woods, R., *Electroanalytical Chemistry, vol 9*, ed. D. M. 1976, New York: A.J. Bard.
47. Brown, P., K. DeAntonois, and P. Hall, *High Performance Liquid Chromatography.* Handbook of Instrumental Techniques for Analytical Chemistry, ed. F. Settle. 1997. 147-164.
48. *NIST/EPA/NIH Mass Spectral Database.*
49. Skoog, Holler, and Nieman, *Principles of Instrumental Analysis.* 5th ed. 1998: Saunders College Publishing. 673-697, 725-766.
50. Yang, H., et al., *Methanol tolerant oxygen reduction on carbon-supported Pt–Ni alloy nanoparticles.* Journal of Electroanalytical Chemistry, 2004. **576**: p. 305-313.